

# **A molecular approach towards tethered bilayer lipid membranes: Synthesis and characterization of novel anchor lipids**

Dissertation zur Erlangung des Grades  
`Doktor der Naturwissenschaft`

am Fachbereich Chemie, Pharmazie und Geowissenschaften  
der Johannes Gutenberg Universität Mainz

Petia Atanasova  
Geboren in Pleven, Bulgarien

Mainz, April 2007

Tag der mündlichen Prüfung: 06.06.07

# Contents

<b>1. Introduction</b> .....	<b>1</b>
1.1. The cell membranes.....	1
1.2. Model lipid membranes.....	2
1.2.1. Vesicles.....	2
1.2.1. Black lipid membranes.....	3
1.2.3. Membranes on solid supports.....	4
1.2.3.1. Supported Bilayer Lipid Membranes.....	4
1.2.3.2. Tethered Bilayer Lipid Membranes.....	5
1.3. Motivation.....	6
Literature.....	8
<b>2. Synthesis of thiolated lipids</b> .....	<b>10</b>
2.1. Characterisation methods.....	10
2.1.1. NMR.....	10
2.1.2. FD-MS.....	11
2.1.3. ATR.....	11
2.1.4. TGA, DSC .....	11
2.1.5. Materials .....	12
2.2. Synthesis of lipids with a different length in the tethering part (DPTT, DPHT and DPOT).....	13
2.2.1. Introduction.....	13
2.2.2. Motivation.....	16
2.2.3. Results and discussion.....	18
2.2.4. Conclusion.....	21

2.2.5. Experimental part.....	22
2.3. Synthesis of lipid with longer tethering part.....	29
2.3.1. Introduction and motivation.....	29
2.3.2. Results and discussion.....	31
2.3.3. Conclusion.....	33
2.3.4. Experimental part.....	33
2.4. Synthesis of lateral spacer molecules.....	38
2.4.1. Introduction and motivation.....	38
2.4.2. Results and discussion.....	40
2.4.3. Conclusion.....	41
2.4.4. Experimental part.....	42
2.5. Synthesis of lipid with bulky anchor - “self-diluted” molecule (DPHDL)..	45
2.5.1. Introduction and motivation.....	45
2.5.2. Results and discussion.....	48
2.5.3. Conclusion.....	51
2.5.4. Experimental part.....	51
2.6. Synthesis of thiolated lipid with extended hydrophobic part (DDPTT)..	57
2.6.1. Introduction and motivation.....	57
2.6.2. Results and discussion.....	60
2.6.3. Conclusion.....	62
2.6.4. Experimental part.....	63
2.7. Synthesis of fluorescent labeled lipids.....	68
2.7.1. Introduction and motivation.....	68
2.7.2. Results and discussion.....	69

2.7.3. Conclusion.....	76
2.7.4. Experimental part.....	77
Literature.....	85
<b>3. Investigation the properties of thiolated lipid monolayers (DPTT, DPHT, DPOT and DDPTT).....</b>	<b>89</b>
3.1. General principles of Langmuir – Blodgett technique.....	89
3.2. Introduction and motivation.....	93
3.3. Results and discussion.....	94
3.3.1. Influence of the lipid structure.....	94
3.3.2. Influence of the temperature.....	97
3.3.3. Investigation of anchor and free lipids mixed monolayers.....	98
3.3.4. Investigation of miscibility of lipid monolayers.....	102
3.3.5. Hysteresis of the pure anchor lipids.....	105
3.3.6. Relaxation time investigation of the monolayers.....	106
3.4. Conclusion.....	107
Literature.....	108
<b>4. Electrical properties of diluted tBLMs.....</b>	<b>110</b>
4.1. Introduction.....	110
4.2. Characterisation techniques.....	111
4.2.1. Electrochemical Impedance Spectroscopy.....	111
4.2.1.1. Theory.....	111
4.2.1.2. Measurements.....	113
4.2.2. Atom Force Microscopy.....	114
4.2.3. Contact angle.....	114
4.3. Materials and methods.....	115

4.3.1. Anchor and free lipids, solutions.....	115
4.3.2. Substrates.....	116
4.3.3. Monolayer formation.....	116
4.3.4. Bilayer formation.....	117
4.3.5. Incorporation of valinomycin.....	119
4.4. Results and discussion.....	120
4.4.1. Application of DDPTT, DPHT and DPHDL.....	120
4.4.2. Membrane formation based on LB-diluted monolayers.....	120
4.4.3. Membrane formation of DPOT-based self-assembled monolayer	124
4.4.4. Membrane formation of DDPTT-based self-assembled monolayers.....	126
4.5. Conclusion.....	128
Literature.....	130
<b>5. Conclusion and outlook.....</b>	<b>131</b>
<b>Abbreviations.....</b>	<b>135</b>
<b>Curriculum vitae .....</b>	<b>139</b>

# 1. Introduction

## 1.1. The cell membranes

Cells are the fundamental building block of all living organisms. They are as well as different organelles in the eukaryotic cells surrounded and protected by a membrane. The study of the cell membrane has a long and extensive history. First, W. Pfeffer in 1877 has discovered that the cell is surrounded by a discrete, but invisible semi-permeable membrane.<sup>1</sup> Around 20 years later, E. Overton proposed that the membrane consists of an oily or lipid-like substance.<sup>2</sup> In 1910, Höber has shown that the membrane possesses a high electrical resistivity although the cytoplasm in the cell has a high conductivity.<sup>3</sup> A substantial effort has been made last century to gain more information about structure and function of the cell membrane.

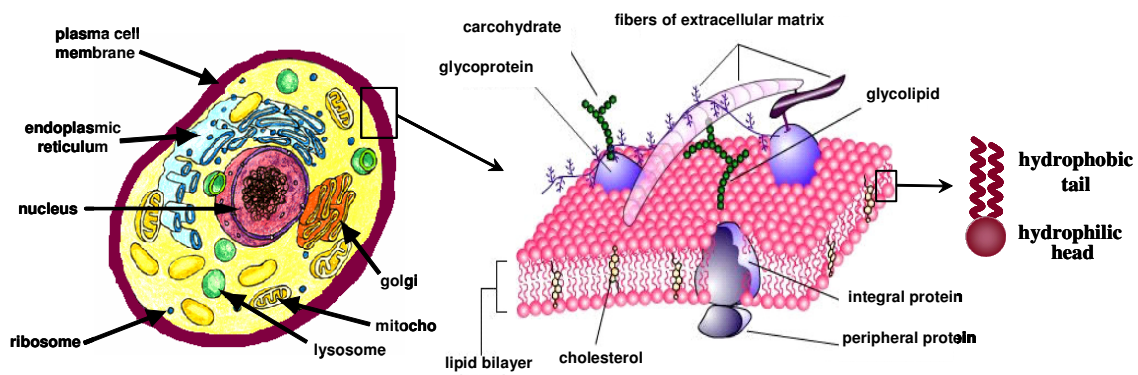


Figure 1.1. Schematic representation of a biological cell, cell membrane and phospholipid

The membrane forms a barrier for most molecules and even ions. Water is almost the only polar molecule able to pass easily. A membrane is mainly composed of lipids and proteins. The lipids are amphoteric molecules (Figure 1.1) with a polar hydrophilic “head” attached via an ester or ether bond to two non polar hydrophobic fatty acid tails. In an aqueous environment, they assemble into a double layer (bilayer) to form the membrane. The hydrophobic fatty tails face the inside of the membrane, while the hydrophilic head points outwards. The assembled bilayer

behaves like a low dielectric material with capacitance  $0.5-1 \mu\text{F cm}^{-2}$ . The diverse functions of the membrane are primarily due to associated proteins. They can be structural and functional, and depending on the degree of association can be divided in two groups. Membrane bound proteins are strongly associated or bound and function on one side of the membrane. The second group includes proteins partly inserted into the membrane, or traverses the membrane as channels from the outside to the inside of the cell.

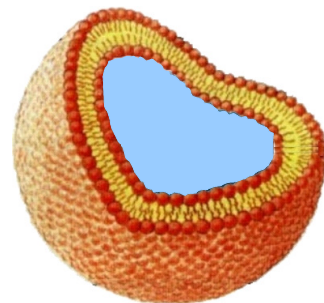
Many models were proposed to explain the organization of the proteins in the lipid bilayer structure. The most common is the fluid mosaic model proposed by S.J. Singer and G.L. Nicolson in 1972<sup>4</sup>. It is schematically depicted in Figure 1.1. According to this model, the membranes proteins are embedded to various degrees in the lipid bilayer providing the structure of the membrane. The movement of the lipids and the other functional components is constrained and controlled to create asymmetrical distribution in a manner still not fully understood. This and many other questions concerning the dynamics of the membrane, structure and functionality of its active parts (especially proteins) are still object of further scientific research.

The complexity of the cell membrane results in lack of detailed knowledge. Therefore, simplified model systems are needed. These could help to find the lacking fundamental knowledge and will give a general platform to investigate their potential applications, for example, as biosensing devices and drug delivery.

## 1.2. Model lipid membranes

### 1.2.1. Vesicles

Historically, the most commonly used model membrane structure is the vesicle or liposome. Vesicles are classified by their size and number of the included bilayers. The simplest and easiest models are multilamellar vesicles. They are spontaneously formed, when pure, dried lipids are dispersed in buffer. The lipids are forced from water to self-suggregate forming concentric shells resulted in giant multilamellar vesicles. They are applied in industry for drug delivery and in the cosmetics. Nevertheless, the application of these type





vesicles is limited because the control of the size or the number of bilayers per vesicles is difficult.

More precise in their structure are unilamellar vesicles. They are surrounded by only one bilayer and can be manufactured in different ways depending from the desired size (extrusion, sonication, film hydration, etc.). These model membranes are used as a matrix for incorporation of proteins measured by patch clamp technique,<sup>5</sup> but their fragility and limited access to the encapsulated solutes in the vesicles make them not the most appropriate model system for this purpose. The need of enhanced stability and controlled permeability led to the synthesis of polymerizable<sup>6</sup> and even polymerizable fluorescent labeled lipids.<sup>7</sup>

Vesicles are especially useful for the investigation of membrane characteristics such as lateral diffusion and homogeneity. Addition of fluorescent probes in the liposomes provides information about the lipid-lipid or lipid-protein interactions as well as insight into the molecular mechanisms of membrane fusion.

The main drawback of this model system is their propensity to aggregate. Therefore, they have defined size distribution only for a few days.

### 1.2.2. Black Lipid Membranes (BLM)

Charge transfer processes through the membrane gain a particular interest in the last years. In order to control the electric properties of the membrane, one needs to



connect both membrane sides. This can be achieved by a planar lipid membrane separating two compartments. Black Lipid Membranes (BLM) are free-hanging bilayers over micrometer sized aperture in thin hydrophobic substrate and are only held by the lateral tension between the lipids.

In 1967, Müller and Rudin first present BLMs as a model systems and the introduced method for their preparation is still the commonly used. In general, BLM are created by painting of an n-alkane solution of lipids across the aperture and continuous thinning of the resulting multilamellar membrane.

The obtained BLM is 4-5 nm thick and covers holes in microscopic diameter (1  $\mu\text{m}$ ). They are highly resistive ( $R > 10^6 \Omega \text{ cm}^2$ ), the capacitance is around  $0.5 \mu\text{F cm}^{-2}$  and are very suitable for electrochemical measurements. Since both the BLMs and the

incorporated proteins are close to their native state, the study of the electrical properties such as conduction, dielectric constant of the membrane or transfer of charges is particularly valuable.

The main drawback of this model system is the lack of stability. Their average lifetime is a few hours before it is destroyed. The presence of even a minute concentration of contaminations leads to rupture of the membrane. Additionally, the thickness, elasticity and electrical properties of the planar membranes are strongly affected from the amount remaining solvent. The latter also affects the conduction of the incorporated ion-channels.

An enhanced stability of the planar membrane could be approached as is described in the next section. Nevertheless, BLMs are still used and have their historical distribution on collection of fundamental knowledge related to the cell membrane and the processes occurred there.

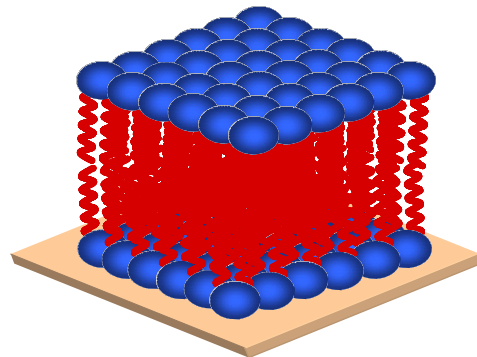
### 1.2.3. Membranes on solid supports

The need of robust model system is of a great importance for both scientific research and further technical applications. One possible system is a bilayer lipid membrane formed on a solid substrate. They could be physisorbed on the surface, then, the membranes are named Supported Bilayer Lipid Membranes (sBLM) or chemisorbed named Tethered Bilayer Lipid Membranes (tBLMs). The properties of these model membranes allow for detailed investigation with a multitude of surface sensitive techniques such as SPR, QCM, AFM, FRAP and EIS.

#### 1.2.3.1. Supported Bilayer Lipid Membranes

sBLMs are only weakly bound to a solid hydrophilic surface (glass, gold, indium-tin oxide or silicon substrates) that retains most of their native properties like hydration and fluidity. The first sBLM has been described by L. K. Tamm and H. M. McConnell in 1985.<sup>8</sup> Small unilamellar

proteoliposomes were fused on glass surface, and cell-cell interactions were



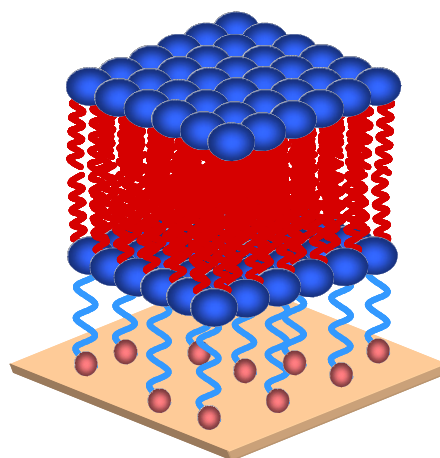
observed. Other methods to obtain sBLMs are Langmuir-Blodgett deposition, self-assembly from lipid dispersion directly on electrodes and detergent dialysis. Bilayers, directly supported on glass or quartz, are separated from the surface by a thin, lubricating film of water (1-2 nm)<sup>9</sup> that is very important to ensure the lateral mobility of the lipids in both leaflets.

Since their introduction, sBLMs have been widely used as a model system for studying the membrane structure,<sup>10</sup> electrochemical properties of the membranes,<sup>11</sup> lipid-protein interactions,<sup>12</sup> and invention of microscopic separation devices.<sup>13</sup>

There is a huge amount of literature dedicated to the charge transfer processes associated with incorporation of different proteins. However, the substrate-exposed domains of large integral proteins could interact with the substrate that causes inhibition of their lateral mobility<sup>14</sup> or even adsorption, hence, denaturation of the proteins. Additionally, the electrical analysis of single membrane channels requires a large ionic reservoir.<sup>15</sup> Therefore, an important goal for further development was to find ways to separate the membrane from the substrate. This was done by inclusion of a polymer cushion<sup>16</sup> that should not interact with the proteins and lipids, allows penetration of water and maintains the protein mobility. Many efforts are put in exploration of such membranes facilitating the protein incorporation.<sup>17</sup> However, these systems are easily damaged or removed that makes their live-time (from hours to days) still not long enough to be systematically used for sensing applications.

### 1.2.3.2. Tethered Bilayer Lipid Membranes

The idea for a functional coupling of the bilayer inner leaflet to the substrate was given by Sackmann in 1996. The attachment with a covalent bond yields more robust supported membrane. In general, the preparation includes a two-step procedure. The proximal layer, terminated with an anchor group, is first attached to the surface. Most of the connections are based on the strong S-Au,<sup>18-20</sup> S-Hg<sup>27,21</sup> or Si-O<sup>22,23</sup> affinity. Secondly, the outer leaflet consisted of free lipids is assembled to complete the bilayer. Two different kinds anchor lipids can be used. Within the first approach, a thiol-alkane is self-



assembled on the gold surface, further covered with a second lipid layer. The resulted membrane is named supported hybrid bilayer membranes (HBMs).<sup>24-27</sup> The main drawback of HBMs is in the absence of aqueous ionic reservoir particularly needed for incorporation of intrinsic membrane proteins. Therefore, a novel class of synthetic tether lipids was developed. These anchor lipids contain a spacer part that serves as a linker between the inner part of the membrane and the anchor attached to the solid support. The biomimetic membranes based on such tether lipids are referred to as tethered bilayer lipid membranes. This system provides a stable bilayer required for nanoelectrical investigations, retain the biocompatibility for biosensor applications as well as allow for investigation the functions of the embedded proteins.

The expected stability and flexibility of tBLMs was proved and successfully used for incorporation of various highly sensitive and selective proteins: ion channels, pores, ion-carriers, etc. For instance, Cornell *et al.*<sup>20</sup> have first presented tBLMs with highly insulating properties allowed development of a biosensing technique in which the conduction of the embedded ion channel is switched by a recognition event.

Later on, many researchers reported the usefulness of tBLMs for biosensing devices on different electrodes.<sup>23,28-30</sup> Giess *et al.*<sup>31</sup> present a new concept of tBLM formation on previously tethered protein. Bushby *et al.*<sup>32</sup> reported investigation the function of a redox-active membrane protein by tethering of vesicles containing total membrane extract onto gold surface modified with cholesterol based thiols.

The length of the spacer part is varied from small, well defined structures<sup>20,23,28,29,33-35</sup> to polymers<sup>22,36,37</sup> in order to tune the space beneath the membrane.

### 1.3. Motivation

Recently, tBLMs based on a new thiolated tether lipid, synthesized in our group,<sup>28</sup> have shown high insulating properties, and allowed incorporation of several membrane proteins. However, the high densely packed monolayers (51-75 Å<sup>2</sup>/molecule) may lower the fluidity of the resulting bilayers. At such a high density, the submembrane space is practically completely occupied by the tethering linker. Thus, incorporation of proteins with large submembrane domains is hindered.

Therefore, further optimization of the lipid structure is needed in order to dilute the monolayers (enhance the fluidity) without increasing the defect probability. The latter is crucial for a proper monitoring of the protein function.

Several parallel approaches were realized to achieve controllable dilution within the inner leaflet of the tBLMs: (i) preparation of tethering lipids with larger tethering linker part is thought to provide bigger space beneath the membrane due to its conformational changes; (ii) lateral spacer molecules were synthesized in order to ensure concurrent to the tethering lipid assembly on the surface, and thus to create more lateral space; (iii) the use of a tethering lipid with a bulky anchor is supposed to increase both the area per lipid molecule and the probability free lipids to be inserted into the inner lipid layer. The latter will increase the mobility of the whole membrane; (iv) increasing the volume of the hydrophobic part of the lipid will increase the mean area per anchored molecule and density in the hydrophobic region required for better electrical-sealing properties of the membrane.

Therefore, the interest in the current study is focused on the synthesis and characterization of a small library of thiolated tether lipids as well as investigation of their ability to form tBLMs suitable to host transport membrane proteins.

The work is divided in three chapters. The first one includes the synthesis and characterization of a series of tether lipids with structures designed to fulfill the desired properties.

Since the anchor lipids, obtained in this study, act as surfactants on the water surface, the characteristic properties of the monolayers prepared either of pure lipids or mixtures (anchor lipids / free lipids) at the air-water interface are described in the second chapter.

Finally, monolayers were assembled on gold substrate applying different techniques. In the third chapter, some preliminary EIS measurements of bilayer formation and protein incorporation will be discussed.

## Literature

1. Pfeffer, W., *Osmotische Untersuchungen. Studien zur Zellmechanik*, Leipzig, **1877**.
2. Overton, E.,: *Über die osmotischen Eigenschaften der Zelle in ihrer Bedeutung für die Toxikologie und Pharmakologie*, Vjschr. Naturforsch. Ges., Zürich, **1895**, 41, 383.
3. Höber, R., *Pflüg. Arch. Phys.*, **1910**, 183, 237.
4. Singer, S. J.; Nicolson, G. L., *Science*, **1972**, 175, 720.
5. Sackman, B.; Neher, E., *Single-Channel Recording*, Plenum Press, New York, **1995**.
6. O'Brien, D. F.; Armitage, B.; Benedicto, A.; Bennett, D. E.; Lamparski, H. G.; Lee, Y. S.; Srisiri, W.; Sisson, T. M., *Acc. Chem. Res.*, **1998**, 31, 861-868.
7. Roy, B. C.; Fazal, M. A.; Arruda, A.; Mallik, S.; Campiglia, A.D., *Organic letters*, **2000**, 2(20), 3067-3070.
8. Tamm, L. K.; McConnell, H. M., *Biophysical Journal*, **1985**, 47, 105-113.
9. Johnson, S. J.; Bayerl, T. M.; McDermott, D. C.; Adam, G.W.; Rennie, A.R.; Thomas, R. K.; Sackmann, E., *Biophysical Journal*, **1991**, 59, 289-294.
10. Tamm, L. K.; Shao, Z., *Biomembrane Structure*, **1998**, Chapman, D. and Harris, P., editors, Amsterdam, 169-185.
11. Stelzle, M.; Weismüller, G.; Sackmann, E., *Journal of Physical Chemistry*, **1993**, 97, 2974-2981.
12. Silvestro, L.; Axelsen, P. H., *Chem. Phys. Lipids*, **1998**, 96, 69-80.
13. van Oudenaarden, A.; Boxer, S. G., *Science*, **1999**, 285(5430), 1046-1048.
14. Poglisch, C. L.; Sumner, M. T.; Thompson, N. L., *Biochemistry*, **1991**, 30, 6662-6671.
15. Costello, R. F.; Peterson, I. R.; Heptinstall, J.; Byrne, N. G.; Miller, L. S., *Adv. Mater. Opt. Electron.*, **1998**, 8, 47-52.
16. Sackmann, E., *Science*, **1996**, 271, 43-48.
17. Shao, Z.; Tamm, L. K., *Langmuir*, **2003**, 19, 1838-1846.
18. Boden, N.; Bushby, R. J.; Liu, Q. Y., *Tetrahedron*, **1998**, 54, 11537-11548.
19. Heyse, S.; Ernst, O. P.; Dienes, Z.; Hofmann K. P.; Vogel, H., *Biochemistry*, **1998**, 37(2), 507-522.
20. Cornell, B. A.; Braach-Maksvytis, V. L. B.; King, L. G.; Osman, P. D. J.; Raguse, B., Wiczorek, L.; Pace, R. J., *Nature*, **1997**, 387, 580-583.
21. Krysinski, R.; Zebrowska, A.; Michota, A.; Bukowska, J.; Becucci, L.; Moncelli, M. R., *Langmuir*, **2001**, 17, 3852-3857.
22. Wagner, M. L.; Tamm, L. K., *Biophys. J.*, **2000**, 79, 1400-1414.

- 
23. Atanasov, V.; Knorr, N.; Duran, R. S.; Ingebrandt, S.; Offenhaeusser, A.; Knoll, W.; Köper, I., *Biophysical Journal*, **2005**, *89*, 1780-1788.
  24. Steinem, C.; Janshoff, A.; Ulrich, W. P.; Sieber, M.; Galla, H. J., *Biochim. Biophys. Acta-Biomembranes*, **1996**, *1279(2)*, 169-180.
  25. Plant, A. L., *Langmuir*, **1999**, *15*, 5128-5135.
  26. Lingler, S.; Rubinstein, I.; Knoll, W.; Offenhäusser, A., *Langmuir*, **1997**, *13*, 7085-7091.
  27. Tadini Buoninsegni, F.; Herrero, R.; Moncelli, M. R., *J. Electroanal. Chem.*, **1998**, *452(1)*, 33-42.
  28. Schiller, S. M.; Naumann, R.; Lovejoy, K.; Kunz, H.; Knoll, W., *Angew. Chem. Int. Ed.*, **2003**, *42(2)*, 208-211.
  29. Terrettaz, S.; Mayer, M.; Vogel, H., *Langmuir*, **2003**, *19*, 5567-5569.
  30. Moncelli, M. R., Becucci, L.; Schiller, S. M., *Bioelectrochemistry*, **2004**, *63(1-2)*, 161-167.
  31. Giess, F.; Friedrich, M. G.; Heberle, J.; Naumann, R. L.; Knoll, W., *Biophysical Journal*, **2004**, *87*, 3213-3220.
  32. Jeuken, L. J.; Connell, S. D.; Nurnabi, M.; O'Reilly, J.; Henderson, P. J. F.; Evans, S. D.; Bushby, R. J., *Langmuir*, **2005**, *21*, 1481-1488.
  33. Vockenroth, I.; Atanasova, P.P.; Knoll, W.; Köper, I., *IEEE sensors*, **2005**.
  34. Vockenroth, I.; Atanasova, P.P.; Long, J. R.; Jenkins, A. T. A.; Knoll, W.; Köper, I., *Biochemica et Biophysica Acta*, **2007**, *paper in press*.
  35. Breffa, C., *New synthetic strategies to tethered bilayer lipid membranes*, **2005**, Johannes Gutenberg Universität: Mainz.
  36. Munro, J. C.; Frank, C. W., *Langmuir*, **2004**, *20*, 10567-10575.
  37. Purucker, O.; Fortig, A.; Jordan, R.; Tanaka, M., *ChemPhysChem.*, **2004**, *5*, 327-335.

## 2. Synthesis of thiolated lipids

### 2.1. Characterization methods

#### 2.1.1. Nuclear magnetic resonance (NMR)

Nuclear magnetic resonance is a powerful technique used in the investigation of the structure of unknown organic compounds in their liquid or solid state. It exploits the magnetic properties of nuclei in atoms. When placed in a magnetic field, NMR active nuclei (like  $^1\text{H}$  or  $^{13}\text{C}$ ) resonate at a specific frequency, dependant on strength of the magnetic field. However, depending on the local chemical environment, different protons in a molecule each resonate at slightly different frequency. Since this frequency is dependant on the strength of the magnetic field, it is converted into a field independent value known as a chemical shift. The latter is reported as a relative measure from some reference resonance frequency. In the case of  $^1\text{H}$  or  $^{13}\text{C}$  NMR, tetramethylsilane is commonly used as a reference.

The  $^1\text{H}$  NMR spectrum of an organic compound provides information concerning:

- the number of different types of hydrogen atoms presented in the molecule
- the relative numbers of the different types of hydrogen atoms
- the electronic environment of the different types of hydrogen atoms
- the number of hydrogen "neighbor" a hydrogen has

In this research, the  $^1\text{H}$  and  $^{13}\text{C}$  NMR spectra were recorded on a Bruker DXP 250 MHz NMR spectrometer. NMR spectra were recorded at ambient conditions at 250 and 62.5 MHz for  $^1\text{H}$  and  $^{13}\text{C}$  NMR, respectively. The spectra were calibrated to the solvent signal as follows: 7.24 ( $^1\text{H}$ ) and 77.0 ( $^{13}\text{C}$ ) ppm for  $\text{CDCl}_3$  and 5.23 ( $^1\text{H}$ ) and 54.0 ( $^{13}\text{C}$ ) ppm for  $\text{CD}_2\text{Cl}_2$ . The processing of the spectra was done with WinNMR software.



### **2.1.2. Field desorption mass spectrometry (FD-MS)**

Mass spectrometry provides information about the mass-to-charge ratio of ions. This is achieved by ionization the sample and separating ions of different masses and recording their relative abundance by measuring intensities of ion flux. Field desorption mass spectrometry is used to detect organic molecules with low molecular weight in the range of 250 to 3500 g/mol.

Mass spectroscopy was performed using a VG ZAB2-SE-FPD Spectrofield spectrometer.

### **2.1.3. Attenuated total reflection infrared (ATR-IR) spectroscopy**

ATR technique is used in conjunction with infrared spectroscopy and enables examination of samples directly in solid or liquid state without further preparation.

The sample is pressed into optical contact with the top of the ATR crystal surface. A beam of infrared light is passed through the crystal having a high refractive index, allowing the radiation to reflect within it several times. The reflection forms an evanescent wave which penetrates into the sample typically by a few microns. At the output end of the crystal, the beam is then collected by a detector.

For our IR spectra measurements, a Nicolet 730 FTIR spectrometer was used with endurance diamant-ATR.

### **2.1.4. Thermogravimetric analysis (TGA) and differential scanning calorimetry (DSC)**

Thermogravimetric analysis is an analytical technique used to determine a material's thermal stability and its fraction of volatile components by monitoring the weight change that occurs as the sample is heated. The measurement is carried out in air or in an inert atmosphere, and the weight is recorded as a function of increasing temperature.

TGA measurements were derived using Mettler 300 Thermogravimetric analyzer.

Differential scanning calorimetry is a thermoanalytical technique, where the difference in the amount of heat required to increase the temperature of a sample and reference are measured as a function of temperature. Both the sample and a reference are maintained at very nearly the same temperature throughout the experiment.

When the sample undergoes a physical transformation such as phase transition, more (or less) heat will need to flow to it than the reference to maintain both at the same temperature. Whether more or less heat must flow to the sample depends on whether the process is exothermic or endothermic. By observing the difference in heat flow between the sample and reference, the amount of heat absorbed or released during such transitions is measured.

DSC analyses were performed on Mettler Digital Scanning Calorimeter 300, with a heating rate of 10 K/min.

### **2.1.5. Materials**

Triethylamine (TEA, Acros) and tetrahydrofuran (THF, Fisher) were dried over  $\text{CaH}_2$  and potassium-benzophenone complex, respectively. Thioacetic acid (Acros) was distilled prior to use. 2,2'-azobis(2-methylpropionitrile) (AIBN, Acros) was recrystallized in ethanol. All other chemicals were used without further purification.

The developer used by TLC monitoring called Zuckerreagenz consists of resorcinmonomethylether and sulphuric acid mixture in ethanol 1/1.

## 2.2. Synthesis of lipids with a different chain length in the tethering part (DPTT, DPHT and DPOT)

### 2.2.1. Introduction

In the last decade, diverse synthetic tether lipids have been synthesized and used for formation of tBLMs. The scientific interest in tBLMs has increased due to the high practical potential of tBLMs as one of the most attractive model system to mimic the structural and transport roles of biological membranes.

In general, the tether lipids reported in the literature differ in their hydrophobic, spacer and anchor moieties. Numerous tether lipids have been synthesized with a hydrophobic part consisting of fully saturated straight hydrocarbonyl chains<sup>1-4</sup> or of a mixture of fully saturated and unsaturated chains<sup>5</sup>. The length of the chains has been varied between 16 and 20 methylene units with a typical length of 16 units.<sup>6</sup> However, these lipids suffer from relatively high glass transition temperatures ( $T_g$ ) (e.g.,  $T_g$  of dipalmitoylphosphatidylcholine is 41.5°C)<sup>7</sup> and thus do not form fluid membranes at room temperature. Lipids with straight aliphatic chains larger than 12 C-atoms form crystalline monolayers leading to domain boundaries and crystal defects within the membrane.<sup>28</sup> To overcome this problem, Cornell *et al.*<sup>8</sup> have introduced a new approach utilizing the excellent barrier properties of archaeobacterial lipids. Archaeobacteria proliferate in environments such as volcanic hot springs, salt lakes, and acidic or alkaline spots.<sup>9</sup> The major structural feature, which distinguishes these lipids from the others, is that the hydrophobic part contains branched hydrocarbon units such as an isoprenoid phytanol. These methyl branches ensure low phase transition temperatures, hinder the crystallization of the membrane, and keep it fluid under ambient conditions.<sup>30</sup> Terrettaz *et al.*<sup>10</sup> and Schiller *et al.*<sup>11</sup> have presented tBLMs based on similar phytanyl units with very good sealing properties.

The hydrocarbon tail of the lipids is coupled to a polar head group. Among various linkage functionalities such as oxyethylenes,<sup>12,13</sup> sulfides,<sup>14</sup> and 2-hydroxymethylglycerol,<sup>15</sup> the glycerol linker is most often used.<sup>16</sup> In natural lipids, this stable moiety occurs in a defined *sn*-2 stereochemical configuration. In the case of tether lipids the polar head group is replaced with a spacer unit. This spacer unit

separates the lipid bilayer from the solid substrate while serving as a polymer cushion. This cushion compensates for surface roughness effects and protects embedded biomaterial from touching the surface, which may cause a loss of functionality due to denaturation. Furthermore, the spacer provides an ion reservoir underneath the membrane, which is of great importance for the electrical properties of the tBLM<sup>17</sup> and proper functionality of the membrane. Various materials such as oligosaccharides,<sup>18</sup> polymers based on acrylamide and its derivatives,<sup>19</sup> ethylene glycol esters/amides of succinic acid/succinamide<sup>20</sup>, and polyethylene glycol<sup>21,3</sup> have been used. It has been shown that these moieties form a gel-like hydrophilic layer between the lipid membrane and the substrate surface which is permeable for ionic species.<sup>15</sup> An important factor for electrical properties of the membrane is the type of linkage. Krishna *et al.*<sup>17</sup> have investigated the ion flow through the bilayer comparing two lipid molecules – one with an ester linkage and another with an ether linkage. The flow of ions has been found to be higher in membranes where the tethering chains are formed of tetraethylene glycol units with all-ether linkages. This phenomenon has been attributed to the stronger physical adsorption of ions to ester than to ether linkage.

Finally, surface immobilization of the tether lipids is achieved by an anchor group, which forms a covalent bond with the surface. Several anchor groups have been tested on gold surfaces; most of them are based on gold-sulfur interactions.<sup>1-5,8</sup> Thiolated tether lipids have also been attached on different electrodes such as mercury.<sup>22</sup>

The first tBLM with phytanyl units in Mainz was developed in 2003. The lipid synthesized for this purpose termed DPTL consists of two phytanyl chains, TEG spacer and lipoic acid anchor. tBLMs prepared with this molecule have demonstrated good electrical sealing properties.<sup>11</sup> The high electrical resistance of the membrane (2-12 MΩcm<sup>2</sup>) has allowed further incorporation and investigation of several membrane proteins. Furthermore, a family of thiolipids (analogs of DPTL) with longer spacers and slightly different lipid head groups has been prepared and investigated.<sup>23</sup> DPTL and its analogs are functionalized with an anchor appropriate for gold surfaces. However, for biosensing applications it is interesting to combine the biological system of the membrane with an electronic read-out system. These systems are mostly based on silicon technology. Therefore, a tether lipid with ability to couple to silicon or silicon oxide surface is of high importance. Tamm *et al.*<sup>24</sup> presented tBLMs on silicon oxide substrates using PEG-phospholipid conjugates with a triethoxysilane anchor group.

In the current section of this work, a generic approach will be described towards the synthesis of a “universal” lipid precursor, which possesses double bond functionality. Using different synthetic routes, the double bond can be modified to different anchor groups suitable either for noble metal surfaces (e.g., Au, Ag, Pt, Cu, Fe, Ni, or Hg) or for metal oxide surfaces<sup>25</sup> (e.g., SiO<sub>2</sub>) (Figure 2.1).

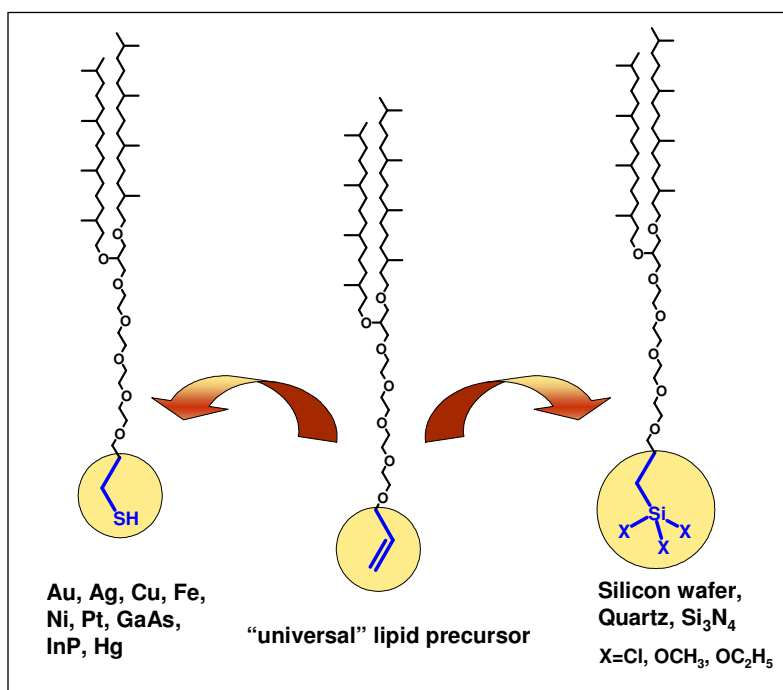


Figure 2.1. Conversion of the “universal” lipid precursor to thiolated or silanated tether lipid

Additionally, the length of the spacer unit can be varied in order to tune the lipid structure for preparation of tBLMs with both high sealing and high fluidic properties.

### 2.2.2. Motivation

The interest in the current study will focus on the synthesis of a series of thiolated tether lipids similar to the structure of DPTL. However, the synthetic route is modified including a synthesis of “universal” lipid precursor. Furthermore, this precursor can be used for preparation of either thiolated or silanated anchor lipids. In comparison with DPTL, where lipoic acid is used as an anchor group, the target lipids have a thiol anchor. It is well known, that lipoic acid tends to polymerize with time.<sup>26</sup> The proposed new thiolipids can only dimerize.

The ion reservoir beneath the membrane is of a great importance for incorporation of larger proteins. Therefore, a range of tether lipids with different ethylene glycol chain lengths in the spacer can be obtained in order to optimize the space between the gold substrate and the bilayer.

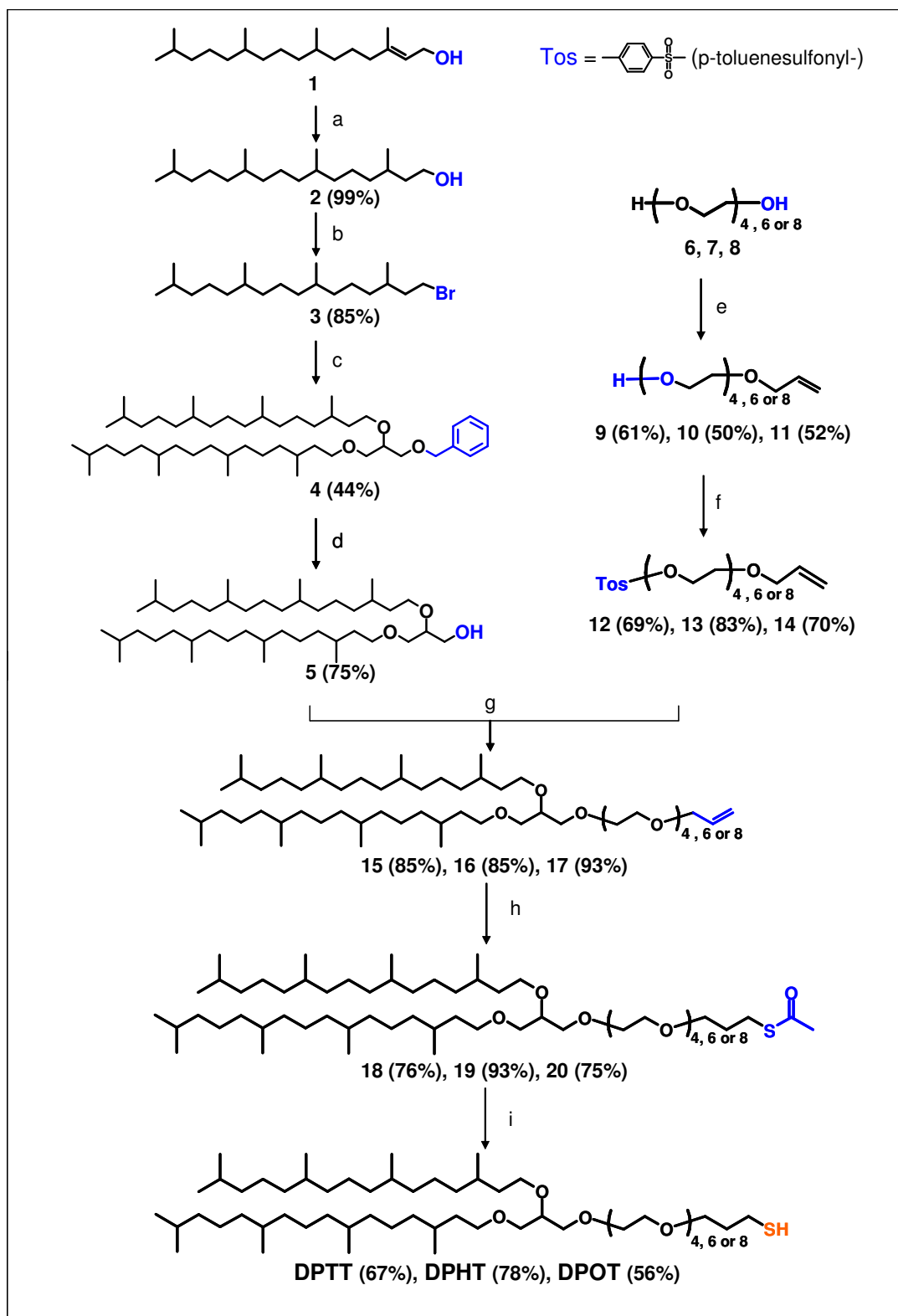


Figure 2.2. Synthetic route for preparation of DPTT, DPHT and DPOT

### 2.2.3. Results and discussion

The synthetic route of the thiolated lipids is shown in Figure 2.2 and consists initially of two parallel reactions: (i) preparation of the hydrophobic part (DPG) and (ii) functionalization of the corresponding ethylene glycol as a hydrophilic moiety. The synthesis of DPG (i) is already described in *Atanasov et al.*<sup>27</sup> The different ethylene glycols (ii) were firstly functionalized with average yield and secondly activated with p-toluenesulfonyl chloride.

Further, the products of (i) and (ii) were coupled by a Williamson reaction. The lipid precursors **15**, **16** and **17** were synthesized successfully with yields up to 93%.

The structure of the obtained precursors was verified by <sup>1</sup>H NMR and <sup>13</sup>C NMR.

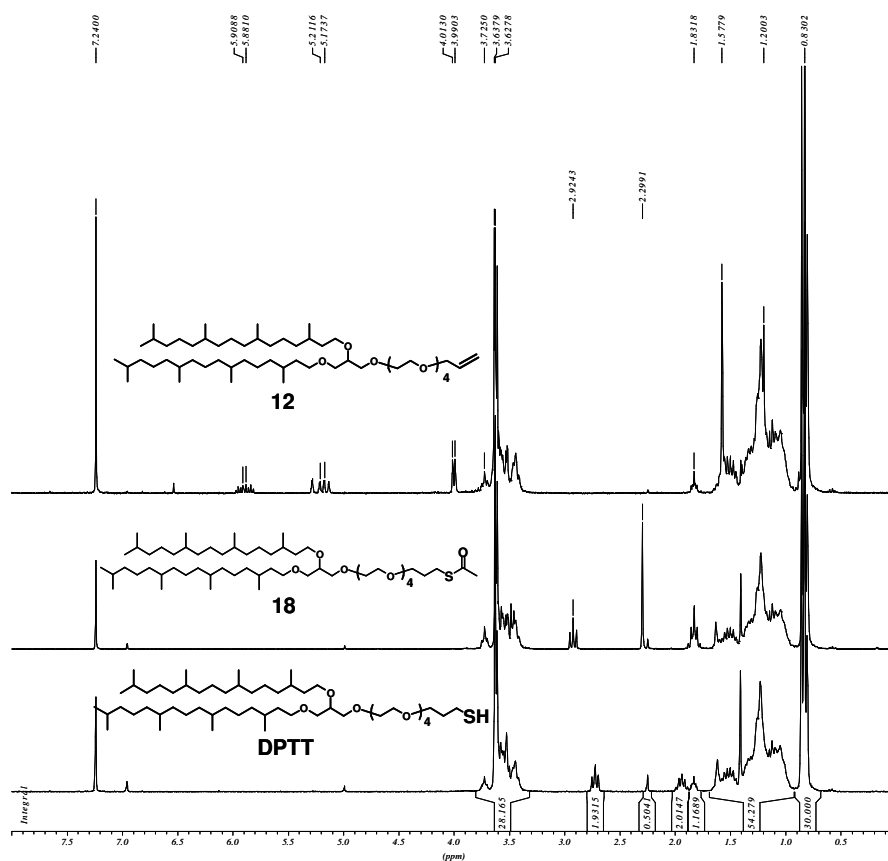


Figure 2.3. <sup>1</sup>H NMR spectra of the lipid precursor **12**, the intermediate **18** and DPTT

Related multiplets at 5.1 – 5.3 and 5.8 – 6.0 ppm in the <sup>1</sup>H NMR, as shown in Figure 2.3, and 135.5 and 116.8 ppm in the <sup>13</sup>C NMR indicate the presence of the double bond functionality. The signal integrals in the region 0.8 - 1.9 ppm correspond to the protons



in the phytanyl chains, the multiplet at 3.35 - 3.8 ppm corresponds to the protons in the ethylene glycol chain, and the signal at 4.0 ppm is related to the methylene protons next to the double bond. At the same time, the signal integrals corresponding to the tosyl group at 7.3 and 7.8 ppm disappeared after the reaction. Very high purity of the precursors was achieved by column chromatography. The isolated products show a sequence of signals in the FD-mass spectrum related to single, double and triple  $m/z$  values of the monomolecular weight. These signals appear probably due to cluster formation.

As the glass-transition temperature ( $T_g$ ) is a very important characteristic of the lipids used as a platform for bilayer formation, DSC analysis was performed in order to compare the  $T_g$  values of the lipids in the current study and the phytanyl based lipids reported in the literature. The measurements have shown that with increasing the length of the ethylene oxide chain  $T_g$  increases (Figure 2.4).

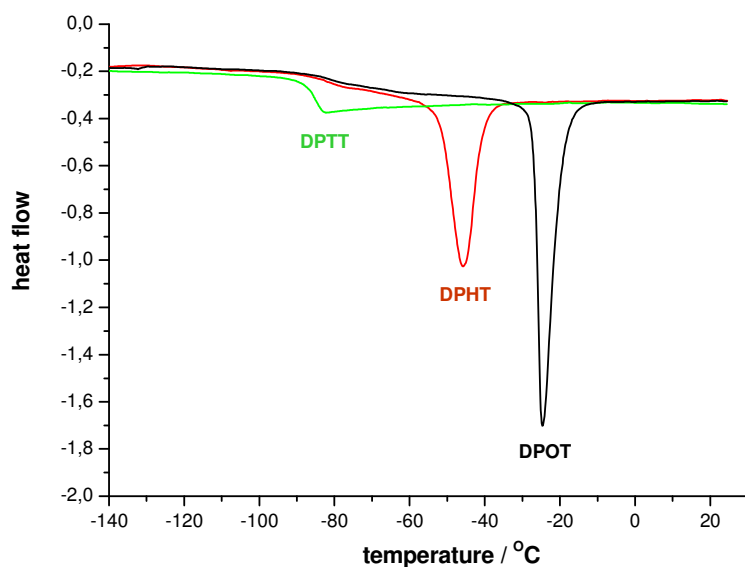


Figure 2.4. DSC graphs of DPTT, DPHT and DPOT

For instance, the precursor with OEG as a spacer unit has a  $T_g = -24.70^\circ\text{C}$ , with HEG it has a  $T_g = -45.79^\circ\text{C}$ , while this with TEG has a  $T_g$  below  $-80^\circ\text{C}$ . This data is comparable to  $T_g$  of phytanyl based lipids reported in the literature.<sup>28-30</sup> DPhyPC as a representative of phytanyl lipids, which does not have any ethylene oxide unit, shows a  $T_g$  below  $-40^\circ\text{C}$ .

Finally, the corresponding lipid precursor with double-bond functionalities is transformed

into a thiol via a thioacetate. This well-known reaction<sup>31,32</sup> leads to lipids with thiol anchor that can be used for tBLM formation on gold surfaces. The complete conversion of the double bond to the thioacetate in the first step is shown indirectly by disappearance of the multiplets in the  $^1\text{H}$  NMR and the signals at 135.5 and 116.8 ppm in the  $^{13}\text{C}$  NMR corresponding to the double bond functionality. Additionally, signals at 2.3 ppm in the  $^1\text{H}$  NMR and 28 ppm in the  $^{13}\text{C}$  NMR related to the methyl protons of the thioacetyl group appeared. The final step was performed in basic conditions to release the thiol group. The typical yields achieved were up to 78%. After column chromatography, the purity and the structure of DPTT, DPHT and DPOT were verified again by  $^1\text{H}$  NMR,  $^{13}\text{C}$  NMR and FD-MS.

The signals corresponding to the thioacetyl group disappeared in the  $^1\text{H}$  NMR and  $^{13}\text{C}$  NMR. A single peak in the FD-MS (Figure 2.5) with  $m/z = 1804.9$  (DPTT), 1981.6 (DPHT), 2156.9 (DPOT) corresponds to dithio-linked dimers of the lipids, which are formed through an oxidation process. The mechanism of thiol oxidation is well established<sup>32</sup>. Here it leads to a disulfide bridge formation and dimerization. It is well-known, that all thiols are in equilibrium with their dimers.

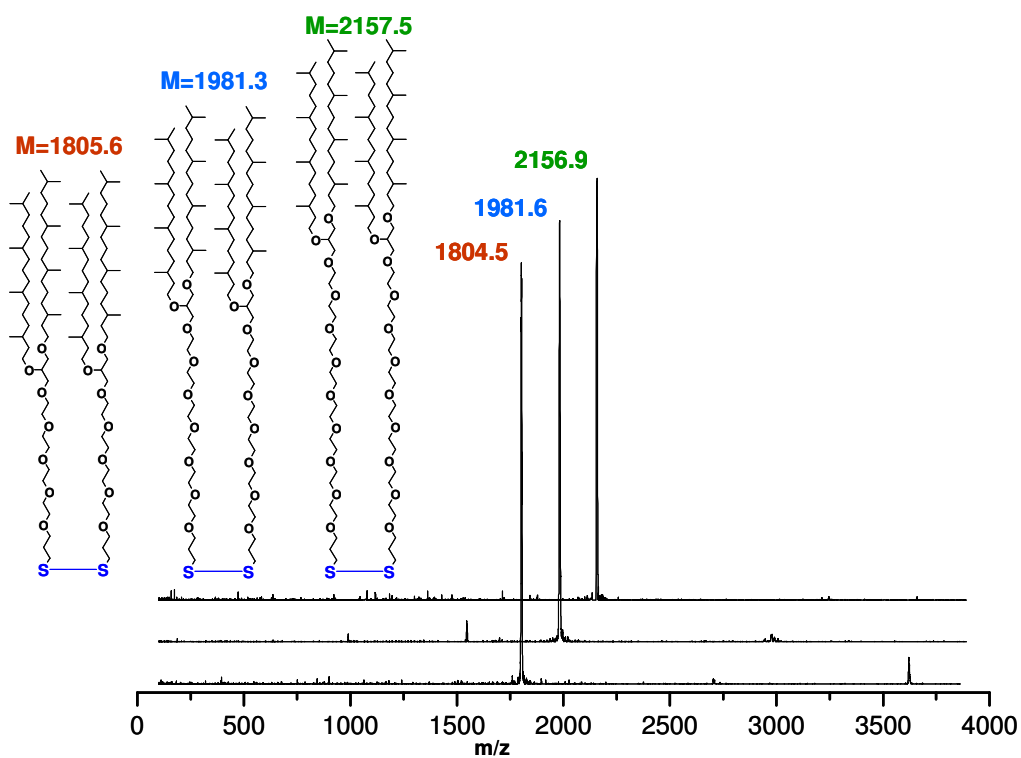


Figure 2.5. FD-MS spectra of DPTT, DPHT and DPOT

This equilibrium is mostly shifted to the disulfides, and thus, only signals of dimers can be observed. In order to prove that dimerization is due to the thiol coupling and not to any other side reaction, a reduction of the dimers was done by tris(2-carboxyethyl)phosphine hydrochloride,<sup>33,34</sup> and signals corresponding to monomers were observed by FD-MS.

However, these dimers are well soluble and surface active and do not influence monolayer homogeneity.<sup>35</sup> The alternatively used lipoic anchor<sup>11</sup> has shown some instability with time, probably due to polymerisation.

#### 2.2.4. Conclusion

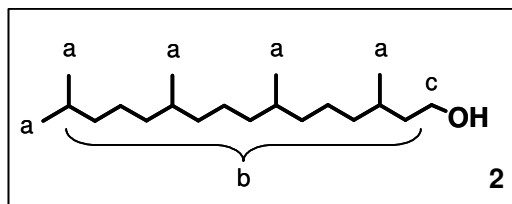
A new synthetic strategy for the preparation of tether lipids suitable for different substrates was established. This approach includes the synthesis of a “universal” lipid precursor with double bound functionality. This functional group serves as an adaptor, and using different synthetic procedures can be modified to the appropriate anchor. Since the goal in this work was the synthesis of thiolated lipids, a very simple and fast procedure was applied, and the lipid precursors were modified with a thiol group.

The synthetic route demonstrates another important advantage: the spacer part can be tuned varying the length of the ethylene glycol chains. Following this method, a series of three new thiolated lipids DPTT, DPHT and DPOT with TEG, HEG and OEG respectively in the spacer part were obtained with high yields up to 93%. The obtained lipids were isolated via column chromatography and characterized by TLC, <sup>1</sup>H NMR, <sup>13</sup>C NMR, FD-MS and ATR. Differential scanning calorimetry has shown T<sub>g</sub> values lower than -20 °C, which is a requirement for preparation of fluid membranes. FD-MS shows that DPTT, DPHT and DPOT exist as dimers; however, all lipids are well soluble and surface active.

### 2.2.5. Experimental part

#### Reaction a:

#### Hydrogenation of phytol



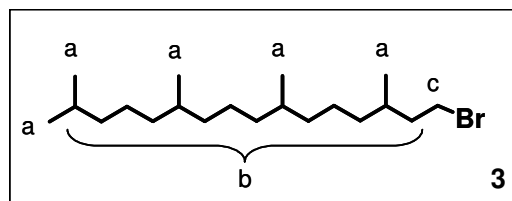
Phytol **1** (60 g, 0.2 mol, 296.54 g/mol) was introduced in a 350 ml autoclave. The catalyst PtO<sub>2</sub>/C (500 mg, 2.2 mmol, 227.08 g/mol) was added and the mixture was diluted with methanol (80 ml). The autoclave was evacuated, and was purged twice with H<sub>2</sub>, while a persistence pressure of 85 bars was maintained. The reaction mixture was stirred at 80°C for 7 days. The termination of the reaction was followed by <sup>1</sup>H NMR. The reaction mixture was filtered through a G4 glass-filter to remove the catalyst, and the filter residues were rinsed thoroughly with EtOH. The filtrates were collected, and the solvent was evaporated under reduced pressure. Phytanol **2** was obtained as colourless oil.

**Yield:** 59.71 g, (99%)

<sup>1</sup>H NMR (250 MHz, CDCl<sub>3</sub>, RT) δ<sub>H</sub>, ppm: 0.8 (t, 15H<sub>a</sub>), 0.9 - 2.0 (m, 24H<sub>b</sub>), 3.6 (m, 2H<sub>c</sub>)

#### Reaction b:

#### Conversion of hydroxide to bromide



Phytanol **2** (75 g, 0.25 mol, 298.56 g/mol) and triphenylphosphine (75.78 g, 0.29 mol, 262.3 g/mol) were introduced in a 2 neck round bottom flask, and were diluted with DCM (700 ml). The mixture was cooled to 0°C. Then N-bromosuccinimide (47.4 g, 0.27 mol, 177.99 g/mol) was added in small portions at 0°C. Finally, the reaction mixture was stirred at room temperature overnight. The reaction was monitored by TLC. After complete conversion of **2**, the reaction was stopped. The solvent was removed under vacuum. The solid residue was washed several times with hexane through G4 glass-filter to extract the product. The filtrates were collected, and the solvent was evaporated. Phytanyl bromide **3** was purified by column chromatography. Eluent: PE.

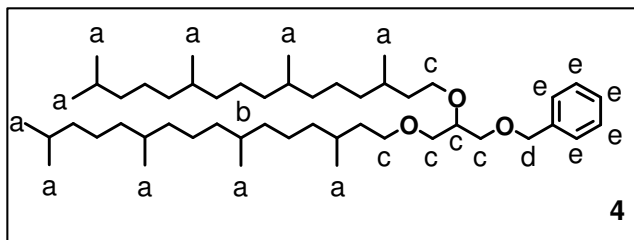
**Yield:** 55.69 g, (85%)

**TLC:** PE,  $R_f = 0.89$

**$^1\text{H NMR}$**  (250 MHz,  $\text{CDCl}_3$ , RT)  $\delta_{\text{H}}$ , ppm: 0.8 (t, 15 $\text{H}_a$ ), 0.9 - 2.0 (m, 24 $\text{H}_b$ ), 3.4 (m, 2 $\text{H}_c$ )

**Reaction c:**

**Synthesis of protected  
diphytanyl glycerol**



All glassware used in reactions **c**, **e**, **f** and **g** was dried and purged with Ar prior to use. NaH (5.15 g, 0.22 mol, 24 g/mol) was placed in a 2 neck round bottom flask. Dry THF (260 ml) was added which formed a suspension. Benzylglycerol (10.63 g, 0.06 mol, 182.21 g/mol) was added dropwise using a syringe at RT with vigorous stirring. The reaction mixture became gel-like, and was stirred overnight.

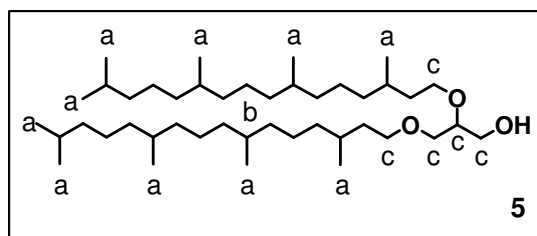
The mixture was transferred to a dropping funnel. Then, it was added dropwise to phytanyl bromide (63.25 g, 0.18 mol, 361.43 g/mol) placed in a 2 neck round bottom flask and dissolved in dry THF (45 ml). The reaction mixture was stirred for 10 days. The reaction was monitored by TLC. Additional amounts of NaH were added in order to keep the reaction conditions dry. After completion of the reaction, some drops of water were added to hydrolyse the remaining NaH.

The solid residue was precipitated by centrifugation (6000 rpm, 15 min) followed by washing with THF (repeated three times) to extract all THF soluble compounds. The solvent was evaporated under reduced pressure. The product **4** was purified by column chromatography. Eluents: PE to PE / THF gradually to 10/1.

**Yield:** 19.11 g, (44%)

**TLC:** CH/EtAc: 30/1,  $R_f = 0.71$

**$^1\text{H NMR}$**  (250 MHz,  $\text{CDCl}_3$ , RT)  $\delta_{\text{H}}$ , ppm: 0.8 (t, 30 $\text{H}_a$ ), 0.9 - 1.9 (m, 48 $\text{H}_b$ ), 3.6 (m, 9 $\text{H}_c$ ), 4.5 (s, 2 $\text{H}_d$ ), 7.3 (m, 5 $\text{H}_e$ )

**Reaction d:****Cleavage of the benzyl group**

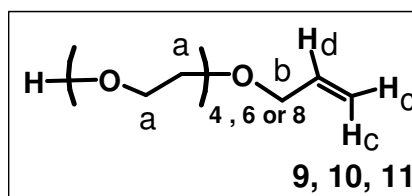
The protected diphytanyl glycerol **4** (7 g, 9.42 mmol, 743.30 g/mol) was dissolved in a mixture of CH<sub>3</sub>OH/THF (50/20 ml) in a 2 neck round bottom flask, and spatula full of catalyst Pd/C was added. The reaction mixture was fed with a stream of hydrogen. The reaction was followed by TLC. After 24 h, the reaction was stopped, and the mixture was centrifuged (6000 rpm, 15 min), followed by washing of the solid residue with THF (repeated three times). The solvent was evaporated under reduced pressure giving colourless oil. Diphytanyl glycerol **5** was purified by flash chromatography. Eluents: CH/EtAc (30/1)

**Yield:** 4.54 g, (74%)

**TLC:** PE/THF (3/1), R<sub>f</sub> = 0.47

**<sup>1</sup>H NMR** (250 MHz, CDCl<sub>3</sub>, RT) δ<sub>H</sub>, ppm: 0.8 (t, 30H<sub>a</sub>), 0.9 - 1.7 (m, 48H<sub>b</sub>), 3.4 - 3.8 (m, 9H<sub>c</sub>)

**FD-MS** (m/z): 653.1 (M<sup>+</sup>), calculated (C<sub>43</sub>H<sub>88</sub>O<sub>3</sub>) = 653.18; 1305.6 (M+M<sup>+</sup>), calculated (2 x C<sub>43</sub>H<sub>88</sub>O<sub>3</sub>) = 1306.36; 1959.0 (2M+M<sup>+</sup>), calculated (3 x C<sub>43</sub>H<sub>88</sub>O<sub>3</sub>) = 1959.54

**Reaction e:****Functionalization of ethylene glycols**

TEG **6** (12.07 g, 62.1 mmol, 194.23 g/mol), HEG **7** (11.97 g, 42.40 mmol, 282.34 g/mol) or OEG **8** (1 g, 2.69 mmol, 370.44 g/mol) was dissolved in dry THF (20 ml, 100 ml, and 20 ml, respectively). NaH (2.12 g, 88.3 mmol; 1.21 g, 50.42 mmol; and 0.1 g, 4.05 mmol respectively) was added portionwise to the solution. The reaction mixture was stirred at RT for 2 hrs. Then, allylbromide (3.21 g, 26.5 mmol; 3.42 g, 0.028 mmol; and 0.33 g, 2.69 mmol, 120.98 g/mol, respectively) was added dropwise. The temperature was increased to 40 °C, and the reaction was monitored by TLC. After 3 days, the reaction was stopped, and the mixture was centrifuged (6000 rpm, 15 min) followed by washing of the solid residue with THF (repeated three times). The solvent was evaporated under

reduced pressure. The products **9**, **10** and **11** were purified by flash chromatography. Eluents: **9** EtAc gradually to EtAc/Ac (2/1), **10** THF/PE (1/1 gradually to 2.5/1), and **11**: THF/PE (2/1 gradually to 4/1), respectively.

**Yield: 9:** 3.79 g, (61%), **10:** 6.36 g, (50%), **11:** 580 mg, (52%)

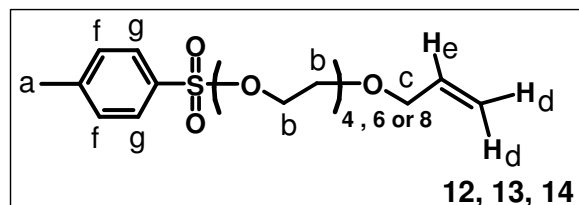
**TLC: 9** EtAc/Ac (2.5/1),  $R_f = 0.54$ ; **10** PE/THF (1/1),  $R_f = 0.19$ ; **11** PE/THF (1/2),

$R_f = 0.32$

**$^1\text{H NMR}$**  (250 MHz,  $\text{CDCl}_3$ , RT)  $\delta_{\text{H}}$ , ppm: 3.5 - 3.75 (m, **9:** 16 $\text{H}_a$ , **10:** 24 $\text{H}_a$ , **11:** 32 $\text{H}_a$ ), 4.0 (d, 2 $\text{H}_b$ ), 5.1 - 5.3 (m, 2 $\text{H}_c$ ), 5.85 - 5.95 (m, 1 $\text{H}_d$ )

**Reaction f:**

**Tosylation of ethylene glycols**



**9** (3.79 g, 16.1 mmol, 234.29 g/mol), **10** (3 g, 9.30 mmol, 322.4 g/mol), or **11**

(580 mg, 1.41 mmol, 410.51 g/mol) was added dropwise at RT in a 2 neck round bottom flask containing a suspension of NaH (0.57 g, 24.15 mmol; 0.33 g, 13.95 mmol and 0.05 g, 2.12 mmol, 24 g/mol, respectively) in THF (10 ml, 20 ml and 12 ml, respectively). The mixture was stirred overnight at RT. The corresponding alkoxide was then transferred in a dropping funnel, and was added dropwise to solution of tosyl chloride (6.14 g, 32.2 mmol; 3.55 g, 18.6 mmol, and 539 mg, 2.83 mmol, respectively) and TEA (1 eq) in dry THF (10 ml, 30 ml, and 9 ml, respectively). The reaction was followed by TLC. After 3 days the reaction was stopped, and the mixture was centrifuged (6000 rpm, 15 min) followed by washing of the solid residue with THF (repeated three times). The solvent was evaporated under reduced pressure. The products **12**, **13** and **14** were purified by flash chromatography. Eluents: **12** CH/EtAc (10/1 gradually to 2/1), **13** PE/THF (4/1 gradually to 1/1), and **14** DCM/Ac (10/1 gradually to 1/1).

**Yield: 12:** 4.32 g, (69%), **13:** 3.66 g, (83%), **14:** 560 mg, (70%)

**TLC: 12** CH/EtAc (1/1),  $R_f = 0.42$ ; **13** PE/THF (1/1),  $R_f = 0.54$ ; **14** PE/THF (1/2),

$R_f = 0.66$

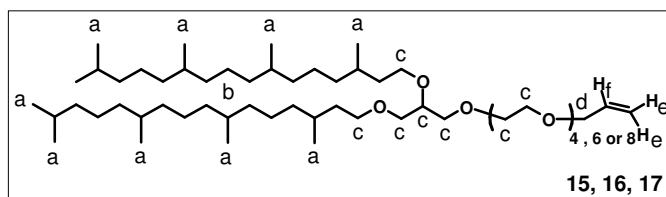
**$^1\text{H NMR}$**  (250 MHz,  $\text{CDCl}_3$ , RT)  $\delta_{\text{H}}$ , ppm: 2.4 (s, 3 $\text{H}_a$ ), 3.5 - 3.7 (m, **12:** 16 $\text{H}_b$ , **13:** 24 $\text{H}_b$ , **14:** 32 $\text{H}_b$ ), 4.0 (d, 2 $\text{H}_c$ ), 4.1 (t,  $-\text{CH}_2\text{O-Tos}$ ), 5.1 - 5.3 (m, 2 $\text{H}_d$ ), 5.8 - 6.0 (m, 1 $\text{H}_e$ ), 7.3 (d,

2H<sub>f</sub>), 7.8 (d, 2H<sub>g</sub>)

**FD-MS** (m/z): **14**: 587.1 (M + Na<sup>+</sup>), calculated (C<sub>26</sub>H<sub>44</sub>O<sub>11</sub>S + Na) = 587.7

**Reaction g:**

**Preparation of universal lipid precursors**



DPG **5** (8.74 g, 13.38 mmol; 4.83 g, 7.40 mmol, and 0.78 g, 1.19 mmol for preparation of **15**, **16** and **17**, respectively) dissolved in dry THF (30 ml, 30 ml and 12 ml, respectively) was placed in a 2 neck round bottom flask supplied with a dropping funnel. NaH (0.64 g, 26.8 mmol; 0.36 g, 14.8 mmol, and 48 mg, 1.98 mmol, respectively) was added in small portions at RT. After several hours, **12** (5.2 g, 13.38 mmol, 388.48 g/mol), **13** (3.53 g, 7.40 mmol, 476.59 g/mol) or **14** (560 mg, 0.99 mmol, 564.66 g/mol) diluted with THF (30 ml, 30 ml, and 10 ml, respectively) was added dropwise with a dropping funnel at 40°C. The reaction mixture was stirred at 40°C for 2, 4 and 1 days, respectively. The reaction was monitored by TLC of aliquots taken from the reaction mixture. After the completion of reaction, the mixture was centrifuged (6000 rpm, 15 min) followed by washing of the solid residue with THF (repeated three times). The solvent was evaporated. The products **15**, **16** and **17** were purified by flash chromatography. Eluents: **15** PE/THF (6/1 gradually to 4/1), **16** PE/THF (5/1 gradually to 3/1), and **17** DCM/Ac (10/1 gradually to 1/1).

**Yield: 15:** 9.89 g, (85%), **16:** 5.98 g, (85%), **17:** 960 mg, (93%)

**TLC:** **15** PE/THF (4/1), R<sub>f</sub> = 0.61; **16** PE/THF (3/1), R<sub>f</sub> = 0.56; **17** DCM/Ac (5/1),

R<sub>f</sub> = 0.46

**<sup>1</sup>H NMR** (250 MHz, CDCl<sub>3</sub>, RT) δ<sub>H</sub>, ppm: 0.8 (t, 30H<sub>a</sub>), 0.9 - 1.9 (m, 48H<sub>b</sub>), 3.35 - 3.8

(m, **15:** 25H<sub>c</sub>, **16:** 33H<sub>c</sub>, **17:** 41H<sub>c</sub>), 4.0 (d, 2H<sub>d</sub>), 5.1 - 5.3 (m, 2H<sub>e</sub>), 5.8 - 6.0 (m, 1H<sub>f</sub>)

**<sup>13</sup>C NMR:** (CD<sub>2</sub>Cl<sub>2</sub>) δ<sub>C</sub>, ppm: 135.5, 116.8, 78.4, 72.4, 71.7, 71.2, 70.9, 70.2, 70.0, 69.0, 39.8, 37.8, 37.2, 33.2 30.3, 28.4, 25.2, 24.8, 22.9, 22.8 and 19.9

**FD-MS** (m/z): **15:** 869.3 (M<sup>+</sup>), calculated (C<sub>54</sub>H<sub>108</sub>O<sub>7</sub>) = 869.46, 1738.5 (M + M<sup>+</sup>),

calculated (2 × C<sub>54</sub>H<sub>108</sub>O<sub>7</sub>) = 1738.9, **16:** 957.4 (M<sup>+</sup>), calculated (C<sub>58</sub>H<sub>116</sub>O<sub>9</sub>) = 957.6,

1915.8 (M + M<sup>+</sup>), calculated (2 × C<sub>58</sub>H<sub>116</sub>O<sub>9</sub>) = 1915.2, **17:** 1068.5 (M + Na<sup>+</sup>), calculated

(C<sub>62</sub>H<sub>124</sub>O<sub>11</sub> + Na<sup>+</sup>) = 1068.7; 2090.9 (M + M<sup>+</sup>), calculated (2 × C<sub>62</sub>H<sub>124</sub>O<sub>11</sub>) = 2091.3

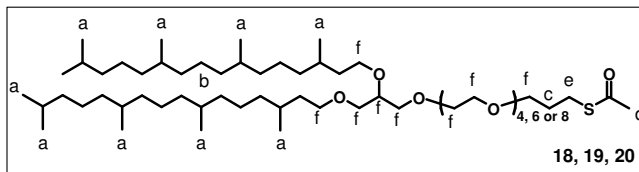
**ATR** (cm<sup>-1</sup>): 2952, 2925, 2868, 1462, 1377, 1300, 1250, 1107, 1043, 995, 992, 879, 735



**TGA/DSC: 15:**  $T_g < -80^\circ\text{C}$ ; **16:** Decomposition interval  $130 - 570^\circ\text{C}$  (99.32%) with maximum rate of degradation at  $390^\circ\text{C}$ .  $T_g = -45.79^\circ\text{C}$ ; **17:** Decomposition interval  $155 - 820^\circ\text{C}$  (101.80%) with maximum rate of degradation at  $385^\circ\text{C}$ .  $T_g = -24.70^\circ\text{C}$

**Reaction h:**

**Functionalization of the lipid precursor (first step)**



Product **15** (1.85 g, 2.14 mmol, 869.46 g/mol), **16** (1 g, 1.04 mmol, 957.57 g/mol) or **17** (0.3 g, 0.29 mmol, 1045.67 g/mol) was introduced in a Schlenk flask tube and dissolved in toluene (5.6 ml, 3 ml and 1.5 ml, respectively). Thioacetic acid (2 g, 26.3 mmol; 3 g, 39.48 mmol, and 0.71 g, 9.34 mmol, 76 g/mol, respectively) and the catalyst AIBN (7 mg, 42.6  $\mu\text{mol}$ ; 6.6 mg, 40.1  $\mu\text{mol}$  and 1.4 mg, 8.5  $\mu\text{mol}$ , 164.21 g/mol, respectively) was added. The reaction mixture was degassed 3 times. The reaction mixture was stirred at  $70^\circ\text{C}$  for 24 h. The completion of the reaction was checked by TLC. The solvent was evaporated. The products **18**, **19** and **20** were purified by flash chromatography. Eluents: **18** PE/THF (6/1), **19** DCM/Ac (10/1 gradually to 5/1), and **20** DCM/Ac (10/1 gradually to 1/1).

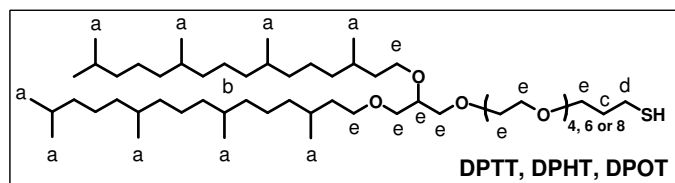
**Yield: 18:** 1.53 g, (76%), **19:** 1 g, (93%), **20:** 240 mg, (75%)

**TLC: 18** PE/THF (6/1),  $R_f = 0.39$ ; **19** DCM/Ac (10/1),  $R_f = 0.38$ ; **20** DCM/Ac (5/1),  $R_f = 0.50$

**$^1\text{H NMR}$**  (250 MHz,  $\text{CDCl}_3$ , RT)  $\delta_{\text{H}}$ , ppm: 0.8 (t, 30 $H_a$ ), 0.9 - 1.7 (m, 48 $H_b$ ), 1.8 (p, 2 $H_c$ ), 2.3 (s, 3 $H_d$ ), 2.9 (t, 2 $H_e$ ), 3.35 - 3.8 (m, **18:** 27 $H_f$ , **19:** 35 $H_f$ , **20:** 43 $H_f$ )

**FD-MS** (m/z): **18:** 945.4 ( $M^+$ ), calculated ( $\text{C}_{56}\text{H}_{112}\text{O}_8\text{S}$ ) = 945.58, **19:** 1035.0 ( $M^+$ ), calculated ( $\text{C}_{60}\text{H}_{120}\text{O}_{10}\text{S}$ ) = 1033.68, **20:** 1123.0 ( $M^+$ ), calculated ( $\text{C}_{64}\text{H}_{128}\text{O}_{12}\text{S}$ ) = 1121.79; 2243.0 ( $M + M^+$ ), calculated ( $2 \times \text{C}_{64}\text{H}_{128}\text{O}_{12}\text{S}$ ) = 2243.58

**Reaction i:**  
**Functionalization of the**  
**lipid precursor (second step)**



The corresponding thioacetate **18** (1.53 g, 1.62 mmol, 945.58 g/mol), **19** (390 mg, 0.38 mmol, 1033.68 g/mol), and **20** (240 mg, 0.21 mmol, 1121.79) was introduced in a round bottom flask and dissolved in THF (40 ml, 10 ml and 5 ml, respectively).

1 M NaOH (6.3 ml, 1.6 ml, and 0.83 ml, 40 g/mol, respectively) was added. The heterogeneous mixture was stirred vigorously at 50 °C overnight. Completion of the reaction was observed by TLC. After the termination of the reaction, 1 M H<sub>2</sub>SO<sub>4</sub> (16 ml, 4 ml, and 2 ml, respectively) was added and stirred for 5 min to neutralize the reaction mixture. Then, all solvents were removed under vacuum. The obtained oil was dissolved in DCM and washed twice with 1 M H<sub>2</sub>SO<sub>4</sub>, and sat. Na<sub>2</sub>CO<sub>3</sub> respectively. The organic layers were collected and dried over Na<sub>2</sub>SO<sub>4</sub>. After filtration, the solvent was removed under vacuum. The products were purified by column chromatography. Eluents: **DPTT** PE/THF (6/1 gradually to 3/1), **DPHT** DCM/Ac (5/1 gradually to 3/1), and **DPOT** DCM/Ac (7/1 gradually to 1/1).

**Yield: DPTT:** 980 mg, (67%), **DPHT:** 290 mg, (78%), **DPOT:** 130 mg, (56%)

**TLC: DPTT** PE/THF (4/1), R<sub>f</sub> = 0.40; **DPHT** PE/THF (3/1), R<sub>f</sub> = 0.28; **DPOT** DCM/Ac (5/1), R<sub>f</sub> = 0.42

**<sup>1</sup>H NMR** (250 MHz, CDCl<sub>3</sub>, RT) δ<sub>H</sub>, ppm: 0.8 (t, 30H<sub>a</sub>), 0.9 - 1.8 (m, 48H<sub>b</sub>), 1.9 (p, 2H<sub>c</sub>), 2.7 (t, 2H<sub>d</sub>), 3.35 - 3.8 (m, **DPTT:** 27H<sub>e</sub>, **DPHT:** 35H<sub>e</sub>, **DPOT:** 43H<sub>e</sub>)

**<sup>13</sup>C NMR:** (CD<sub>2</sub>Cl<sub>2</sub>) δ<sub>C</sub>, ppm: 78.4, 71.7, 71.2, 70.9, 70.6, 70.2, 69.6, 69.0, 68.1, 39.7, 37.8, 37.1, 35.8, 33.2, 30.5, 30.3, 29.7, 28.4, 26.0, 25.1, 24.8, 24.7, 22.8, 22.7, 19.8

**FD-MS** (m/z): **DPTT:** 1804.9 (M + M<sup>+</sup>), calculated (2 x C<sub>54</sub>H<sub>109</sub>O<sub>7</sub>S) = 1805.6, **DPHT:** 1981.6 (M + M<sup>+</sup>), calculated (2 x C<sub>58</sub>H<sub>117</sub>O<sub>9</sub>S) = 1981.3, **DPOT:** 2156.9 (M + M<sup>+</sup>), calculated (2 x C<sub>62</sub>H<sub>125</sub>O<sub>11</sub>S) = 2157.5

**ATR** (cm<sup>-1</sup>): br 2952, 2925, 2865, s 1462, s 1377, s 1292, s 1248, s 1111, s 1070, s 916, s 860, s 737

## 2.3. Synthesis of a lipid with an even longer tethering part

### 2.3.1. Introduction and motivation

Recently, the investigation of protein functions and interactions within the cell membrane has been studied extensively.<sup>10,15,36-38</sup> Membrane proteins play an essential role in mediating the cell processes. However, their principle of function is not fully understood. Therefore, the need of reliable biomimetic environment makes tBLMs a promising candidate as a stable and suitable platform for this study.

As it was described in section 2.2, the lipids in tBLMs are tethered to the substrate via polar spacer increasing the hydrophilic region beneath the membrane. The existence of such hydrophilic region is important for successful incorporation of large trans-spanning membrane proteins with large submembrane units. In general, longer linkers beneath the membrane exclude protein-surface interactions, provides a solvent compartment adjacent to the solid surface that may accommodate solvent-exposed proteins domains. Additionally, increasing the linker length increases both the lateral space between the tether lipids and the fluidity of the membrane.

Many strategies to obtain spacers with different lengths have been investigated. Most of them are based on ethylene glycol chains as a spacer. McGillivray *et al.*<sup>39</sup> have recently reported on tBLMs consisted of lipids containing thiolated hexaethylene oxide spacer. However, neutron reflectometry (NR) measurements have shown that these membranes do not contain a solvent reservoir. Recently, in our group (see section 2.2), a family of thiolipids (analogs of DPTL) with longer spacers have been obtained by C. Breffa.<sup>23</sup> The NR local structure investigation of octaethylene glycol spacer lipid has also shown unexpected low content of water.<sup>40</sup> However, the usage of longer well-defined spacer molecules has demonstrated formation of tBLMs with reproducible electrical properties comparable with those of the biological membranes.<sup>8,17,41,42</sup>

Another approach consists of inclusion of polymer cushion between the substrate and the bilayer. The utility of using such cushion is to provide a soft, deformable layer with high degree of mobility. The authors have employed telechelic PEG chains functionalized with anchors for SiO<sub>2</sub><sup>22</sup> and gold surface.<sup>43</sup>

The aim in the present study is to find a proper synthetic strategy for preparation of thiolated lipid with longer (n=18) ethylene glycol chain. In a former study<sup>23</sup> it was verified

that the use of oligoethylene glycol spacers obtained by anionic polymerization has resulted in tBLMs with low quality. The latter can be attributed to the polydispersity of the oligoethylene glycols in the spacer part. Thus, the synthesis of monodispersed compound achieved by well-defined chemistry is the main advantage of the method used in the current study and is crucial for preparation of smooth monolayers.

The approach towards the synthesis of the aimed lipid precursor is shown in Figure 2.5.

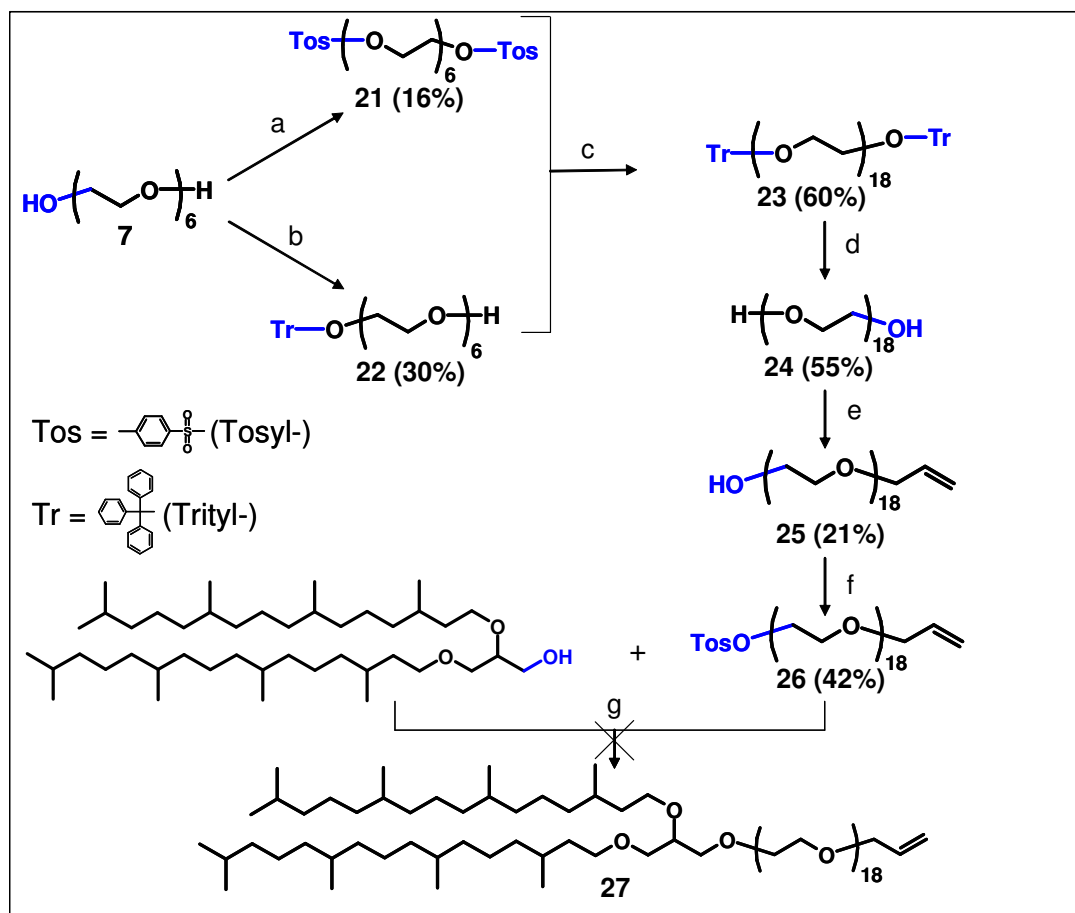


Figure 2.5. Synthesis of lipid precursor with longer tethering spacer unit (octadecaethylene glycol)

### 2.3.2. Results and discussion

The synthesis includes two main steps: synthesis of well-defined double bond functionalized octadecaethylene glycol (ODEG) as a tethering part and its coupling to the hydrophobic part (DPG) forming the lipid precursor.

HEG was chosen as an initial compound. It underwent two different reactions. Firstly, a certain amount of ethylene glycol was modified from both sides with *p*-toluenesulfonyl chloride. The product of this reaction was obtained in a very low yield may be due to the hygroscopic properties of HEG and inactivation of the catalyst. Secondly, another HEG was monoprotected with triphenylmethyl (trityl) chloride. This protecting group has been chosen due to its UV activity and ease of cleavage. Additionally, trityl group provides significant hydrophobicity that helps for isolation of the very hydrophilic ODEG chain by FC.

The next step was a nucleophilic substitution reaction between the monoprotected HEG (**22**) and tosylated HEG (**21**) in molar ratio 2:1 to obtain protected octadecaethylene glycol (**23**) on both sides. After completion of the reaction, the crude product was purified by flash chromatography. It was established that the product **23** is partially deprotected already in the chromatographic column. This was supported by the FD-mass spectrum where signals corresponding to the main product (both sides protected **23**), the monoprotected and completely deprotected ODEG were observed.

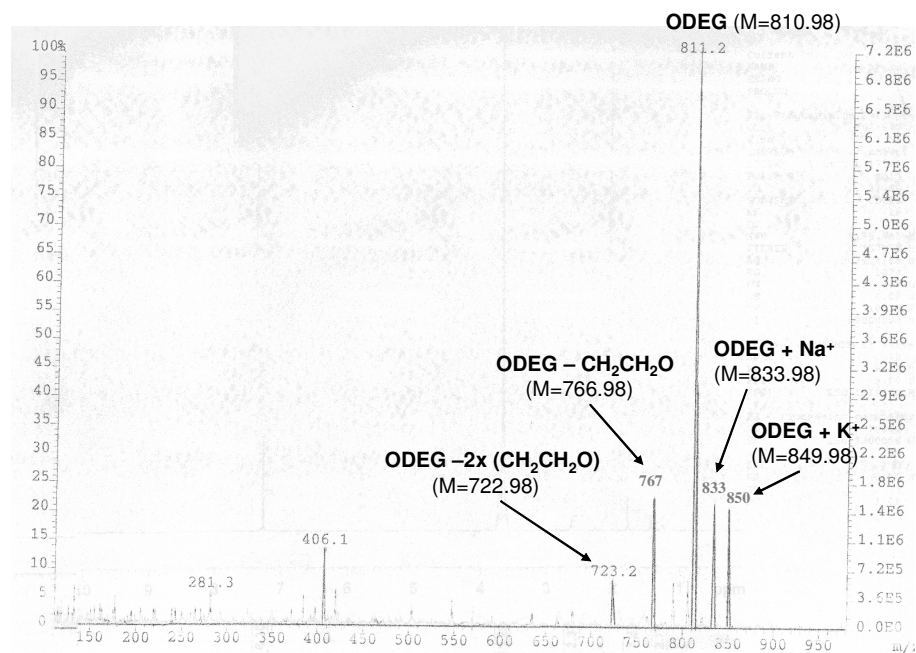


Figure 2.6. FD-mass spectrum of ODEG (**24**)

The trityl groups were successfully cleaved, but the mass spectrum of ODEG (Figure 2.6) revealed defragmentation of the main compound. Then, ODEG was consecutive functionalized with a double bond from one side (**25**) and with a tosyl group from the other (**26**) (see reaction **f** in 2.2.5).

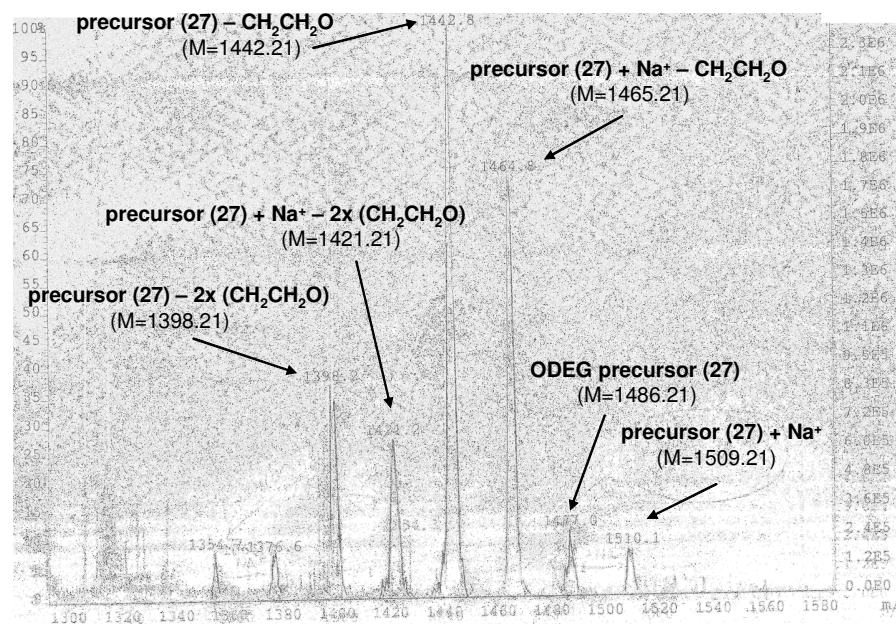


Figure 2.7. FD-mass spectrum of ODEG precursor (**27**)

Unfortunately, the yields of both last steps (reactions **e**, **f**) were low (20 – 40%) due to significant material loss by chromatography of polar substances such as monoprotected and completely deprotected ODEG. Thus, **26** was isolated in an insignificant amount of 50 mg. Therefore, the final step (introduction of the lipid part, reaction **g**) failed and only few milligrams of the final lipid precursor (**27**) were isolated. Due to the previously occurred defragmentation of ODEG, precursor products with shorter ethylene glycol chains are detected by FD-MS (Figure 2.7).

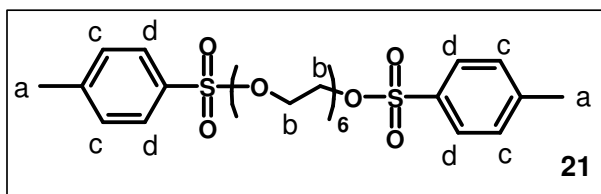
### 2.3.3. Conclusion

The synthesis of tether lipid precursor with ODEG in the spacer part was investigated. Following a multiple step procedure, ODEG was synthesized starting from HEG. It was further functionalized with double bond suitable for preparation of both thiols and silanes. However, mainly due to purification and detection problems, the products were obtained in very low yields. Thus, the last coupling reaction between the hydrophobic and the hydrophilic moiety was not efficient.

As an outlook, changes in the synthetic strategy like coupling with the hydrophobic part from the beginning could improve the yield. This strategy would help by TLC detection, because the phytanyl chains are well visible after treatment with resorcin based developer. Moreover, they would lower the polarity of the product, and thus accelerate the movement through the column.

### 2.3.4. Experimental part

#### Reaction a: Tosylation of HEG



The glassware used in reactions **a**, **b**, **c**, **e** and **f** was dried and purged with Ar prior to use.

HEG **7** (3 g, 10.6 mmol, 282.33 g/mol) dissolved in THF (40 ml) was introduced in a 2 neck round bottom flask. NaH (0.77 g, 32.08 mmol, 24 g/mol) was added in small portions and the mixture was stirred overnight at RT. Then, tosyl chloride (8.1 g, 42.5 mmol, 190.6 g/mol) was added dropwise to the reaction mixture. The reaction was

monitored by TLC of aliquots taken from the reaction mixture. After 3 days, the reaction was stopped, and the mixture was centrifuged (6000 rpm, 15 min). The solid residue was resuspended in THF and centrifuged again. This procedure was repeated three times. The organic phases were combined and the solvent was evaporated under vacuum. The residue was purified by flash chromatography to afford product **21**. Eluents: PE/THF (3/1 gradually to 1/2.5).

**Yield:** 1 g, (16%)

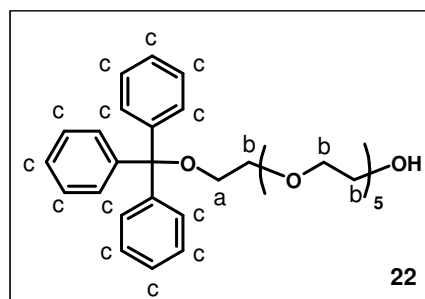
**TLC:** PE/THF (1/1),  $R_f = 0.38$

**$^1\text{H NMR}$**  (250 MHz,  $\text{CDCl}_3$ , RT)  $\delta_{\text{H}}$ , ppm: 2.4 (s, 6 $\text{H}_a$ ), 3.5 - 3.8 (m, 24 $\text{H}_b$ ), 4.1 (t, 4- $\text{CH}_2\text{OTos}$ ), 7.3 (d, 4 $\text{H}_c$ ), 7.7 (d, 4 $\text{H}_d$ )

**FD-MS** (m/z): (100%) 589.3 ( $\text{M}^+$ ), calculated ( $\text{C}_{26}\text{H}_{38}\text{O}_{11}\text{S}_2$ ) = 590.71

**Reaction b:**

**Asymmetric protection of HEG**



NaH (1.1 g, 45.8 mmol, 24 g/mol) was placed in a 2 neck round bottom flask. Dry THF (30 ml) was added forming a suspension. By vigorous stirring, HEG **7** (6.98 g, 24.72 mmol, 282.33 g/mol) dissolved in dry THF (20 ml) was added dropwise using a syringe at RT. The reaction mixture was stirred overnight. Triphenylmethyl chloride (6.41 g, 22.99 mmol, 278.78 g/mol) was dissolved in dry THF (50 ml) and transferred in dropping funnel. Then, it was added dropwise to the reaction mixture at 40°C. The reaction mixture was stirred for 3 days, while the reaction was monitored by TLC. Additional amounts of NaH were added in order to keep the reaction conditions dry. After completion of the reaction, some drops of water were added to quench the excess NaH. The solid residue was precipitated by centrifugation (6000 rpm, 15 min). The solid residue was resuspended in THF and centrifuged again. This procedure was repeated three times. The organic phases were combined and the solvent was evaporated under vacuum. The residue was purified by column chromatography to afford product **22**. Eluents: THF/PE (1/1 gradually to 3/1).

**Yield:** 3.8 g, (30%)

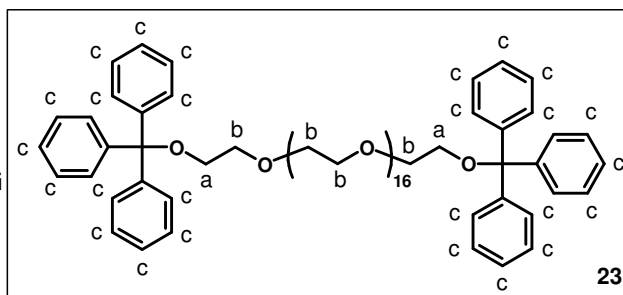


**TLC:** PE/THF (1/1),  $R_f = 0.19$

**$^1\text{H NMR}$**  (250 MHz,  $\text{CDCl}_3$ , RT)  $\delta_{\text{H}}$ , ppm: 3.2 (t,  $2\text{H}_a$ ) 3.5 - 3.8 (m,  $22\text{H}_b$ ), 7.1 - 7.55 (m,  $15\text{H}_c$ )

**Reaction c:**

**Synthesis of doubly protected ODEG**



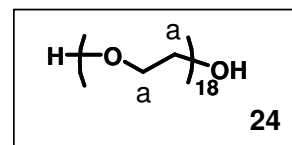
Product **22** (1.95 g, 3.72 mmol, 524.66 g/mol) dissolved in dry THF (30 ml) was placed in a 2 neck round bottom flask. NaH (0.12 g, 6.67 mmol, 24 g/mol) was added with vigorous stirring at RT. The reaction mixture turned dark green and stirred for 6 hrs at RT. Product **21** (1 g, 1.69 mmol, 590.71 g/mol) was dissolved in dry THF (20 ml) and transferred in a dropping funnel. It was added dropwise to the reaction mixture and stirred overnight. The colour turned to dark red. The reaction was monitored by TLC. Additional amounts of NaH (0.16 g) were added. After completion of the reaction, some drops of water were added to quench NaH. The solid residue was precipitated by centrifugation (6000 rpm, 15 min). The solid residue was resuspended in THF and centrifuged again. This procedure was repeated three times. The organic phases were combined and the solvent was evaporated under vacuum. The residue was purified by flash chromatography to afford product **23**. Eluents: THF/PE (1/1 gradually to 3.5/1).

**Yield:** 1.33 g, (60%)

**TLC:** THF/PE (2/1),  $R_f = 0.37$

**$^1\text{H NMR}$**  (250 MHz,  $\text{CDCl}_3$ , RT)  $\delta_{\text{H}}$ , ppm: 3.5 (t,  $4\text{H}_a$ ), 3.8 - 4.15 (m,  $68\text{H}_b$ ), 7.4 - 7.8 (m,  $30\text{H}_c$ )

**FD-MS** (m/z): (100%) 810.9 ( $\text{M}^+$ ), calculated (**24**:  $\text{C}_{36}\text{H}_{74}\text{O}_{19}$ ) = 810.98, (80%) 1295.9 ( $\text{M}^+$ ), calculated (**23**:  $\text{C}_{74}\text{H}_{102}\text{O}_{19}$ ) = 1295.63, (75%) 1075.7 ( $\text{M}^+ + \text{Na}$ ), calculated (**MonoTrODEG**:  $\text{C}_{55}\text{H}_{88}\text{O}_{19} + \text{Na}$ ) = 1076.3

**Reaction d:****Deprotection of ODEG**

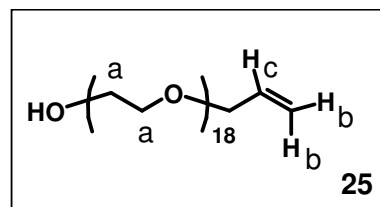
Product **23** (1.3 g, 1 mmol, 1295.63) and finely powdered zinc bromide (2.25 g, 10 mmol, 225.19 g/mol) were dissolved in DCM (2 ml) in a round bottom flask. The reaction mixture was stirred for 2 hrs at RT. The deprotection was monitored by TLC. After the reaction was completed, the mixture was washed thrice with sat. NaHCO<sub>3</sub>. NaHCO<sub>3</sub> fraction was thoroughly washed several times with small amounts of DCM. The DCM layers were collected and dried over MgSO<sub>4</sub>. After filtration, the organic solvent was evaporated. Thus, the initially obtained oil was crystallized. Octadecaethylene glycol (**24**) was used without further purification.

**Yield:** 450 mg, (55%)

**TLC:** THF/PE (2/1), R<sub>f</sub> = 0.37

**<sup>1</sup>H NMR** (250 MHz, CDCl<sub>3</sub>, RT) δ<sub>H</sub>, ppm: 3.8 - 4.15 (m, 72H<sub>a</sub>)

**FD-MS** (m/z) (100%) 811.2 (M<sup>+</sup>), calculated (**24**: C<sub>36</sub>H<sub>74</sub>O<sub>19</sub>) = 810.98

**Reaction e:****Allyl functionalization of ODEG**

Product **24** (450 mg, 0.56 mmol, 810.98 g/mol) dissolved in dry THF (20 ml) was introduced in a 2 neck round bottom flask. NaH (0.02 g, 0.83 mmol, 24 g/mol) was added and the reaction mixture was stirred for 2 hrs at RT.

Allyl bromide (0.08 g, 0.56 mmol, 120.98 g/mol) dissolved in dry THF (13 ml) was added dropwise through dropping funnel to the reaction mixture. The mixture was stirred overnight at 40 °C. The reaction was monitored by TLC. After 3 days, the reaction was stopped. The solid residue was precipitated by centrifugation (6000 rpm, 15 min). The solid residue was resuspended in THF and centrifuged again. This procedure was repeated three times. The organic phases were combined and the solvent was evaporated under vacuum. The residue was purified by column chromatography to afford product **25**. Eluent: THF.

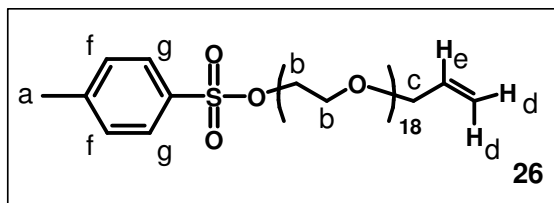
**Yield:** 100 mg, (21%)

**TLC:** THF,  $R_f = 0.38$

**$^1\text{H NMR}$**  (250 MHz,  $\text{CDCl}_3$ , RT)  $\delta_{\text{H}}$ , ppm: 3.4 - 4.15 (m, 72 $H_a$ ), 5.1 - 5.3 (m, 2 $H_b$ ), 5.8 - 5.95 (m, 1 $H_c$ )

**FD-MS** (m/z): (100%) 851.3 ( $M^+$ ), calculated (**25**:  $\text{C}_{39}\text{H}_{78}\text{O}_{19}$ ) = 851.05, (70%) 873.6 ( $M + \text{Na}^+$ ), calculated (**25**:  $\text{C}_{39}\text{H}_{78}\text{O}_{19} + \text{Na}$ ) = 874.05, (48%) 807.0 ( $M^+ - \text{CH}_2\text{CH}_2\text{O}$ ), calculated (**25**:  $\text{C}_{39}\text{H}_{78}\text{O}_{19} - \text{CH}_2\text{CH}_2\text{O}$ ) = 807.05

**Reaction f:**  
**Tosylation of 25**



Product **25** (100 mg, 0.12 mmol, 851.05 g/mol) dissolved in dry THF (3 ml) was introduced in a 2 neck round bottom flask. NaH (4 mg, 0.18 mmol, 24 g/mol) was added and the reaction mixture was stirred for 2 hrs at RT. TEA (20  $\mu\text{l}$ , 0.12 mmol, 101.2 g/mol) was added to the mixture, and tosyl chloride (45 mg, 0.24 mmol, 190.6 g/mol) dissolved in dry THF (3 ml) was added dropwise. The reaction was monitored by TLC. Additional amounts of NaH and tosyl chloride were added. After 5 days, the reaction was stopped. The solid residue was precipitated by centrifugation (6000 rpm, 15 min). The solid residue was resuspended in THF and centrifuged again. This procedure was repeated three times. The organic phases were combined and the solvent was evaporated under vacuum. The residue was purified by flash chromatography to afford product **26**. Eluents: THF/PE (4/1).

**Yield:** 50 mg, (42%)

**TLC:** THF/PE (4/1),  $R_f = 0.29$

**$^1\text{H NMR}$**  (250 MHz,  $\text{CDCl}_3$ , RT)  $\delta_{\text{H}}$ , ppm: 2.4 (s, 3 $H_a$ ), 3.5 - 3.7 (m, 72 $H_b$ ), 4.0 (d, 2 $H_c$ ), 4.1 (t,  $-\text{CH}_2\text{OTos}$ ), 5.15 - 5.3 (m, 2 $H_d$ ), 5.8 - 6.0 (m, 1 $H_e$ ), 7.3 (d, 2 $H_f$ ), 7.7 (d, 2 $H_g$ )

**FD-MS** (m/z) (100%) 962.7 ( $M^+ - \text{CH}_2\text{CH}_2\text{O}$ ), calculated (**26**:  $\text{C}_{46}\text{H}_{84}\text{O}_{21}\text{S} - \text{CH}_2\text{CH}_2\text{O}$ ) = 961.23, (70%) 1006.9 ( $M^+$ ), calculated (**26**:  $\text{C}_{46}\text{H}_{84}\text{O}_{21}\text{S}$ ) = 1005.23, (30%) 918.7 ( $M^+ - 2x (\text{CH}_2\text{CH}_2\text{O})$ ), calculated (**26**:  $\text{C}_{46}\text{H}_{84}\text{O}_{21}\text{S} - 2x (\text{CH}_2\text{CH}_2\text{O})$ ) = 917.23, (27%) 1031.0 ( $M^+ + \text{Na}$ ), calculated (**26**:  $\text{C}_{46}\text{H}_{84}\text{O}_{21}\text{S} + \text{Na}$ ) = 1028.23

## 2.4. Synthesis of lateral spacer molecules

### 2.4.1. Introduction and motivation

A possible approach to decrease the two-dimensional lipid density usually observed by self-assembly is the use of small hydrophilic thiolated molecules. They act as diluting molecules termed also as spacers (Figure 2.9). Mixed with tethering lipids, they take part in the fabrication of laterally diluted SAM. In principle, diluting molecules are attached to the gold surface concurrently with the tethering lipids, and thus increase the lateral space. This helps to produce a hydrated reservoir beneath the membrane from one side, and to enhance the membrane fluidity from the other.

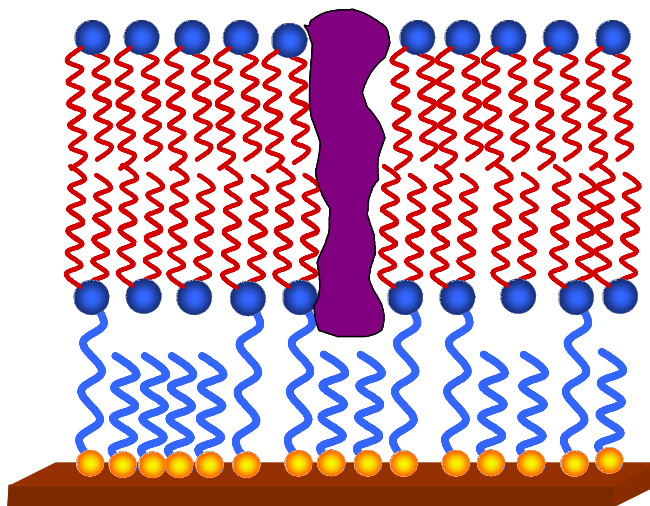


Figure 2.9. Protein incorporation in tBLM prepared from lateral diluted monolayer

Several examples are given in the literature exploring this approach.<sup>41-46</sup> In general, two types of spacer molecules have been used. The strategy which has mostly been applied includes small hydrophilic disulfide-containing molecules such as dithiodiglycolic acid<sup>41,42,45</sup> and 2-mercaptoethanol.<sup>44,46</sup> However, Nauman *et al.*<sup>47</sup> have reported that their attempt to dilute the thiolipid monolayers with short molecules, such as 2-mercaptoethanol or lipoic acid have resulted in bilayers with poor electrical properties. Their recent work<sup>48</sup> has demonstrated preparation of highly insulating tBLMs

based on mixed SAMs, prepared by mixing thiolated tether lipid (DPTL) with a spacer molecule (TEGL), an ester of TEG and lipoic acid.

A similar approach has been used by Munro *et al.*<sup>43</sup> where thiolipids have been diluted with lateral spacer molecules (especially polyethylene glycols) identical with the hydrophilic and anchor moieties of the corresponding tethering lipid.

Principally following the same strategy, the synthesis of two new lateral spacer molecules slightly different from TEGL is presented. In this part, starting from monoprotected TEG, the free hydroxyl group was modified with thiol and lipoic acid

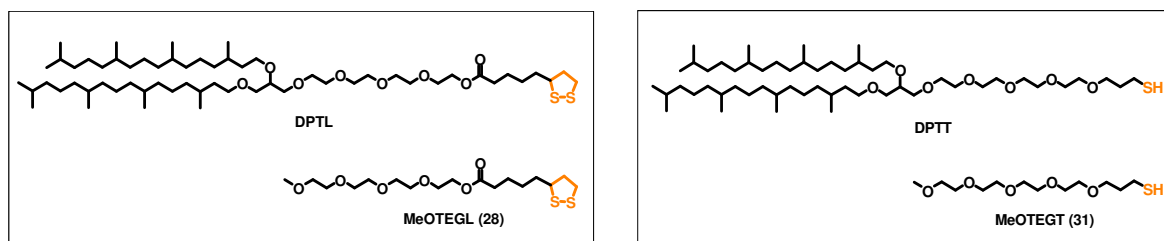


Figure 2.10. Chemical structures of the tether thiolipids DPTL and DPTT and their corresponding lateral spacer molecules

anchors resembling DPTT and DPTL respectively (Figure 2.10). The synthesis of these diluting molecules was done for the need of TEGL analogs in Naumann's group for further investigations. The synthesis was conducted according to Figure 2.11.

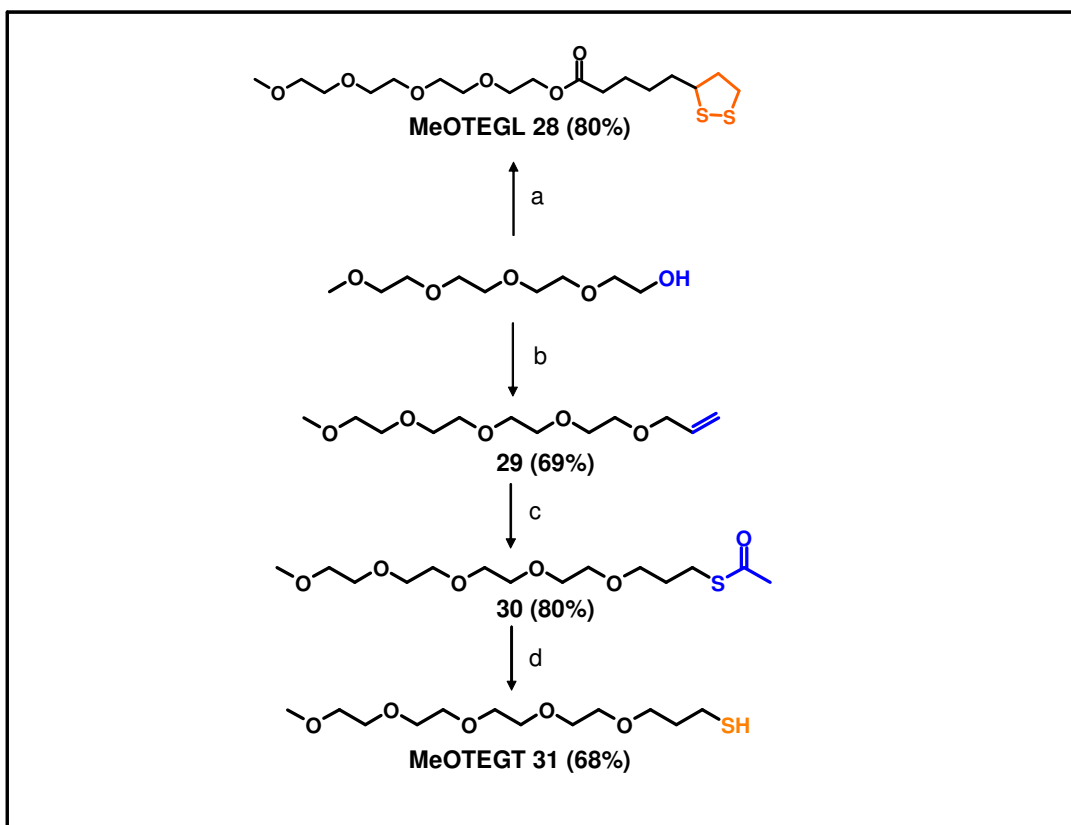


Figure 2.11. Synthetic pathway to obtain the lateral spacer molecules

#### 2.4.2. Results and discussion

The initial molecule in reactions **b** and **c** (Figure 2.11) is tetraethylene glycol monomethylether. The advantage of using MeOTEG compared to TEG (used by synthesis of TEGL) is that the methoxy group protects one of the terminating hydroxyl groups of TEG, and thus only the other one can be modified. On the other hand, after completion of the reaction, the methoxy group is not removed in order to prevent side reactions (e.g. ether or ester coupling) during the SAM investigation.

MeOTEGGL was synthesized in a one step reaction by ester coupling of MeOTEG with lipoic acid. The mechanism of the ester coupling reaction is given below.

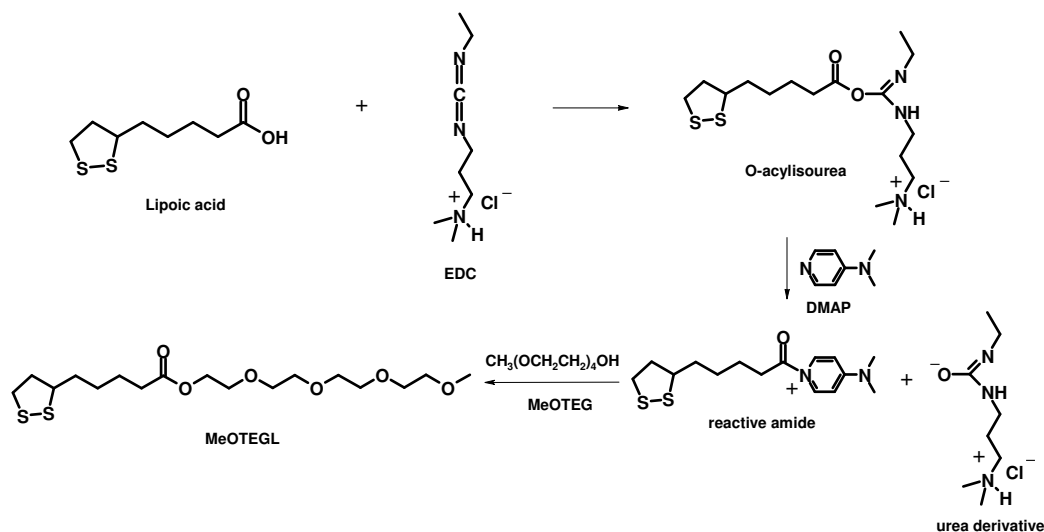


Figure 2.12. Mechanism of ester coupling reaction with EDC

First, lipoic acid was activated by coupling with 1-Ethyl-3-(3-dimethylaminopropyl)-carbodiimide hydrochloride (EDC). The obtained corresponding ureaester reacts with 4-N,N-dimethylaminopyridine (DMAP) to give a so called “reactive amide”. This intermediate reacts rapidly with alcohols (MeOTEG) giving the ester MeOTEG-L. DMAP acts as a catalyst for acyl (lipoic) transfer. The target product MeOTEG-L was obtained with a yield of 80%.

MeOTEG-T was synthesized following a 3 step procedure including first functionalization of double bond, then thiolation via thioacetat, and finally, cleavage of the acyl group. Every step was followed by column chromatography yielding finally a pure product characterized with TLC, <sup>1</sup>H NMR and FD-MS.

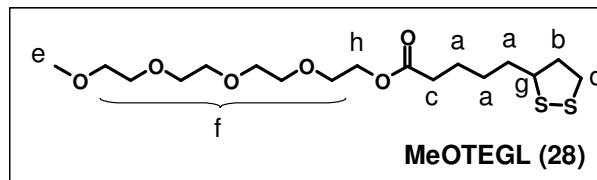
### 2.4.3. Conclusion

In the frame of this section, the synthesis of two new thiolated spacer molecules was described. This was done by modifying the free hydroxyl group of MeOTEG with thiol and lipoic anchors, which are suitable for gold surface. Both products MeOTEG-L and MeOTEG-T are obtained in good yields. The molecules have been used by Jing Li (thesis in preparation).

### 2.4.4. Experimental part

#### Reaction a:

#### Ester coupling of tetraethylenglycolmonomethylether with lipoic acid



Lipoic acid (1.11 g, 5.38 mmol, 206.34 g/mol) was dissolved in DCM in a 2 neck round bottom flask. EDC (1.57 g, 8.19 mmol, 191.71 g/mol) was added, and the solution was stirred for 1 h at RT. The preparation of the EDC activated lipoic acid is checked by TLC (PE/EtAc: 2/1). Tetraethylenglycolmonomethylether (0.67 g, 3.23 mmol, 208.23 g/mol) diluted in DCM was added dropwise to the reaction mixture. DMAP (0.4 g, 3.27 mmol, 122.2 g/mol) was added, and the solution was stirred overnight. The reaction was monitored by TLC. After completion of the reaction, the solution was washed with sat.  $\text{Na}_2\text{CO}_3$  and  $\text{H}_2\text{O}$ . The organic layer was dried over  $\text{Na}_2\text{SO}_4$  and filtered. The solvent was evaporated, and the product **MeOTEGl (28)** was purified by column chromatography. Eluents: EtAc/DCM (4/1)

**Yield:** 1.03 g, (80%)

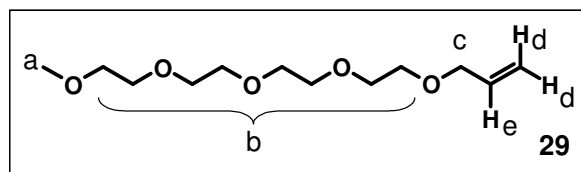
**TLC:** EtAc/DCM (4/1),  $R_f = 0.44$

**$^1\text{H NMR}$**  (250 MHz,  $\text{CDCl}_3$ , RT)  $\delta_{\text{H}}$ , ppm: 1.25 - 1.7 (m,  $6\text{H}_a$ ), 1.7 - 2.45 (d/h,  $2\text{H}_b$ ), 2.2 (t,  $2\text{H}_c$ ), 2.9 - 3.15 (m,  $2\text{H}_d$ ), 3.3 (s,  $3\text{H}_e$ ), 3.35 - 3.7 (m,  $15\text{H}_{f+g}$ ), 4.1 (t,  $2\text{H}_h$ )

**FD-MS** (m/z): 396.7 ( $\text{M}^+$ ), calculated ( $\text{C}_{17}\text{H}_{32}\text{O}_6\text{S}_2$ ) = 396.57; 793.1 ( $\text{M}+\text{M}^+$ ), calculated ( $2 \times \text{C}_{17}\text{H}_{32}\text{O}_6\text{S}_2$ ) = 793.14

#### Reaction b:

#### Allylation of MeOTEG



Tetraethylenglycolmonomethylether (4.32 g, 20.74 mmol, 208.26 g/mol) was dissolved in dry THF (23 ml) in a 2 neck round bottom flask. NaH (0.75 g, 31.3 mmol, 24 g/mol) was added in small portions at RT. After 1 h, allyl bromide (2.51 g, 20.7 mmol, 120.98 g/mol) diluted with dry THF (20 ml) was added dropwise through a dropping funnel to the alkoxide at  $40^\circ\text{C}$ . After 24 hrs, the reaction was stopped, and the mixture was centrifuged (6000 rpm, 15 min). The solid residue was resuspended in THF and



centrifuged again. This procedure was repeated three times. The organic phases were combined and the solvent was evaporated under vacuum. The residue was purified by flash chromatography to give product **29**. Eluents: DCM/Ac (10/1 gradually to 5/1).

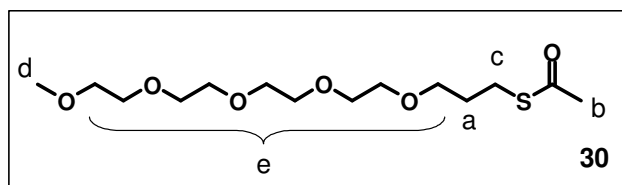
**Yield:** 3.55 g, (69%)

**TLC:** DCM /Ac (10/1),  $R_f = 0.25$

**$^1\text{H NMR}$**  (250 MHz,  $\text{CDCl}_3$ , RT)  $\delta_{\text{H}}$ , ppm: 3.3 (s,  $3\text{H}_a$ ), 3.45 - 3.7 (m,  $16\text{H}_b$ ), 3.99 (d,  $2\text{H}_c$ ), 5.1 - 5.3 (m,  $2\text{H}_d$ ), 5.8 - 5.95 (m,  $1\text{H}_e$ )

**Reaction c:**

**Synthesis of the thiolated spacer molecule MeOTEGT (first step)**



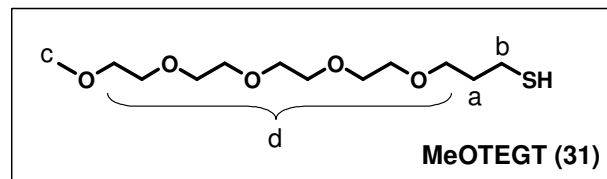
Product **29** (3.55 g, 14.3 mmol, 248.32 g/mol), thioacetic acid (43.5 g, 572 mmol, 76 g/mol) and AIBN (94 mg, 0.572 mmol, 164.21 g/mol) were placed in a Schlenk flask and dissolved in toluene (10 ml). The solution was degassed three times. The flask was purged with Ar and stirred at 70 °C for 24 h. The reaction was stopped, and the solvent was evaporated under vacuum. The product **30** was purified by column chromatography. Eluents: DCM/Ac (5/1 gradually to 1/1).

**Yield:** 3.72g, (80%)

**TLC:** DCM /Ac (5/1),  $R_f = 0.53$

**$^1\text{H NMR}$**  (250 MHz,  $\text{CDCl}_3$ , RT)  $\delta_{\text{H}}$ , ppm: 1.8 (p,  $2\text{H}_a$ ), 2.3 (s,  $3\text{H}_b$ ), 2.9 (t,  $2\text{H}_c$ ), 3.3 (s,  $3\text{H}_d$ ), 3.4 - 3.7 (m,  $18\text{H}_e$ )

**FD-MS** (m/z): 325.6 ( $\text{M}^+$ ), calculated ( $\text{C}_{14}\text{H}_{28}\text{O}_6\text{S}$ ) = 324.44

**Reaction d:****Preparation of the thiolated spacer molecule MeOTEGT (second step)**

The thioacetate **30** (3.72 g, 11.5 mmol, 324.44 g/mol) was dissolved in THF (100 ml) in a round bottom flask, and 1 M NaOH (62 ml) was added. The heterogeneous mixture was stirred vigorously overnight at 50°C. The reaction was monitored by TLC. After the completion of the reaction, 1 M H<sub>2</sub>SO<sub>4</sub> (62 ml) was added to neutralize the mixture and stirred for 30 min at RT. The solvent was evaporated under vacuum. The product was dissolved in DCM (120 ml) and washed with H<sub>2</sub>O, 1 M H<sub>2</sub>SO<sub>4</sub> and sat. Na<sub>2</sub>CO<sub>3</sub> solution. The organic layers were collected and dried over Na<sub>2</sub>SO<sub>4</sub>. After filtration, the solvent was evaporated, and the product **MeOTEGT (31)** was purified by column chromatography. Eluents: DCM/Ac (5/1 gradually to 2/1).

**Yield:** 2.21g, (68%)

**TLC:** DCM /Ac (5/1), R<sub>f</sub> = 0.32

**<sup>1</sup>H NMR** (250 MHz, d-THF, RT) δ<sub>H</sub>, ppm: 1.9 (p, 2H<sub>a</sub>), 2.8 (t, 2H<sub>b</sub>), 3.3 (s, 3H<sub>c</sub>), 3.4 - 3.7 (m, 18H<sub>d</sub>)

**FD-MS** (m/z): 562.6 (M + M<sup>+</sup>), calculated (2 x C<sub>12</sub>H<sub>25</sub>O<sub>5</sub>S) = 562.8, 1124.4 (2x (M + M<sup>+</sup>)), calculated 2x (2 x C<sub>12</sub>H<sub>25</sub>O<sub>5</sub>S) = 1125.6

## 2.5. Synthesis of lipid with a bulky anchor - “self-diluted” molecule (DPHDL)

### 2.5.1. Introduction and motivation

The study of the lipid lateral organization within the tBLMs is highly important to mimic biomembranes. Since the preparation of tBLMs as a biosensor platform is the main object in our group, control over membrane structure and composition is necessary. In order to achieve such control over the lateral space between tethered lipids, Cornell *et al.*<sup>42</sup> have used an approach to design their thiolipids in a way to provide bigger lateral space and an ionic reservoir. The lipids were attached to the surface via benzyl alkyl disulfide moiety. This anchor acts as a tether for the thiolipids, and it introduces a benzyl spacer group that lowers the two-dimensional packing density of the membrane. However, in spite of the special anchor design, they have used additional spacer molecule. Mixed SAMs (tethered and spacer molecules) has been object of many researchers.<sup>42-48</sup>

However, the use of diluting molecules for the preparation of SAMs with higher planar fluidity might raise some disadvantages. First of all, smaller spacer molecules compared to the thiolated lipids attach to the gold surface with priority. Thus, the mixing ratio on the gold surface is different compared to the one in the solution. Therefore, additional experiments need to be done to determine the relative proportion of thiols on the surface.<sup>48</sup> On the other hand, phase separation between tether lipids and spacer molecules can result in inhomogeneous SAMs.

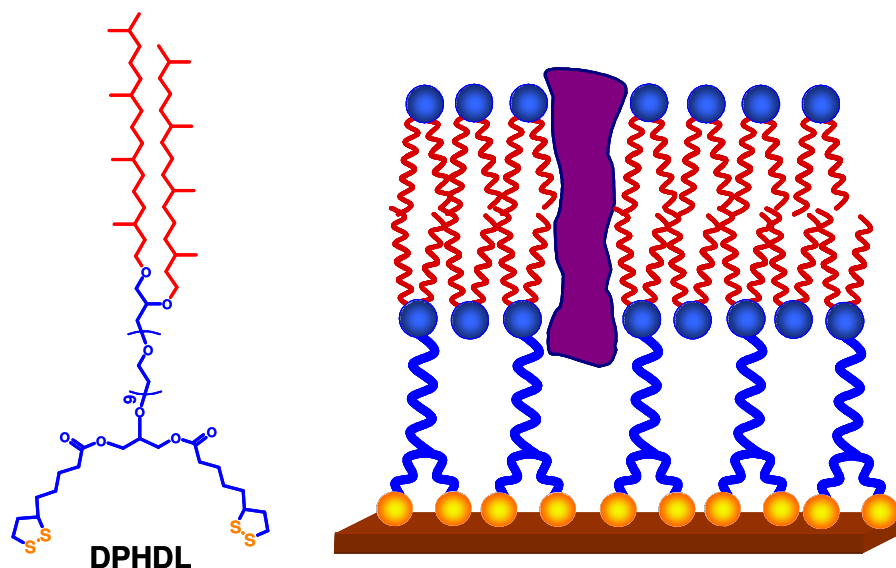


Figure 2.13. Chemical structure of DPHDL and schematic representation of the structure of tBLM prepared with this molecule

In order to exclude the need of two different molecules by SAM fabrication we designated a new tethering lipid (DPHDL) with relatively bulky anchor. This molecule is “self-diluting”, because the anchor facilitates the dilution process by the monolayer formation without the need of additional spacer molecule. The structure of the “self-diluted” molecule resembles the one of DPTL but instead of one it contains two lipoic anchors (Figure 2.13). Thus, once the lipid molecules assemble on the surface, the bulky double anchors provide larger lateral space needed for higher mobility of the monolayer and bigger ionic reservoir beneath the membrane.

The use of such molecules offers two main advantages: preparation of more homogeneously distributed and more stable monolayers, preventing the known possibility of desorption of the tethered lipids from the gold surface.

The synthesis of DPHDL is conducted following the synthetic pathway shown in Figure 2.14.

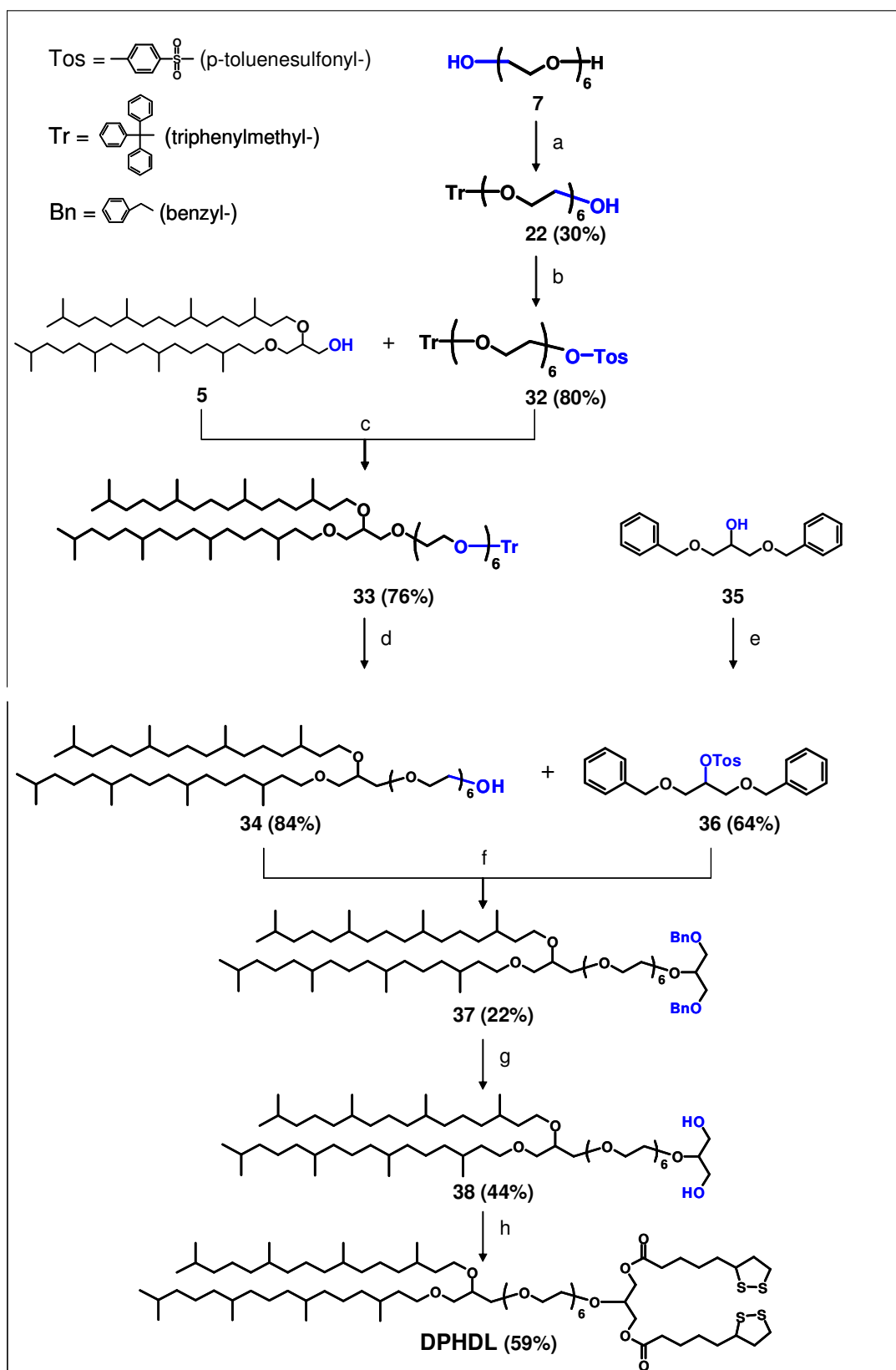


Figure 2.14. Synthetic pathway of “self-diluted” tether lipid DPHDL

### 2.5.2. Results and discussion

Hereby, we report the design, synthesis and characterization of a tether lipid molecule (DPHDL) with a bulky anchor. The structure of DPHDL was designed in a way that once the molecule is immobilized on a substrate surface, the covered area per molecule will be larger compared with the area occupied from a molecule of DPTL, DPTT, DPHT or DPOT. This statement was supported initially by theoretically simulated statistical 3D-conformational modelling (Figure 2.15) and later the better ability for incorporation of large proteins was verified experimentally (Chapter 4).

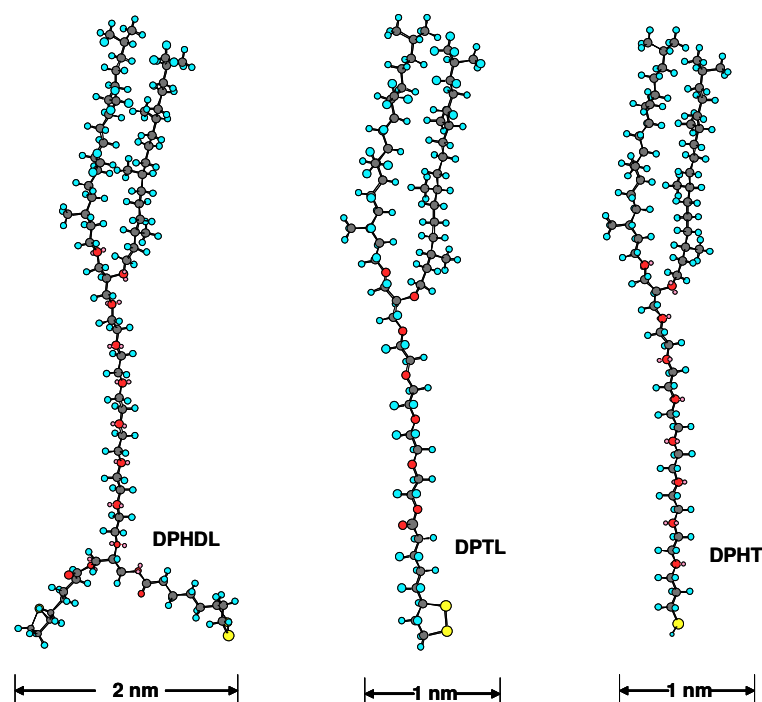


Figure 2.15. Molecular modelling of DPHDL, DPTL and DPHT by CS Chem 3D Ultra 6.0

All molecular models were simulated by using MM2 force field method. This method takes into account the energy minimization of the structure, which will result in the most favourable conformational structure. Interaction calculations were approximated for a molecular conformation in vacuum with a minimum gradient of 0.01 units. For the obtained global minimum, the maximal cross-sectional radius resulted in  $\sim 2$  nm for DPHDL and  $\sim 1$  nm for DPTL and DPHT. Moreover, the cross-sectional radius of DPTL

and DPHT is contributed mainly to the hydrophobic part. However, in the case of DPHDL the increase of the molecular cross-sectional radius is due to the bulky (double lipoic acid ester) anchor. Of course, these simulations do not include the influence of factors such as temperature and molecular dynamics, solvation and intra- or intermolecular interactions. Therefore, further mathematical models have to be applied in order to extract additional information for the particular conformations of this molecule.

The synthetic pathway of DPHDL consists of a multiple step procedure (Figure 2.14) involving three main tasks: nucleophilic substitution reaction of a phytanyl based lipid (DPG) with monoprotected HEG (reaction **c**), introduction of a branch in the main tethering part (reaction **f**) and, finally, coupling with the anchor groups (reaction **h**). The sequence of the steps in this synthetic pathway is chosen because of two main reasons. Firstly, the introduction of the hydrophobic phytanyl chains in the beginning compensates the high polarity of HEG. That will facilitate both the purification processes and the TLC monitoring. Secondly, the lipoic acid is coupled to the lipid in the final step in order to exclude an eventual reesterification in the hard conditions of the preceding nucleophilic substitution reactions.

The synthesis starts with consecutive monoprotection and tosylation of HEG (reactions **a**, **b**). Triphenylmethyl group was selected as a suitable protecting group due to the ease of its protecting/cleavage procedure and the significant UV activity (see 2.3.2).

In the next step, the modified HEG (**32**) was coupled to DPG (**5**) (reaction **c**). This nucleophilic Williamson type substitution reaction, illustrated already in the synthesis of lipid precursors in section 2.2.3, is crucial because of the relatively high activation energy required. In spite of the relatively hard reaction conditions, this step was conducted successfully with yield of 76%. Then, the protective group was cleaved yielding product **34** with a free hydroxyl group needed for a branch introduction (reaction **d**). The branch was inserted by using doubly protected glycerol (**35**). Initially, **35** was tosylated introducing a good leaving group that later underwent nucleophilic substitution on pegylated lipid **34** (reaction **f**). This was the second crucial step, because it is known that secondary alcohols can be hardly substituted due to steric reasons. Therefore, the yield of this reaction (22%) was relatively low.

After deprotection of glycerol (reaction **g**), lipoic acid was attached to both hydroxymethyl branches of **38** resulting in the target product DPHDL. As described in section 2.4.3, the reaction was conducted in presence of EDC and DMAP following the

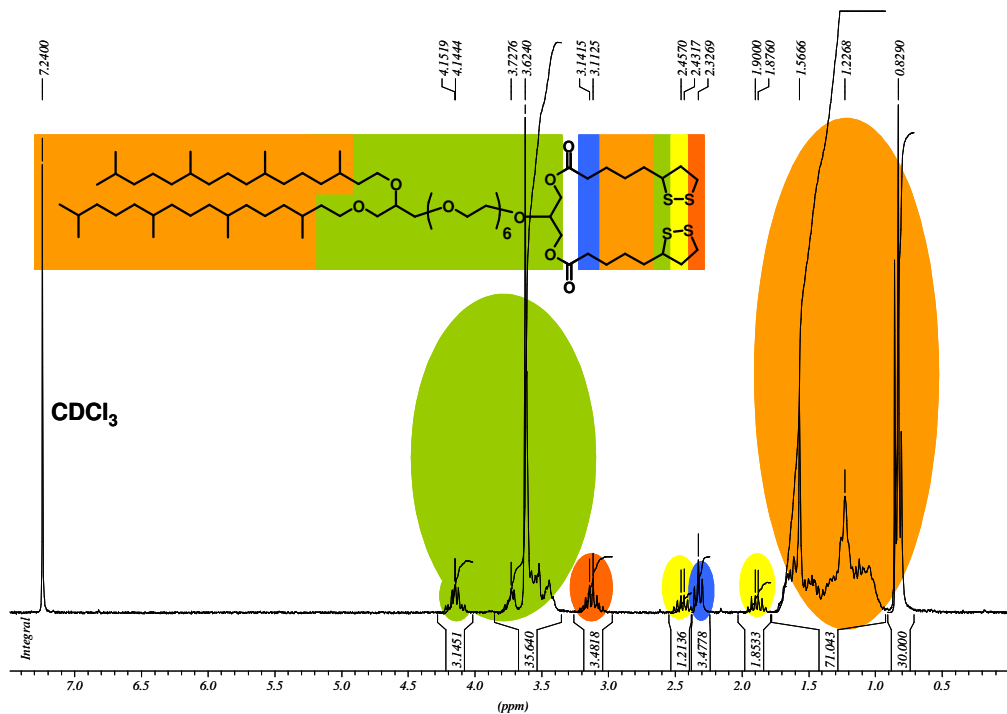


Figure 2.14  $^1\text{H}$  NMR spectrum of DPHDL

same ester coupling mechanism. The product was purified by column chromatography and characterized by  $^1\text{H}$  NMR,  $^{13}\text{C}$  NMR and FD-MS that verified the structure and purity of DPHDL.

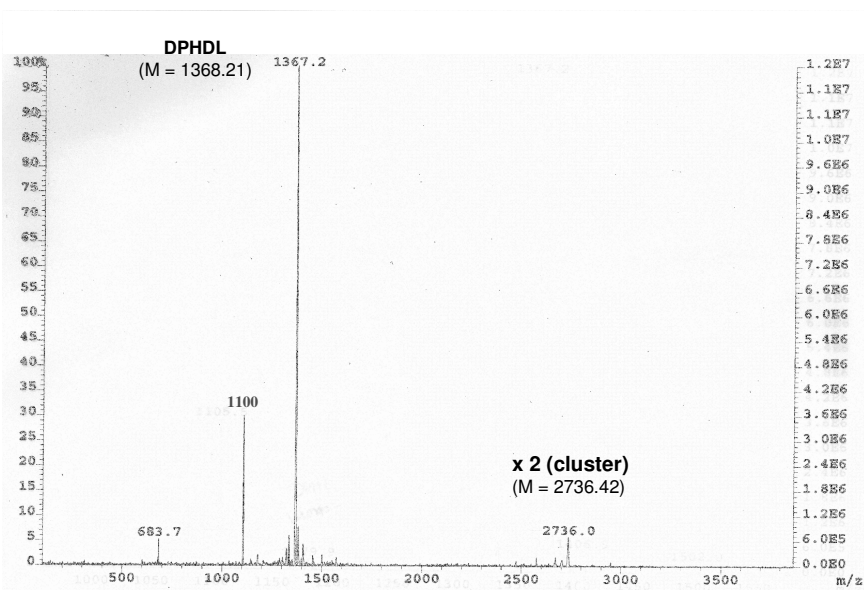


Figure 2.15 FD-mass spectrum of DPHDL



### 2.5.3. Conclusion

In this work, the synthesis of novel tether lipid has been developed. We could thus add a new thiolipid possessing relatively bulky anchor to our lipid toolbox. Assembled on the gold surface, DPHDL molecules provide additional lateral space. This leads to lower two-dimensional packing density of the lipids. The use of such “self-diluted” lipid excludes the need of additional spacer molecules that make the system more complicated. Finally, DPHDL in comparison with DPTL contains two lipoic anchor moieties. The presence of four sulphur-gold chemical bonds per molecule determine strong connection of the monolayer to the surface, preventing eventual lipid desorption in solution. All mentioned advantages make DPHDL a promising lipid with many potential applications.

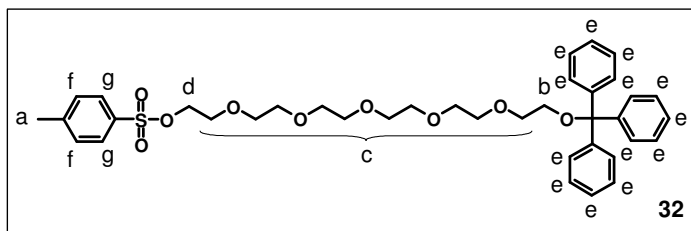
### 2.5.4. Experimental part

#### Reaction a:

This reaction was already described in section 2.3.4 (reaction **b**).

#### Reaction b:

#### Tosylation of **22**



The glassware used in reactions **b**, **c**, **e** and **f** was dried and purged with Ar prior to use. Product **22** (1.75 g, 3.34 mmol, 524.66 g/mol) was dissolved in dry THF (20 ml) in a 2 neck round bottom flask. NaH (0.12 g, 5.0 mmol, 24 g/mol) was added, and the reaction mixture was stirred for 1 h at RT. The obtained alkoxide was added dropwise to a solution of tosyl chloride (1.27 g, 6.67 mmol, 190.6 g/mol), TEA (460  $\mu$ l, 3.3 mmol, 101.2 g/mol) and dry THF (15 ml). The reaction was monitored by TLC. Additional amounts of NaH and tosyl chloride were added. After 48 h, the reaction was stopped. The solid residue was precipitated by centrifugation (6000 rpm, 15 min). The solid residue was resuspended in THF and centrifuged again. This procedure was repeated 3 times. The organic phases were combined and the solvent was evaporated under vacuum. The residue was purified by column chromatography to give product **32**. Eluents: DCM/Ac (20/1 gradually to 10/1).

**Yield:** 1.8 g, (80%)

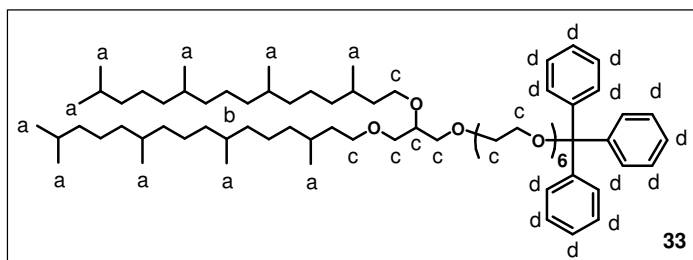
**TLC:** DCM /Ac (15/1),  $R_f = 0.53$

**$^1\text{H NMR}$**  (250 MHz,  $\text{CDCl}_3$ , RT)  $\delta_{\text{H}}$ , ppm: 2.45 (s,  $3\text{H}_a$ ), 3.2 (t,  $2\text{H}_b$ ), 3.5 - 3.8 (m,  $20\text{H}_c$ ), 4.1 (t,  $2\text{H}_d$ ), 7.2 - 7.4 (m,  $15\text{H}_e$ ), 7.5 (d,  $2\text{H}_f$ ), 7.8 (d,  $2\text{H}_g$ )

**FD-MS** (m/z): (100%) 678.7 ( $\text{M}^+$ ), calculated (**32**:  $\text{C}_{38}\text{H}_{46}\text{O}_9\text{S}$ ) = 678.85, (80%) 243.5 ( $\text{Tr}^+$ ), calculated ( $\text{C}_{19}\text{H}_{15}$ ) = 243.34, (20%) 1358.1 ( $\text{M} + \text{M}^+$ ), calculated (**32**:  $2 \times \text{C}_{38}\text{H}_{46}\text{O}_9\text{S}$ ) = 1357.7

**Reaction c:**

**Coupling of 22 with DPG (5)**



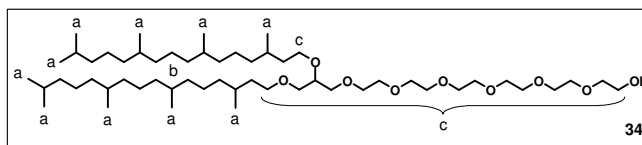
DPG **5** (2.13 g, 3.26 mmol, 653.2 g/mol) was dissolved in dry THF (15 ml) in a 2 neck round bottom flask. NaH (0.13 g, 5.3 mmol, 24 g/mol) was added in small portions at RT. After 2.5 hrs, the obtained alkoxide was transferred to a dropping funnel, and was added dropwise to product **32** (1.8 g, 2.65 mmol, 678.85 g/mol), dissolved in dry THF (20 ml) at RT. The reaction mixture was stirred for 48 h and monitored by TLC. After the completion of the reaction, the mixture was centrifuged (6000 rpm, 15 min). The solid residue was resuspended in THF and centrifuged again. This procedure was repeated 3 times. The organic phases were combined and the solvent was evaporated under vacuum. The residue was purified by column chromatography to give product **33**. Eluents: DCM/Ac (30/1 gradually to 20/1).

**Yield:** 2.36 g, (76%)

**TLC:** DCM/Ac (20/1),  $R_f = 0.57$

**$^1\text{H NMR}$**  (250 MHz,  $\text{CDCl}_3$ , RT)  $\delta_{\text{H}}$ , ppm: 0.8 (t,  $30\text{H}_a$ ), 0.9 - 1.8 (m,  $48\text{H}_b$ ), 3.2 (t,  $-\text{CH}_2\text{OTr}$ ), 3.35 - 3.7 (m,  $31\text{H}_c$ ), 7.1 - 7.4 (m,  $15\text{H}_d$ )

**FD-MS** (m/z): (100%) 243.6 ( $\text{Tr}^+$ ), calculated ( $\text{C}_{19}\text{H}_{15}$ ) = 243.34, (30%) 1160.1 ( $\text{M}^+$ ), calculated (**33**:  $\text{C}_{74}\text{H}_{126}\text{O}_9$ ) = 1159.82, (30%) 918.7 ( $\text{M}^+$ ), calculated (**34**:  $\text{C}_{55}\text{H}_{112}\text{O}_9$ ) = 917.50, (20%) 2319.7 ( $\text{M} + \text{M}^+$ ), calculated (**33**:  $2 \times \text{C}_{74}\text{H}_{126}\text{O}_9$ ) = 2319.64

**Reaction d:****Deprotection of the trityl group**

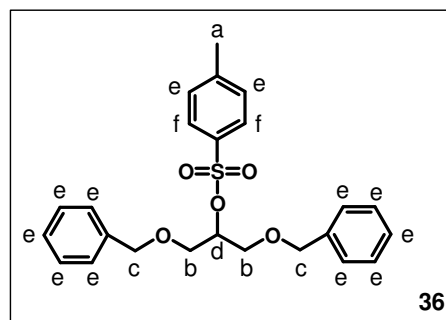
In a round bottom flask, product **33** (2.36 g, 2.03 mmol, 1159.82 g/mol) and powdered zinc bromide (2.26 g, 10.03 mmol, 225.19 g/mol) were dissolved in DCM (4 ml). The reaction mixture was stirred at RT. The completion of the deprotection reaction was monitored by TLC. After 24 h, the reaction was stopped, and the mixture was washed three times with sat. NaHCO<sub>3</sub>. This solution was thoroughly extracted with small amounts DCM. DCM layers were collected and dried over MgSO<sub>4</sub>. After filtration, the organic solvent was evaporated. The product was purified by flash chromatography. Eluents: DCM/Ac (25/1 gradually to 10/1).

**Yield:** 1.54 g, (84%)

**TLC:** DCM /Ac (10/1), R<sub>f</sub> = 0.27

**<sup>1</sup>H NMR** (250 MHz, CDCl<sub>3</sub>, RT) δ<sub>H</sub>, ppm: 0.8 (t, 30H<sub>a</sub>), 0.9 - 1.7 (m, 48H<sub>b</sub>), 3.35 -3.8 (m, 33H<sub>c</sub>)

**FD-MS** (m/z): (100%) 918.7 (M<sup>+</sup>), calculated (**34**: C<sub>55</sub>H<sub>112</sub>O<sub>9</sub>) = 917.50, (45%) 1860.8 (2M + Na<sup>+</sup>), calculated (**34**: 2 x C<sub>55</sub>H<sub>112</sub>O<sub>9</sub> + Na) = 1858.0

**Reaction e:****Tosylation of 1,3-O-dibenzyl glycerol**

**35** (5.1 g, 18.73 mmol, 272.35 g/mol) was dissolved in dry THF (20 ml) in a round bottom flask. NaH (0.8 g, 33.33 mmol, 24 g/mol) was added at RT and the reaction mixture was stirred for 2½ hrs. The alkoxide of **35** was added dropwise to the solution of tosyl chloride (10.5 g, 55.09 mmol, 190.6 g/mol) dissolved in dry THF (25 ml). The reaction was monitored by TLC. Additional amounts of NaH were added. After 7 days, the reaction was stopped. The solid residue was precipitated by centrifugation (6000 rpm, 15 min). The solid residue was resuspended in THF and centrifuged again. This procedure was repeated three times. The organic phases were combined and the solvent was evaporated under vacuum. Product **36** was purified by column

chromatography. Eluent: DCM.

**Yield:** 6.31 g, (79%)

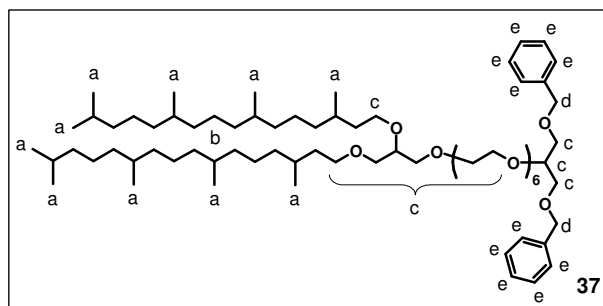
**TLC:** PE /THF (3/1),  $R_f = 0.52$

**$^1\text{H NMR}$**  (250 MHz,  $\text{CDCl}_3$ , RT)  $\delta_{\text{H}}$ , ppm: 2.3 (s,  $3\text{H}_a$ ), 3.6 (d,  $4\text{H}_b$ ), 4.3 (t,  $4\text{H}_c$ ), 4.69 (p,  $1\text{H}_d$ ), 7 - 7.3 (m,  $12\text{H}_e$ ), 7.7 (d,  $2\text{H}_f$ )

**FD-MS** (m/z): (100%) 850.7 ( $\text{M} + \text{M}^+$ ), calculated (**36**:  $2 \times \text{C}_{24}\text{H}_{26}\text{O}_5\text{S}$ ) = 853.08, (47%) 425.2 ( $\text{M}^+$ ), calculated (**36**:  $\text{C}_{24}\text{H}_{26}\text{O}_5\text{S}$ ) = 426.54, (45%) 1277.5 ( $2\text{M} + \text{M}^+$ ), calculated (**36**:  $3 \times \text{C}_{24}\text{H}_{26}\text{O}_5\text{S}$ ) = 1279.62

**Reaction f:**

**Introduction of a splitting junction in the hydrophilic part**



**34** (1.54 g, 1.68 mmol, 917.50 g/mol) was dissolved in dry THF (10 ml) in a 2 neck round bottom flask. NaH (60 mg, 5.52 mmol, 24 g/mol) was added at RT. After 3 hrs, the mixture was transferred to a dropping funnel, and was added dropwise to a solution of **36** (0.72 g, 1.68 mmol, 426.54 g/mol) in dry THF (15 ml). The reaction mixture was stirred for 4 days, while the reaction was monitored by TLC. After the completion of the reaction, the mixture was centrifuged (6000 rpm, 15 min) followed by washing of the solid residue with THF (repeated 3 times). The solid residue was resuspended in THF and centrifuged again. This procedure was repeated 3 times. The organic phases were combined and the solvent was evaporated under vacuum. The residue was purified by flash chromatography to give product **37**. Eluents: DCM gradually to DCM/Ac (30/1 gradually to 20/1).

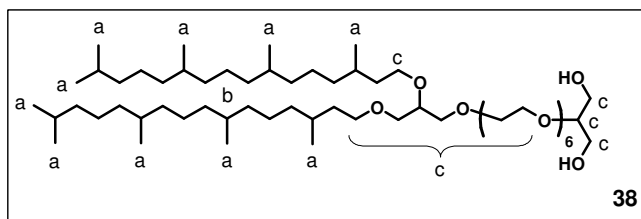
**Yield:** 430 mg, (22%)

**TLC:** PE/THF (5/1),  $R_f = 0.25$

**$^1\text{H NMR}$**  (250 MHz,  $\text{CDCl}_3$ , RT)  $\delta_{\text{H}}$ , ppm: 0.8 (t,  $30\text{H}_a$ ), 0.9 - 1.7 (m,  $48\text{H}_b$ ), 3.5 - 3.8 (m,  $38\text{H}_c$ ), 4.5 (s,  $4\text{H}_d$ ), 7.2 - 7.35 (m,  $10\text{H}_e$ )

**FD-MS** (m/z): (100%) 1171.4 ( $\text{M}^+$ ), calculated (**37**:  $\text{C}_{72}\text{H}_{130}\text{O}_{11}$ ) = 1171.83, (52%) 2345.4 ( $\text{M} + \text{M}^+$ ), calculated (**37**:  $2 \times \text{C}_{72}\text{H}_{130}\text{O}_{11}$ ) = 2343.66

**Reaction g:**  
**Cleavage of the benzyl groups**



**37** (430 mg, 0.37 mmol, 1171.83 g/mol) was dissolved in a mixture of EtOH/Cyclohexene (5/2.5 ml), and the catalyst Pd/C was added. The conversion of the initial compound was monitored by TLC. Additional amounts of catalyst were added to complete the reaction. The reaction was stopped after 4 days, the catalyst was filtered, and the solvent was evaporated under vacuum. The product **38** was purified by flash chromatography. Eluents: DCM/Ac (7/1 gradually to Ac).

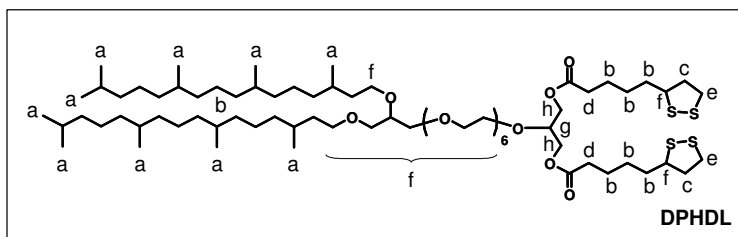
**Yield:** 160 mg, (44%)

**TLC:** DCM /Ac (1/1),  $R_f = 0.37$

**$^1\text{H NMR}$**  (250 MHz,  $\text{CDCl}_3$ , RT)  $\delta_{\text{H}}$ , ppm: 0.8 (t, 30 $H_a$ ), 0.9 - 1.65 (m, 48 $H_b$ ), 3.35 -3.8 (m, 38 $H_c$ )

**FD-MS** (m/z): (100%) 993.8 ( $M^+$ ), calculated ( $\text{C}_{58}\text{H}_{118}\text{O}_{11}$ ) = 991.58, (55%) 1016.2 ( $M + \text{Na}^+$ ), calculated ( $\text{C}_{58}\text{H}_{118}\text{O}_{11} + \text{Na}$ ) = 1014.58

**Reaction h:**  
**Synthesis of DPHDL**



Lipoic acid (330 mg, 1.6 mmol, 206.34 g/mol) was dissolved in DCM (14 ml) in a 2 neck round bottom flask. EDC (410 mg, 2.14 mmol, 191.71 g/mol) was added, and the solution was stirred for 1 h at RT. DMAP (60 mg, 0.48 mmol, 122.2 g/mol) was added. Product **38** (160 mg, 0.16 mmol, 991.58 g/mol) diluted in DCM (3 ml) was added dropwise to the reaction mixture. The solution was stirred overnight at RT. The reaction was monitored by TLC. After completion of the reaction, the solution was washed with sat.  $\text{Na}_2\text{CO}_3$  and  $\text{H}_2\text{O}$ . The organic layers were dried over  $\text{Na}_2\text{SO}_4$  and filtered. The solvent was evaporated, and the **DPHDL** was isolated by column chromatography. Eluents: DCM/Ac (30/1).

**Yield:** 130 mg, (59%)

**TLC:** DCM/Ac (5/1),  $R_f = 0.76$

**$^1\text{H NMR}$**  (250 MHz,  $\text{CDCl}_3$ , RT)  $\delta_{\text{H}}$ , ppm: 0.8 (t, 30H<sub>a</sub>), 0.9 - 1.8 (m, 60H<sub>b</sub>), 1.8 - 2.5 (d/h, 4H<sub>c</sub>), 2.3 (t, 4H<sub>d</sub>), 3.1 (m, 4H<sub>e</sub>), 3.4 - 3.65 (m, 35H<sub>f</sub>), 3.65 - 3.85 (m, 1H<sub>g</sub>), 4.05 - 4.5 (m, 4H<sub>h</sub>)

**$^{13}\text{C NMR}$**  ( $\text{CD}_2\text{Cl}_2$ )  $\delta_{\text{C}}$ , ppm: 173, 78, 76, 71, 70, 69, 63, 56, 40, 39, 38, 37, 35, 34, 33, 30, 29, 28, 25, 24, 23, 20

**FD-MS** (m/z): (100%) 1367.2 ( $\text{M}^+$ ), calculated ( $\text{C}_{74}\text{H}_{142}\text{O}_{13}\text{S}_4$ ) = 1368.21, (7%) 2736.0 ( $\text{M} + \text{M}^+$ ), calculated ( $2 \times \text{C}_{74}\text{H}_{142}\text{O}_{13}\text{S}_4$ ) = 2736.42

## 2.6. Synthesis of thiolated lipid with an extended hydrophobic part (DDPTT)

### 2.6.1. Introduction and motivation

The preparation of tether lipids for tBLMs with diluted tethered inner leaflet was the main task in most of the sections in this work (2.3 - 2.5). Within all these projects the general strategy is to dilute the tethered thiolipids either by varying the ethylene glycol chain length in the tethering part (2.3) or by changes in the lateral space (insertion of small lateral spacer molecules (2.4) or utilization of bulky anchor (2.5)). However, the preparation of more diluted SAMs in this way tends to decrease the hydrophobicity of the inner leaflet which is the main drawback when preparing tBLMs on silicon-wafers.<sup>49</sup> A low hydrophobicity seems to impede the vesicle fusion process. Additionally, the low amount tethered lipids decreases the stability of the membrane and increases the probability for leakage through the tBLM.

An alternative strategy is an increase of the hydrophobic part in the tether lipid. Coupling more than one or two hydrophobic chains to one hydrophilic spacer, one can control the lateral density in the submembrane space. Lipids with more than two alkyl chains in the hydrophobic part are found in nature. For instance, cardiolipin is a tetra acyl lipid, mainly found in energy transducing membranes, such as the bacterial membrane and the inner mitochondrial membranes. Addition of small amounts of bovine heart cardiolipin into egg-yolk phosphatidylcholine liposomal membranes causes a significant decrease in their water permeability associated with stabilization of the membrane structure.<sup>50</sup> As a variation of the tetra acyl lipids, archaeal cardiolipins are composed of four phytanyl chains ether-linked to glycerol. Furthermore, they have two phosphate groups or other highly acidic residues as the polar head groups.<sup>51</sup> Another example for natural lipids with more hydrophobic chains is Lipid A, a part of lipopolysaccharides derived from different groups of Gram-negative bacteria. Lipid A has four (R)-3-hydroxy fatty acids in ester and amide linkages. Two of them are usually further acylated at their 3-hydroxyl group. Lipid A provides a hydrophobic anchor that secures the lipopolysaccharide molecule within the membrane.<sup>52</sup> Some synthetic approaches to mimic these natural lipids were explored. S. M. Schiller tried to mimic

Lipid A by synthesis of glycolipids with 5 chains in the hydrophobic part,<sup>53</sup> while Cornells *et al.* proposed lipid molecule with 3 chains.<sup>15</sup>

Therefore, a new tether lipid molecule (DDPTT) with four phytanyl chains and thus providing significant hydrophobicity was synthesized in our group. The phytanyl chains are attached via three glycerol linkers to TEG as a tethering part (Figure 2.16). The synthetic route includes the synthesis of an intermediate precursor with allyl functionality, appropriate for preparation of lipids for gold and silicon oxide surfaces.

The structure of DDPTT is design to provide two main advantages. First, the extended hydrophobic part allows for the adjustment of the packing constrains within the hydrocarbon region of the membrane and thus simultaneously stabilize the bilayer and decrease the ion-permeability. Second, it defines a lower two-dimensional packing density in the tether region of the assembled membrane, which facilitates incorporation of protein with large sub-membrane domains.



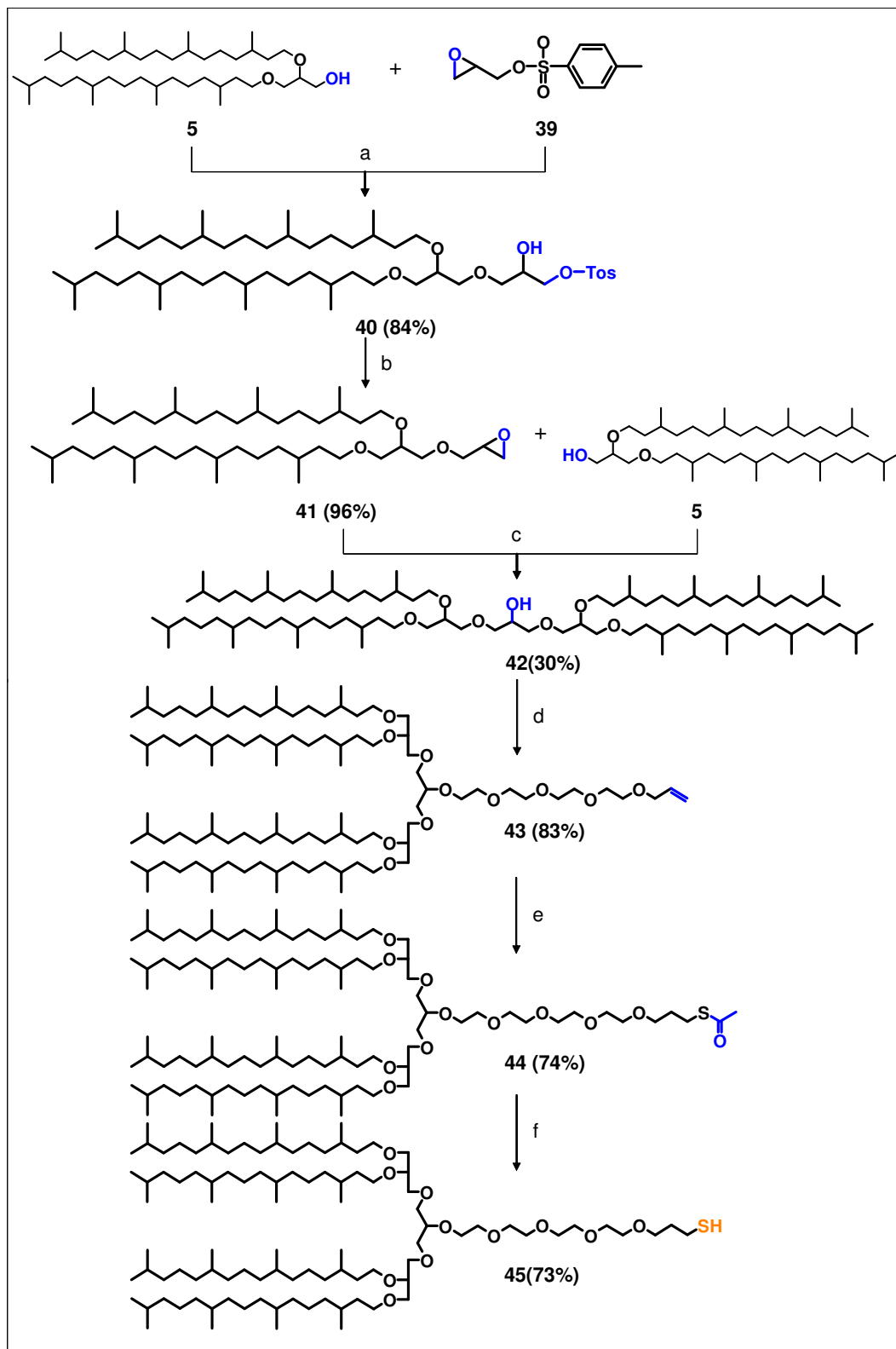


Figure 2.16. Synthesis of tether lipid (DDPTT) with extended hydrophobic part

### 2.6.2. Results and discussion

The central reaction in the presented synthetic pathway (Figure 2.16) is the  $\text{BF}_3 \cdot \text{Me}_2\text{O}$  catalyzed reaction of glycidyl tosylate (**39**) with DPG (**5**). The high reactivity of **39**, caused by the epoxy ring, allows an alternating opening (reactions **a**, **b**) and closing (reaction **c**) of the ring. The latter allows for a selective nucleophilic addition of different substituents to each oxygen atom in the molecule. Moreover, the main priority utilizing glycidyl tosylate over any protected glycerol is the opportunity to simultaneously reduce the number of synthetic steps avoiding additional protection and deprotection of certain hydroxyl groups and activation of the hydroxyl group (dehydrogenation with NaH) in the nucleophile. This method, permitting the introduction of different substituents via  $\text{BF}_3$  – catalyzed alcoholysis of glycidyl derivatives was developed by Bittman *et al.*<sup>54</sup> and successfully applied later by C. Breffa.<sup>23</sup>

The strategy towards the synthesis of lipid with an extended hydrophobic part includes three main steps: synthesis of the hydrophobic head group, introduction of a double bond functionalized spacer part and modification of the double bond with an anchor group.

According to the synthetic strategy, the first reaction was the opening of the epoxy ring of glycidyl tosylate by the nucleophilic addition of DPG (reaction **a**). The reaction was performed in the presence of  $\text{BF}_3 \cdot \text{Me}_2\text{O}$  catalyst that weakens the bonds of the epoxide attracting the oxygen free electrons (Figure 2.17). Then, DPG attacked (due to steric reasons) the less substituted carbon atom in the epoxy ring resulting in monosubstituted glyceryl tosylate (**40**) with a considerable yield of 84%.

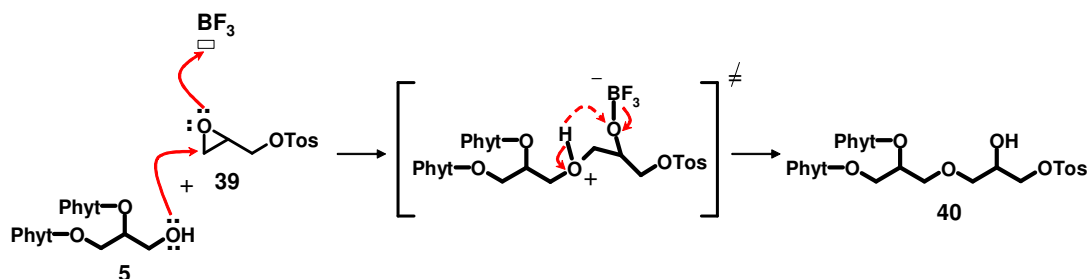


Figure 2.17. Nucleophilic addition to an epoxide in conditions of  $\text{BF}_3 \cdot \text{Me}_2\text{O}$  catalyst

In order to introduce the second DPG molecule, the epoxy ring in product **40** was closed again from the other side. For this purpose, an internal nucleophilic substitution reaction was done (reaction **b**). The free secondary hydroxyl group was deprotonated in presence of base. Then, the leaving (tosyl) group located next to the obtained alkoxide ion was displaced forming an epoxy ring. Similar to results observed previously,<sup>23,54</sup> the reaction was almost quantitative (96%). In this regard, it should be taken into account that no polymerization reaction has occurred.

The most crucial step in the synthesis of DDPTT was the coupling of **41** with a second equivalent of DPG (reaction **c**) conducted in the same conditions applied for the first epoxy ring opening. The problem stems from the fact that once obtained, the main product **42** by releasing a free hydroxyl group can further react with **41** leading to a competing side product (Figure 2.18). The existence of a side product was verified by FD-MS, where signals at 2071.8 m/z corresponding to this compound ( $M_w=2071,67$  g/mol) were observed. The polarity of both main and side products was similar that made the isolation of the target product difficult. The formation of a side product and the purification problems are the main reason for the obtained low yield (30%).

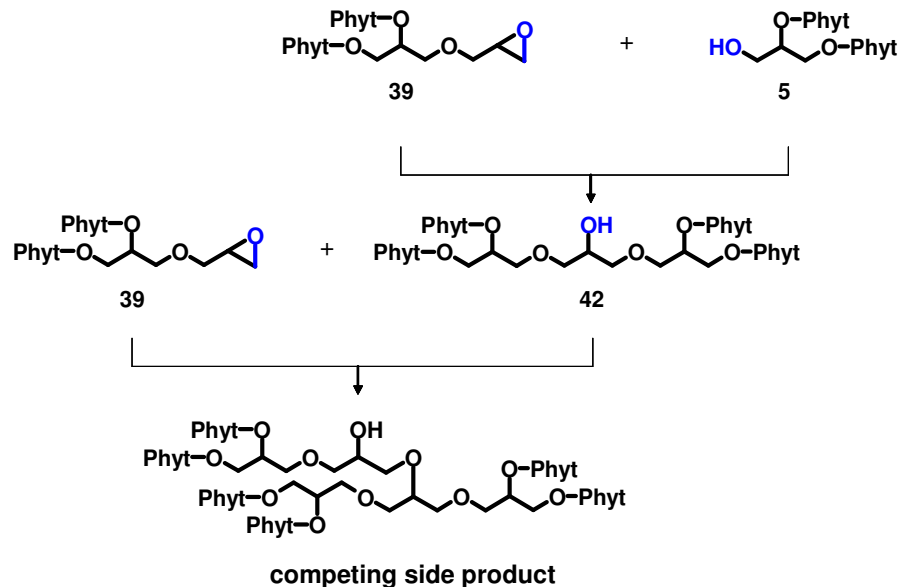


Figure 2.18. Competing side reaction of product **42** to the initial compound **39**

The second main point in the DDPTT synthesis was the coupling of the obtained extended hydrophobic head (**42**) with **12**. This step was accomplished by Williamson

coupling described already in section 2.2.2. Although the nature of the secondary type hydroxyl group participated in the reaction and the possible steric hindrance of the bulky phytanyl chains, the reaction was conducted successfully achieving a yield of 83%.

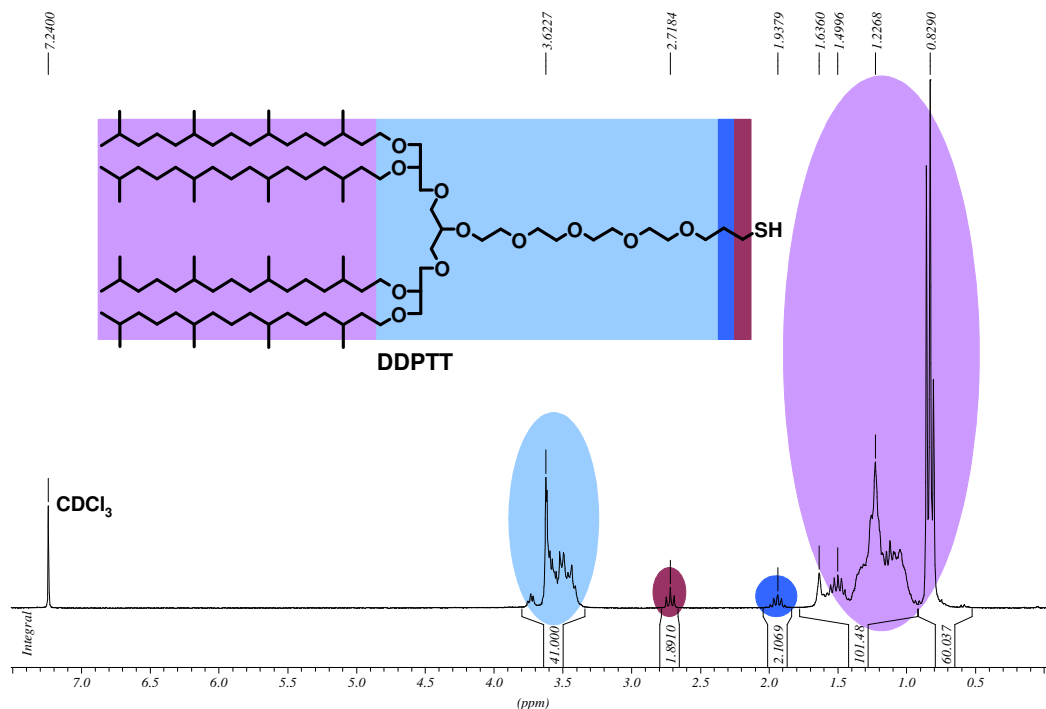


Figure 2.19.  $^1\text{H}$  NMR spectra of DDPTT

Finally, the double bond in **43** was transformed into an anchor. In our case, the lipid was functionalized with a thiol, suitable for gold surface. Following a strategy already described in section 2.2.4 the target thiolipid DDPTT was obtained. The structure was verified by  $^1\text{H}$  NMR (Figure 2.19).

### 2.6.3. Conclusion

The method reported here allowed for the preparation of tether lipids with an extended lipophylic part via combination of  $\text{BF}_3$  – catalyzed alcoholysis of glycidyl derivatives, Williamson coupling and modification of the double bond. The latter can be done according to the substrate chosen for immobilization of the obtained lipid molecule. In our case, the double bond was transferred in thiol group. Future modification with silane

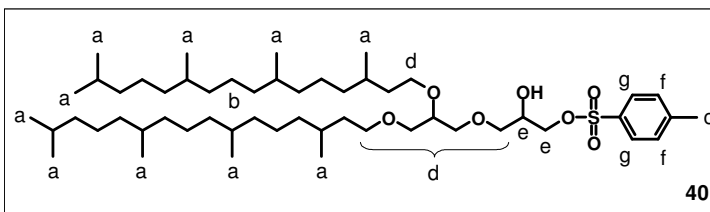
anchor for silicon oxide surfaces may solve the problem with rather diluted SAMs obtained on silicon wafers.

Further application of DDPTT is supposed to contribute to simultaneously preparation of more homogeneously diluted SAMs (the vesicle fusion process will be facilitated). At the same time more densely packed and leakage free proximal layer of the membrane can be formed.

#### 2.6.4. Experimental part

##### Reaction a:

##### Opening of the epoxy ring



The glassware used in reactions **a**, **c**, and **d** was dried and purged with Ar prior to use. DPG **5** (570 mg, 0.87 mmol, 653.18 g/mol) and glycidyl tosylate **39** (176 mg, 0.772 mmol, 230.28 g/mol) were dissolved in dry DCM (2.5 ml) in a 2 neck round bottom flask. One drop of catalyst  $\text{BF}_3 \cdot \text{Me}_2\text{O}$  was added at RT. The reaction continued to stir overnight at RT. After the completion of the reaction (verified by TLC), 5 ml water was added to quench the catalyst. The water layer was extracted 3 times with DCM. The organic layers were collected and the solvent was evaporated. The product **40** was purified by flash chromatography. Eluents: HE/EtAc (5/1 gradually to 1/1).

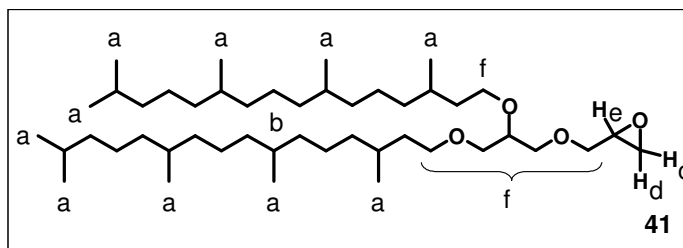
**Yield:** 520 mg, (84%)

**TLC:** HE/EtAc (5/1),  $R_f = 0.25$

**$^1\text{H NMR}$**  (250 MHz,  $\text{CDCl}_3$ , RT)  $\delta_{\text{H}}$ , ppm: 0.8 (t, 30 $H_a$ ), 0.9 - 1.7 (m, 48 $H_b$ ), 2.4 (s, 3 $H_c$ ), 3.35 - 3.65 (m, 11 $H_d$ ), 3.85 - 4.1 (m, 3 $H_e$ ), 7.3 (d, 2 $H_f$ ), 7.7 (d, 2 $H_g$ )

**FD-MS** (m/z): (100%) 882.2 ( $M^+$ ), calculated ( $\text{C}_{53}\text{H}_{100}\text{O}_7\text{S}$ ) = 881.45, (70%) 1762.9 ( $M + M^+$ ), calculated ( $2 \times \text{C}_{53}\text{H}_{100}\text{O}_7\text{S}$ ) = 1762.9, (30%) 2646.3 ( $2M + M^+$ ), calculated ( $3 \times \text{C}_{53}\text{H}_{100}\text{O}_7\text{S}$ ) = 2644.35

**Reaction b:**  
**Formation of oxyrane cycle**



**40** (520 mg, 0.59 mmol, 881.45 g/mol) was dissolved in MeOH (11.5 ml) in a 3 neck round bottom flask. The solution was cooled to 0°C, followed by addition of the catalyst  $K_2CO_3$  (270 mg, 1.974 mmol). The reaction mixture was allowed to slowly warm up to RT, and was stirred for 23 hrs, until TLC revealed the formation of **41** and consumption of the starting materials. The reaction mixture was neutralized with about 15 ml sat.  $NH_4Cl$  solution. Tosylic acid precipitated from the solution. The water layers as well as the precipitated tosylate salts were extracted 3 times with diethyl ether. The organic layers were washed with sat. NaCl solution until the pH reached 7.0 and dried over  $MgSO_4$ . The solvent was evaporated. The product **41** was used without further purification.

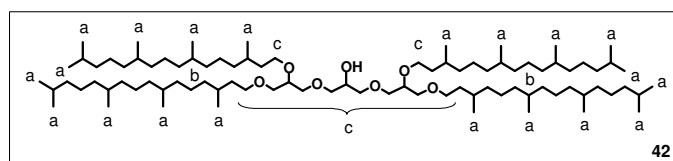
**Yield:** 400 mg, (96%)

**TLC:** HE/EtAc (10/1),  $R_f = 0.37$

**$^1H$  NMR** (250 MHz,  $CDCl_3$ , RT)  $\delta_H$ , ppm: 0.8 (t, 30 $H_a$ ), 0.9 - 1.7 (m, 48 $H_b$ ), 2.55 - 2.63 (m, 1 $H_c$ ), 2.8 (t, 1 $H_d$ ), 3.08 - 3.17 (m, 1 $H_e$ ), 3.35 - 3.8 (m, 11 $H_f$ )

**FD-MS** (m/z): (100%) 710.2 ( $M^+$ ), calculated ( $C_{46}H_{92}O_4$ ) = 709.24, (60%) 1419.2 ( $M + M^+$ ), calculated ( $2 \times C_{46}H_{92}O_4$ ) = 1418.48, (14%) 2125.0 ( $2M + M^+$ ), calculated ( $3 \times C_{46}H_{92}O_4$ ) = 2129.0

**Reaction c:**  
**Coupling of 41 with DPG (5)**



DPG **5** (420 mg, 0.64 mmol, 653.18 g/mol), **41** (400 mg, 0.56 mmol, 709.24 g/mol) and two drops of  $BF_3 \cdot Me_2O$  were placed in 2 neck round bottom flask and dissolved in dry DCM (7 ml). The mixture was allowed to stir at RT for 20 hrs until FD-MS revealed reaction of the product with excess reactants to form a competing side product. About 5 ml water was added to quench the catalyst. The water layers were extracted 3 times with DCM. The organic layers were collected and the solvent was evaporated. The product **42** was purified by flash chromatography. Eluents: HE/EtAc (10/1). Due to

incomplete separation, a second chromatography column was performed. Eluents: HE/DCM (1/30).

**Yield:** 230 mg, (30%)

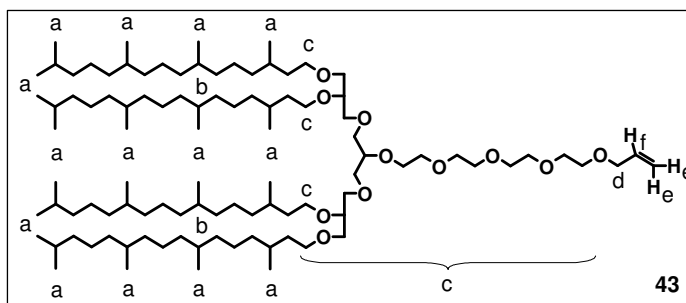
**TLC:** HE/EtAc (10/1),  $R_f = 0.29$

**$^1\text{H NMR}$**  (250 MHz,  $\text{CDCl}_3$ , RT)  $\delta_{\text{H}}$ , ppm: 0.8 (t, 60 $H_a$ ), 0.9 - 1.8 (m, 96 $H_b$ ), 3.35 - 4.0 (m, 23 $H_c$ )

**FD-MS** (m/z): (100%) 1361.9 ( $M^+$ ), calculated ( $\text{C}_{89}\text{H}_{180}\text{O}_7$ ) = 1362.42, (75%) 2726.5 ( $M + M^+$ ), calculated ( $2 \times \text{C}_{89}\text{H}_{180}\text{O}_7$ ) = 2724.84

**Reaction d:**

**Addition of the hydrophilic spacer part**



**42** (230 mg, 0.169 mmol, 1362.42 g/mol) and NaH (40 mg, 1.6 mmol, 24 g/mol) dissolved in dry THF (4 ml) were introduced in a 2 neck round bottom flask. This mixture was stirred at RT for 1.5h. Allyl-tetra(ethylene glycol)-tosylate (**12**) (270 mg, 0.695 mmol, 388.48 g/mol) dissolved in dry THF (4 ml) was added dropwise over 30 min at 40°C, and the mixture was stirred overnight at the same temperature. During the reaction, additional amounts NaH (about 80 mg, 3.3 mmol) were added. After 18 hrs, FD-MS and TLC revealed the formation of the product **43**. A few drops of water were added to quench the excess NaH. Precipitated salts were removed by centrifugation for 15 minutes at 9000 rpm. The solvent was evaporated in vacuum. The product **43** was purified by flash chromatography. Eluents: DCM/EtAc (30/1 gradient to 1/1).

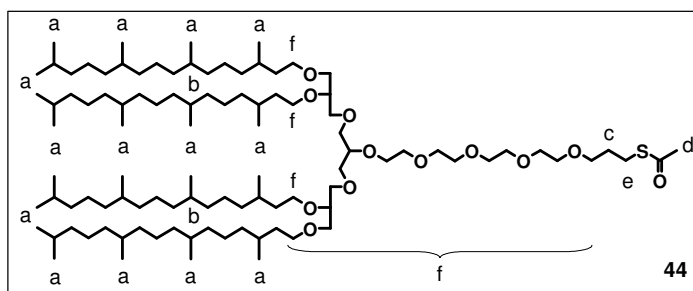
**Yield:** 220 mg, (83%)

**TLC:** DCM/EtAc (30/1),  $R_f = 0.37$

**$^1\text{H NMR}$**  (250 MHz,  $\text{CDCl}_3$ , RT)  $\delta_{\text{H}}$ , ppm: 0.8 (t, 60 $H_a$ ), 0.9 - 1.7 (m, 96 $H_b$ ), 3.35 - 3.8 (m, 39 $H_c$ ), 3.9 (d, 2 $H_d$ ), 5.1 - 5.3 (m, 2 $H_e$ ), 5.8 - 6.0 (m, 1 $H_f$ )

**FD-MS** (m/z): (100%) 1577.0 ( $M^+$ ), calculated ( $\text{C}_{100}\text{H}_{200}\text{O}_{11}$ ) = 1578.70, (15%) 3166.3 ( $M + M^+$ ), calculated ( $2 \times \text{C}_{100}\text{H}_{200}\text{O}_{11}$ ) = 3157.4

**Reaction e:**  
**Thiolation of the lipid**  
**precursor (first step)**



Product **43** (220 mg, 0.14 mmol, 1578.70 g/mol), thioacetic acid (550 mg, 7.24 mmol, 76 g/mol) and AIBN (3.5 mg, 0.02 mmol, 164.21 g/mol) were placed in a Schlenk flask and dissolved in toluene (1 ml). The solution was degassed 3 times. The flask was filled with Ar, and was stirred for 24h at 70°C. A TLC check showed the completion of the reaction. The solvent was evaporated under vacuum. The product **44** was purified by column chromatography. Eluents: DCM/EtAc (10/1 gradient to 3/1).

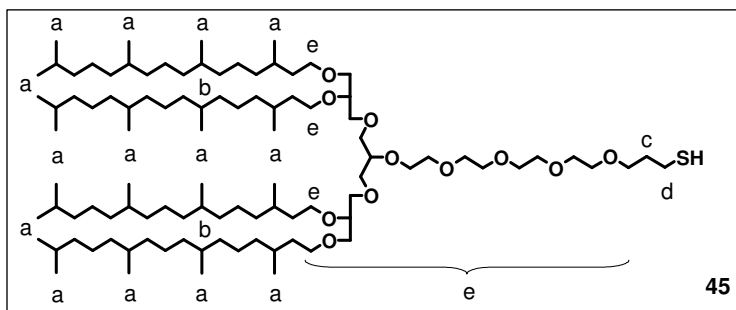
**Yield:** 170 mg, (74%)

**TLC:** DCM/EtAc (10/1),  $R_f = 0.52$

**$^1\text{H NMR}$**  (250 MHz,  $\text{CDCl}_3$ , RT)  $\delta_{\text{H}}$ , ppm: 0.8 (t, 60 $H_a$ ), 0.9 - 1.7 (m, 96 $H_b$ ), 1.8 (p, 2 $H_c$ ), 2.3 (s, 3 $H_d$ ), 2.9 (t, 2 $H_e$ ), 3.3 - 3.8 (m, 41 $H_f$ )

**FD-MS** (m/z): (100%) 1651.6 ( $M^+$ ), calculated ( $\text{C}_{102}\text{H}_{204}\text{O}_{12}\text{S}$ ) = 1654.82

**Reaction f:**  
**Thiolation of the lipid**  
**precursor (second step)**



Thioacetate **44** (170 mg, 0.10 mmol, 1654.82 g/mol) was dissolved in THF (2.4 ml) in a round bottom flask. 1M NaOH (0.4 ml) was added. The heterogeneous mixture was stirred vigorously overnight at 50°C. The reaction was monitored by TLC. After the completion of the reaction, 1M  $\text{H}_2\text{SO}_4$  was added and stirred for 30 min at RT to neutralize the mixture. Then, the solvent was evaporated under vacuum. The product was dissolved in DCM and washed consecutive with  $\text{H}_2\text{O}$ , 1M  $\text{H}_2\text{SO}_4$  and sat.  $\text{Na}_2\text{CO}_3$  solution. The organic layers were collected and dried over  $\text{Na}_2\text{SO}_4$ . After filtration, the solvent was removed, and the product **45** was purified by column chromatography. Eluents: PE/EtAc (5/1 gradient to 2/1).



**Yield:** 120 mg, (72%)

**TLC:** DCM/EtAc (10/1),  $R_f = 0.52$

**$^1\text{H NMR}$**  (250 MHz,  $\text{CDCl}_3$ , RT)  $\delta_{\text{H}}$ , ppm: 0.8 (t, 60 $\text{H}_a$ ), 0.9 - 1.7 (m, 96 $\text{H}_b$ ), 1.9 (p, 2 $\text{H}_c$ ), 2.7 (t, 2 $\text{H}_d$ ), 3.35 - 3.8 (m, 41 $\text{H}_e$ )

**FD-MS** (m/z): (100%) 3223.1 ( $\text{M} + \text{M}^+$ ), calculated ( $2 \times \text{C}_{100}\text{H}_{202}\text{O}_{11}\text{S}$ ) = 3225.56, (12%) 1612.0 ( $\text{M}^+$ ), calculated ( $\text{C}_{100}\text{H}_{202}\text{O}_{11}\text{S}$ ) = 1612.78

**$^{13}\text{C NMR}$**  ( $\text{CD}_2\text{Cl}_2$ )  $\delta_{\text{C}}$ , ppm: 78.4, 77.9, 71.7, 71.1, 70.8, 70.6, 70.0, 69.3, 69.0, 39.38, 37.4, 36.79, 35.31, 32.8, 29.9, 29.1, 27.9, 24.8, 24.5, 22.6, 19.7

## 2.7. Synthesis of fluorescent labeled lipids

### 2.7.1. Introduction and motivation

Fluorescent probes can give useful information about structural and functional properties of a system. Mimicking their natural counterparts, fluorescent labeled lipids have provided specific information about the dynamics of lipids within a membrane and the membrane structure and its properties.

For example, they have been used to investigate membrane fusion, as an important process involved in many cellular processes.<sup>55</sup> Ohki *et al.*<sup>56</sup> have found that a certain degree of hydrophobicity of the vesicle surface is needed to observe vesicle fusion process. It has been shown that the required hydrophobicity can be achieved by increasing the interfacial tension and lowering the surface dielectric constant (insertion of PEG or increasing the fusogenic ion concentration). Additionally, the transmembrane diffusion of phospholipids in biological and artificial membranes (flip-flop effect) has been extensively studied.<sup>57</sup> Furthermore, labeled lipids are used to investigate membrane fluidity<sup>58</sup> (determining the diffusion coefficient of the lipids) and membrane homogeneity<sup>59,60</sup> (investigating the possibility of phase separation).

Some of the most widely used fluorescent dyes for coupling to lipidic structures are pyrene, 7-nitro-2-1,3-benzoxadiazol-4-yl (NBD), 5-dimethylamino-1-naphthalene sulfonyl (dansyl), rhodamine and coumarin. In principle, a dye can be attached to both parts of an amphiphile, the hydrophilic and hydrophobic part. However, the introduction of the fluorescent probe might cause change in the intermolecular structure and the labeling position has to be chosen carefully. For instance, chain-labeled lipid analogues are the probes of choice if the lipid head group may play a functional role.<sup>61,62</sup> Alternatively, head group labeled lipids can be used in cases, when properties of the hydrophobic chain region are important (e.g. phase determination) or for probing the aqueous environment of the membrane (e.g. the attached labels, accessed by the surrounding media, detect the hydrophobicity on the surface<sup>56</sup> and pH values<sup>63</sup> near to the head groups).

The evaluation of the localization, function and interactions of the lipids can be done by exploring the fluorescent properties of the dyes which are sensitive to their environment. Thus, incorporation of fluorescent-tagged lipid analogues within the lipid

bilayer allows investigation of the environment-dependant changes by the commonly used fluorescent quenching, fluorescent recovery after photobleaching, resonance energy transfer and excimer formation.

In order to illustrate assembly properties of tBLMs, we synthesized anchor-lipid precursor with fluorescent tag. Until now, synthesis and properties of fluorescent, polymerizable and metal-chelating lipids have been described in the literature, but they were used only for fabrication of polymerizable liposomes.<sup>64</sup>

Herein, we present the synthesis of fluorescent labeled tether lipids with a double bond functionality enabling the attachment to different surfaces (Figure 2.21). The dansyl group was chosen as a fluorescent dye due to its relatively small size, ease of coupling and expected optical properties. In order to not hinder the intermolecular arrangement and interactions within the hydrophobic region of the membrane, the labeling was done by the glycerol head group.

A suitable technique to study the lipid arrangement within the monolayer is the Langmuir film balance. However, the mechanism of the lipid interaction on the air-water interface is not clear. Therefore, such fluorescent labeled tether lipids will permit directly observation of the lipid redistribution on the air-water interface during the lipid monolayer compression by simultaneous application of LB technique and fluorescence microscopy. Furthermore, tethered lipid distribution after monolayer transfer on glass substrates can be investigated.<sup>25,27</sup>

### 2.7.2. Results and discussion

The structure of the obtained fluorescent labeled tether lipid precursors **51** and **58** are given in Figure 2.21. They have one and two phytanyl chains, respectively connected *via* a glycerol moiety to the TEG spacer part. The tethering spacer is terminated with a double bond functionality. The choice of the dansyl group as a fluorophore was governed from the relatively compact structure of the naphthalene core in this group, because evidently, the bigger the structure is, the higher the mismatch possibility. On the other hand, the fluorescent dye was attached to the glycerol head group coming from the assumption that the fluorescent probe will not hinder the lipid interactions during the monolayer formation.

Two different synthetic pathways were examined to obtain fluorescent labeled tether lipid. The first one is shown in Figure 2.20.

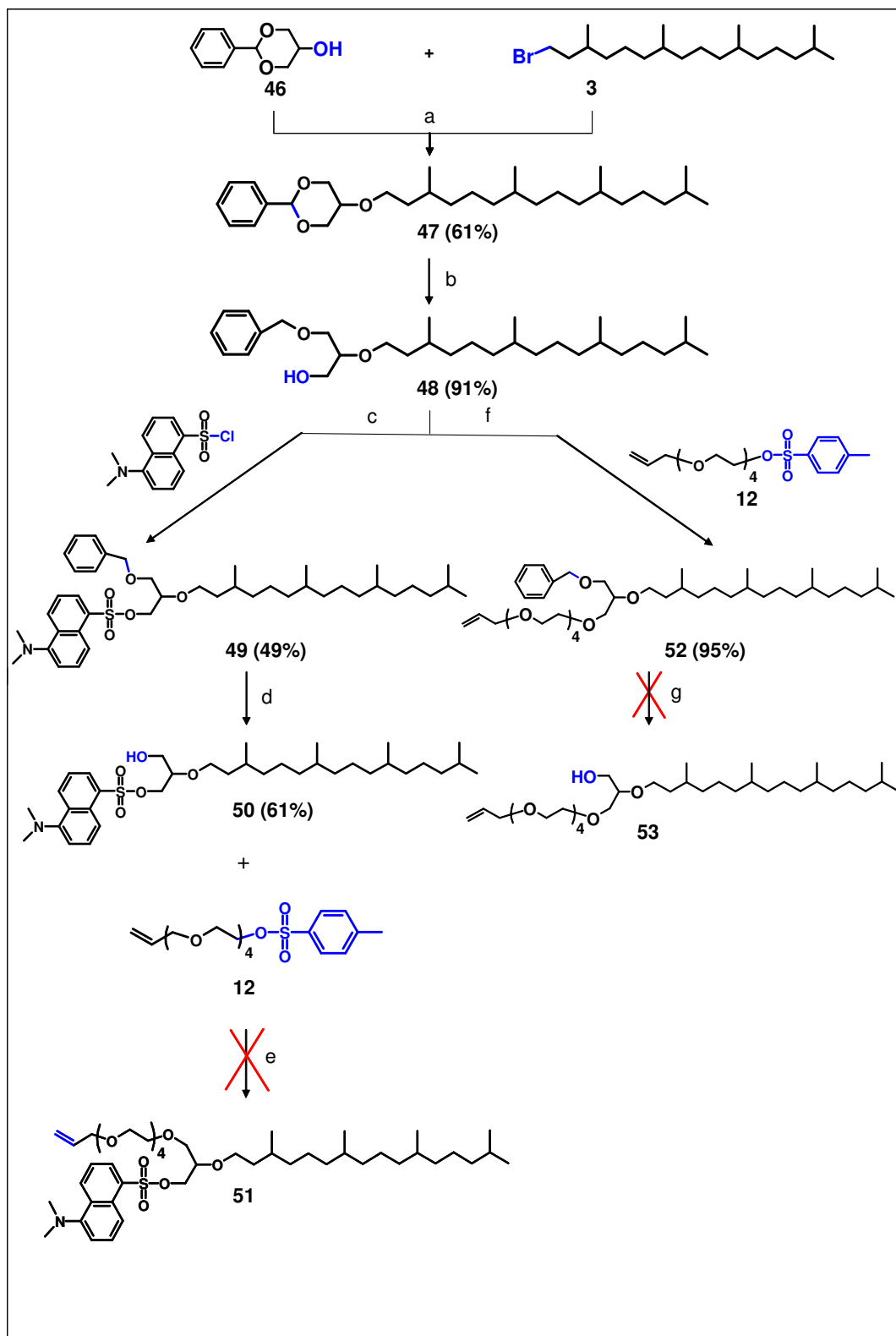


Figure 2.20. Synthetic pathway for preparation of fluorescent labeled tether lipids that failed

The strategy involves consecutive nucleophilic substitution of the hydroxyl groups in the glycerol molecule starting with benzylidene glycerol (**46**). Firstly, the phytanyl group was introduced in order to increase the hydrophobicity of the intermediates, and thus, as it was discussed previously (section 2.5.3), the TLC detection and the isolation of the products will be facilitated. Then, the protected hydroxyl groups were consecutive released. Two opposite approaches for the insertion of the fluorophore and the spacer part were tested. According to the first one, the dansyl group was introduced initially (reaction **c**). After cleavage of the benzyl group (reaction **d**), all attempts towards the attachment of the spacer failed (reaction **e**). The reason for this is most probably the nature of the dansyl group, which can act as a good leaving group in the conditions of  $S_N^2$  reactions. Therefore, a side reaction of intra- and intermolecular  $S_N^2$  reaction of **50** can be observed. During the reaction, the TLC revealed the formation of product **51**, but the conducted column chromatography and further preparative chromatography did not contribute to satisfactory separation and only few milligrams pure product were isolated. The second approach includes the opposite sequence of the reaction steps. The spacer part (product **12**) was initially coupled to the monoprotected phytanyl glycerol (**48**) almost quantitatively (95%). Next, reaction **g** required cleavage of the benzyl group in presence of a double bond and was conducted in milder conditions with chlorosulfonyl isocyanate (CSI).

Deprotection of benzyl and p-methoxybenzyl groups without affecting the other functional groups including double bond has been reported in the literature<sup>65</sup> as a new and mild methodology using CSI-NaOH reaction conditions. The mechanism of the reaction is shown below:

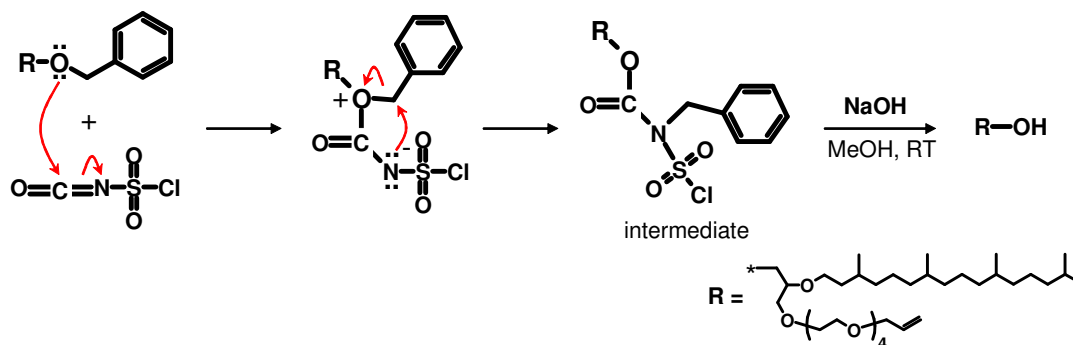


Figure 2.21. Mechanism of benzyl deprotection of product **52** by CSI-NaOH (reaction **g**, Figure 2.20)

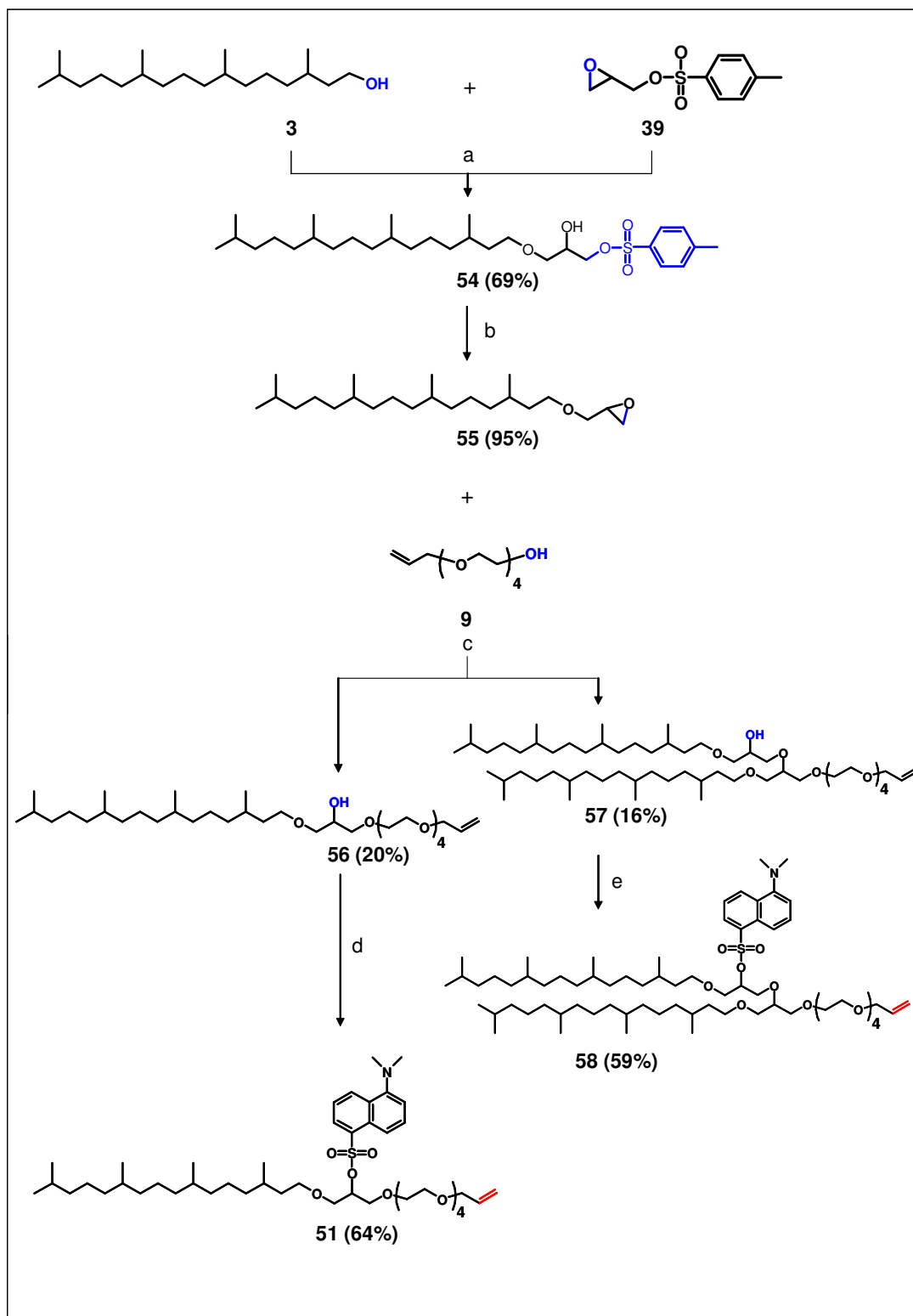


Figure 2.22. Successful synthetic pathway for preparation of fluorescent labeled tether lipids

The protected compound reacts with CSI forming an intermediate. Then, addition of NaOH releases the cleaved product. Unfortunately, in our case, only formation of the intermediate complex was observed by FD-MS and further treatment with NaOH did not result in the cleavage of complex to give product **53**.

The second synthetic pathway towards the synthesis of fluorescent labeled lipid precursor is shown in Figure 2.22. Glycidyl tosylate (**39**) was used as starting material in this synthetic route as in the synthesis of DDPTT in the former section 2.6.2. As already mentioned, the use of glycidyl tosylate is advantageous because of the high reactivity of the epoxy ring and no protection groups are required. Similar to the first approach, the initial step was the introduction of the hydrophobic phytanyl chain accompanied with the opening of the epoxy ring. Then, the ring was closed again in basic conditions to give **55** with almost quantitative yield of 95% (reaction **b**). The crucial reaction in this synthesis was the nucleophilic addition of the double bond functionalized TEG (**9**) to the epoxy ring of **55** (reaction **c**). The second opening of the ring and the release of a hydroxyl group in the target product **56** was prone to a side reaction. This side reaction occurred by competing nucleophilic addition of the target product **56** to compound **55** revealed by TLC. As a result, two different lipid precursors with one (product **56**) and two (product **57**) phytanyl chains in the hydrophobic region were isolated by column chromatography. Both products possess a free hydroxyl group, needed for the final coupling with the fluorophore. The dansyl group was introduced by a nucleophilic substitution reaction with the lipid precursors (reactions **d**, **e**). The obtained target fluorescent labeled lipid precursors **51** and **58** were purified by column chromatography and characterized by  $^1\text{H}$  NMR,  $^{13}\text{C}$  NMR and FD-MS. The  $^1\text{H}$  NMR spectrum shown below confirms the structure of **51**. The  $^1\text{H}$  NMR spectrum of **58** is essentially the same only with doubled integral values corresponding to the signals of the phytanyl chains.

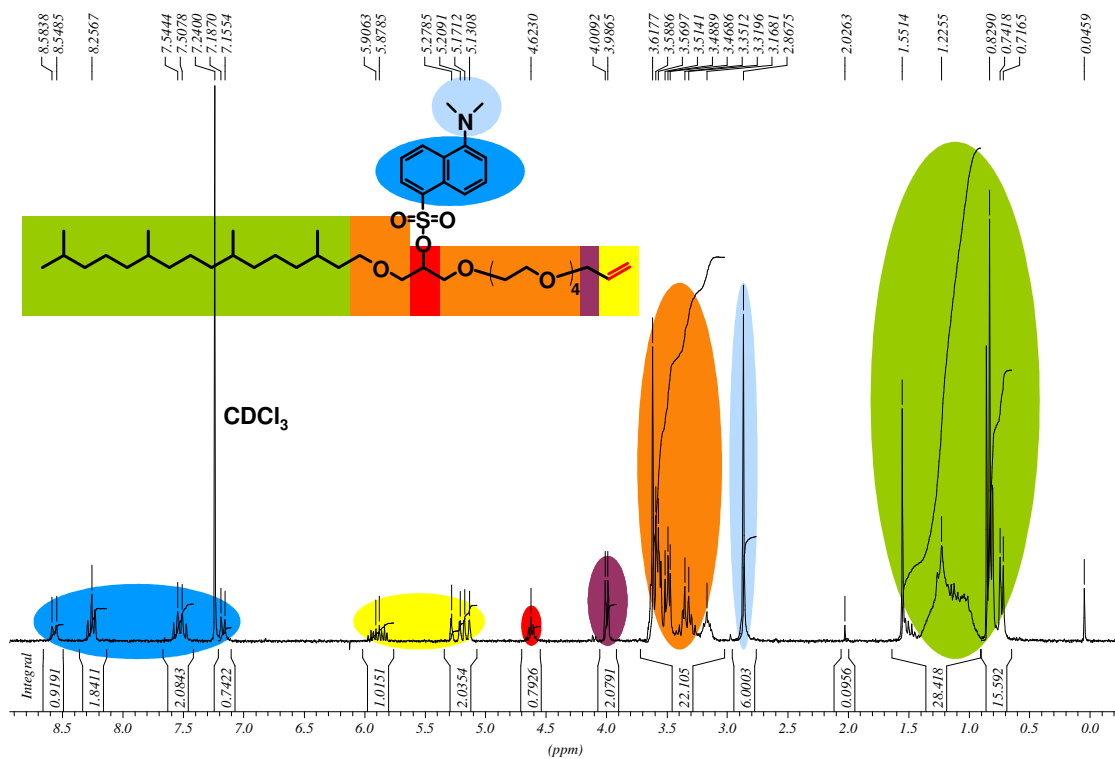


Figure 2.23.  $^1\text{H}$  NMR spectrum of fluorescent precursor **51**

In the FD-mass spectrum (Figure 2.24) the signal at 820.2 m/z corresponds to the molecular weight of the monophytanyl fluorescent precursor **51** (822.2 g/mol). Additionally, signals for di, tri and tetrameric clusters are observed.



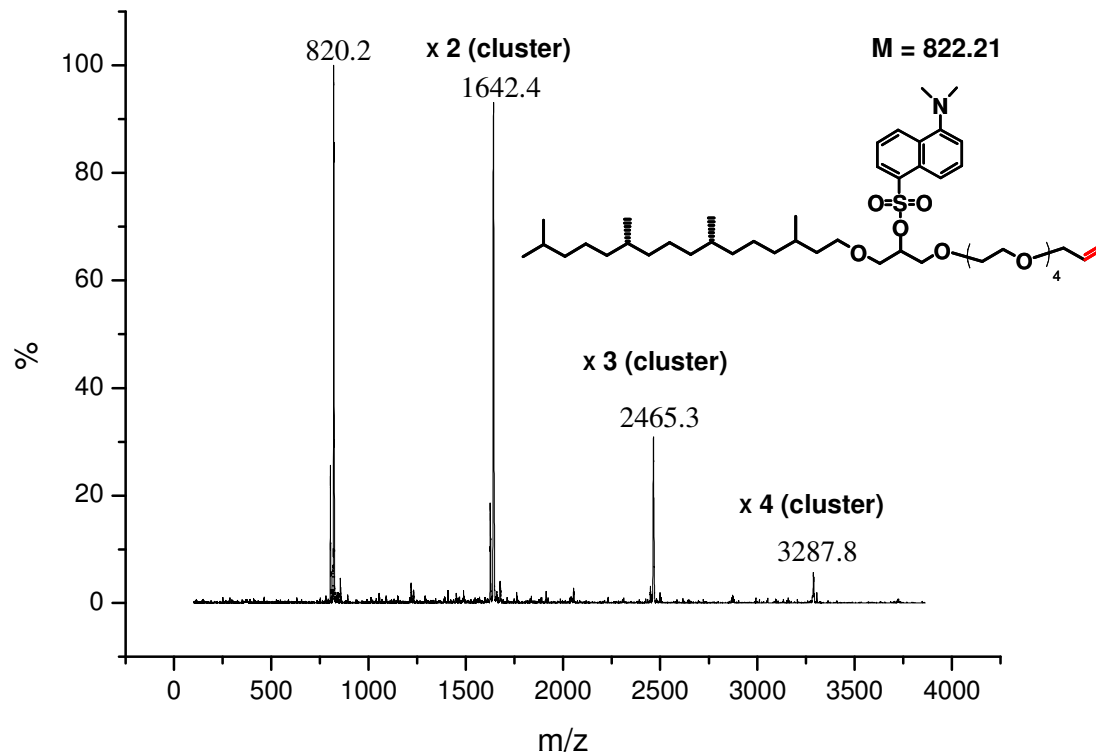


Figure 2.24. FD-mass spectrum of fluorescent precursor **51**

Finally, UV and fluorescent spectroscopy were used to measure the absorption and emission spectra of the fluorescent labeled compounds **51** and **58**. In Figure 2.25, the absorption and emission spectra (the green curves) of the initial fluorescent compound dansyl chloride are shown. The black and red curves represent the absorption and emission of the fluorescent labeled precursors **51** and **58**, and it is well seen that they match each other. Attachment of dansyl group to the lipids may cause conformational changes, hence, change in the energy levels of the fluorophore. Thus, compared to dansyl chloride, the absorption spectra of the labeled lipids are blue shifted and the emission spectra are red shifted.

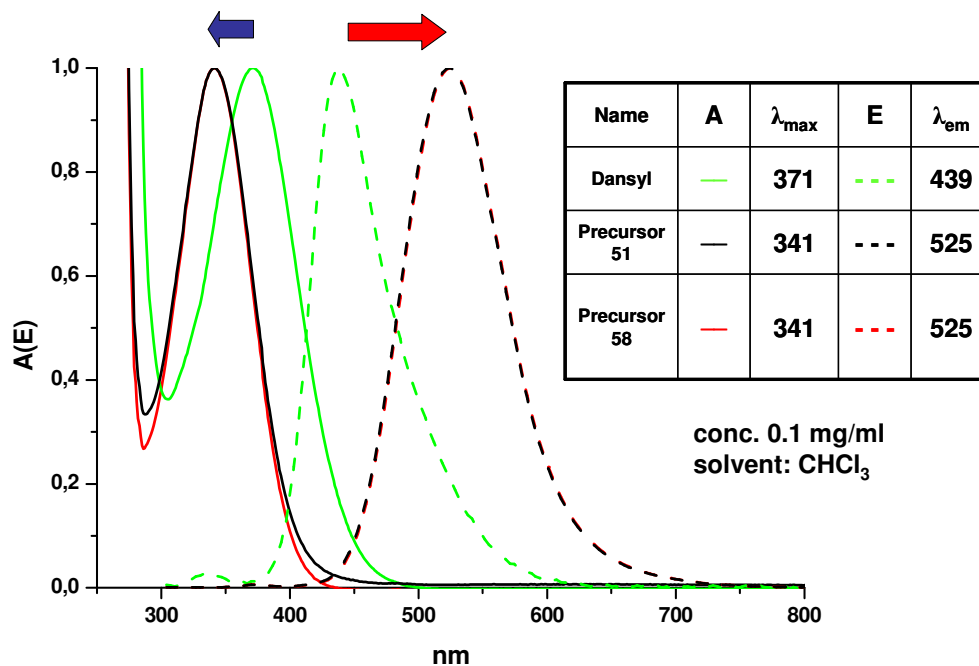


Figure 2.25. Absorption and emission spectra of dansylated compounds **51** and **58**

### 2.7.3. Conclusion

Two different approaches towards the synthesis of fluorescent labeled lipid precursor have been examined. Although, there was a lack of success with the first described synthetic pathway, the second one permitted the synthesis of two fluorescent labeled precursors with one and two phytanyl chains in the hydrophobic region. A dansyl group was successfully coupled to the glycerol head group in the final step. The target products **51** and **58** were characterized by  $^1\text{H}$  NMR,  $^{13}\text{C}$  NMR and FD-MS. The fluorescent activity of the lipids was verified by measuring the absorption and emission spectra compared with those of dansyl chloride.

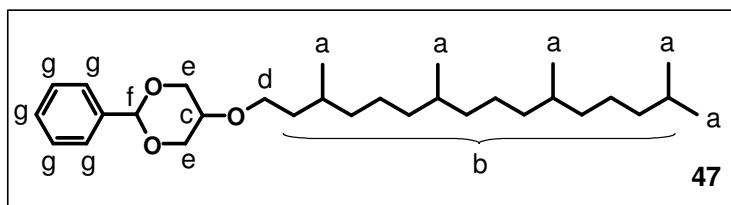
As an overview, the terminating double bond in precursors can be modified in anchors appropriate for different substrates ( $\text{SiO}_2$ , Au,  $\text{Al}_x\text{O}_y$ ). For the purpose of our study, the lipid precursors can be transformed in chloro- or alkoxy silane anchored fluorescent labeled lipids. Further LB-experiments with these lipids should give additional information for the lipid distribution on the water surface and the homogeneity of the deposited monolayers on the silicon oxide substrate. These experiments have not been done due to a lack of time.

## 2.7.4. Experimental part

Figure 2.20

Reaction a:

Introduction of the hydrophobic part



1, 3-O-benzylidene glycerol **46** (4.85 g, 26.91 mmol, 180.2 g/mol), about 20 ml dry THF, and NaH (1.3 g, 54.17 mmol, 24 g/mol) were added to a 2 neck round bottom flask. This mixture turned light green and was stirred for 2.5h at RT. The mixture was added dropwise to phytanyl bromide **3** (10 g, 27.67 mmol, 361.43 g/mol) dissolved in dry THF (25 ml) in a round bottom flask and stirred for 2.5 days at 40°C. Additional amounts of NaH were added in order to keep the reaction conditions dry. The reaction was monitored by TLC. After complete consumption of the starting materials, a few drops of water were added to quench excess of NaH. Precipitated salts were removed by centrifugation for 15 minutes at 9000 rpm. The solvent was evaporated in vacuum. The product **47** was purified by flash chromatography isolating two structural isomers: **47(1)** and **47(2)**. Eluents: HE/Et<sub>2</sub>O (7/1 gradient to 5/1).

**Yield:** **47(1)** 4.93 g, **47(2)** 2.66 g, overall: 7.59 g, (61%)

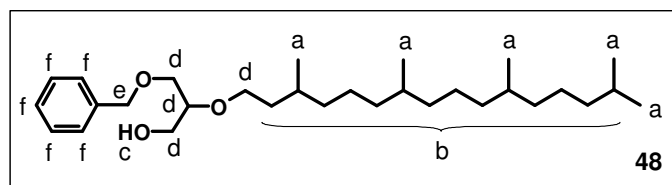
**TLC:** HE/Et<sub>2</sub>O (7/1), **47(1)** R<sub>f</sub> = 0.66; **47(2)** R<sub>f</sub> = 0.33

**<sup>1</sup>H NMR** (250 MHz, CDCl<sub>3</sub>, RT) δ<sub>H</sub>, ppm: **47(1)** 0.8 (t, 15H<sub>a</sub>), 0.9 - 1.7 (m, 24H<sub>b</sub>),

3.5 - 3.8 (m, 5H<sub>c+d+e</sub>), 4.3 - 4.5 (m, 2H<sub>e</sub>), 7.25 - 7.55 (m, 5H<sub>g</sub>); **47(2)** 0.8 (t, 15H<sub>a</sub>), 0.9 - 1.7 (m, 24H<sub>b</sub>), 3.2 (s, 1H<sub>c</sub>), 3.5 - 3.65 (m, 2H<sub>d</sub>), 4.0 (d, 2H<sub>e</sub>), 4.3 (d, 2H<sub>e</sub>), 5.5 (s, 1H<sub>f</sub>), 7.25 - 7.55 (m, 5H<sub>g</sub>)

**FD-MS** (m/z): **47(1)** (100%) 459.8 (M<sup>+</sup>), calculated (C<sub>30</sub>H<sub>52</sub>O<sub>3</sub>) = 460.75, (71%) 921.9 (M + M<sup>+</sup>), calculated (2 x C<sub>30</sub>H<sub>52</sub>O<sub>3</sub>) = 921.5; **47(2)** (100%) 920.9 (M + M<sup>+</sup>), calculated (2 x C<sub>30</sub>H<sub>52</sub>O<sub>3</sub>) = 921.5, (50%) 1382.5 (2M + M<sup>+</sup>), calculated (3 x C<sub>30</sub>H<sub>52</sub>O<sub>3</sub>) = 1382.3, (34%) 460.9 (M<sup>+</sup>), calculated (C<sub>30</sub>H<sub>52</sub>O<sub>3</sub>) = 460.75,

**Reaction b:**  
**Opening of the dioxane ring**



Product **47** (2.66 g, 5.77 mmol, 460.75 g/mol), DIBAH (13.5 ml, 20% w/w solution in toluene) and dry toluene (16 ml) were placed in a Schlenk flask. The reaction mixture was stirred for 24h at RT. A TLC check has shown the completion of the reaction. Some drops H<sub>2</sub>O were added to stop the reaction, while a white solid residue of Al(OH)<sub>3</sub> was formed. The mixture was filtrated over G3 filter, and the solid residue was washed thoroughly with H<sub>2</sub>O. The aqua solution was extracted with DCM 3 times. The organic layers were dried over MgSO<sub>4</sub> and evaporated under vacuum. The product **48** was purified by column chromatography. Eluents: HE/Et<sub>2</sub>O (1/1).

**Yield:** 2.43 g, (91%)

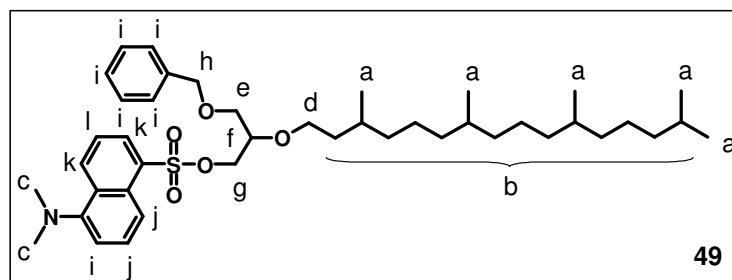
**TLC:** HE/Et<sub>2</sub>O (1/1), R<sub>f</sub> = 0.39

**<sup>1</sup>H NMR** (250 MHz, d<sub>8</sub> - THF, RT) δ<sub>H</sub>, ppm: 0.86 (t, 15H<sub>a</sub>), 1.0 - 1.65 (m, 24H<sub>b</sub>), 2.5 (s, 1H<sub>c</sub>), 3.4 - 3.8 (m, 7H<sub>d</sub>), 4.5 (s, 2H<sub>e</sub>), 7.15 - 7.4 (m, 5H<sub>f</sub>)

**<sup>13</sup>C NMR** (CD<sub>2</sub>Cl<sub>2</sub>) δ<sub>C</sub>, ppm: 138, 128, 127, 78, 74, 70, 69, 63, 39, 38, 33, 30, 28, 25, 24, 23, 20

**FD-MS** (m/z): (100%) 463.2 (M<sup>+</sup>), calculated (C<sub>30</sub>H<sub>54</sub>O<sub>3</sub>) = 462.76, (22%) 925.6 (M + M<sup>+</sup>), calculated (2 x C<sub>30</sub>H<sub>54</sub>O<sub>3</sub>) = 925.5, (40%) 1389.1 (2M + M<sup>+</sup>), calculated (3 x C<sub>30</sub>H<sub>54</sub>O<sub>3</sub>) = 1388.3

**Reaction c:**  
**Addition of the fluorescent moiety**



Product **48** (760 mg, 1.64 mmol, 462.76 g/mol), NaH (90 mg, 3.75 mmol, 24 g/mol) and dry THF (8 ml) were placed in a Schlenk flask. The reaction mixture was stirred for 3 hrs at RT. The alkoxide of **48** and triethylamine (0.23 ml, 1.68 mmol, 101.2 g/mol) were added dropwise to densyl chloride (890 mg, 3.29 mmol, 269.75 g/mol) dissolved in dry THF (10 ml) at 50°C. Additional amounts of NaH and densyl chloride were added during

the reaction. After 3 days, a TLC check revealed the formation of the product. The reaction was stopped. A few drops of water were added to quench excess of NaH. Precipitated salts were removed by centrifugation for 15 minutes at 9000 rpm. The solvent was evaporated in vacuum. The product **49** was purified by column chromatography. Eluents: PE/THF (15/1 gradient to 5/1).

**Yield:** 560 mg, (49%)

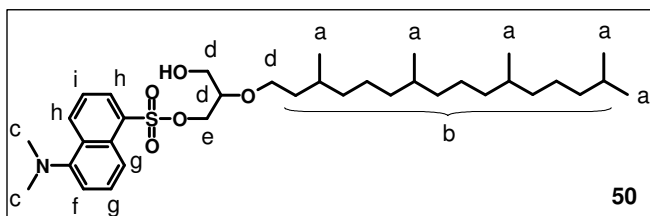
**TLC:** PE/THF (15/1),  $R_f = 0.35$

**$^1\text{H NMR}$**  (250 MHz,  $\text{CDCl}_3$ , RT)  $\delta_{\text{H}}$ , ppm: 0.7 - 0.9 (m, 15 $\text{H}_a$ ), 0.9 - 1.6 (m, 24 $\text{H}_b$ ), 2.8 (s, 6 $\text{H}_c$ ), 3.3 - 3.45 (m, 2 $\text{H}_d$  + 1 $\text{H}_e$ ), 3.55 - 3.65 (m, 1 $\text{H}_f$ ), 3.7 - 3.8 (m, 1 $\text{H}_e$ ), 3.9 - 4.2 (m, 2 $\text{H}_g$ ), 4.25 (s, 2 $\text{H}_h$ ), 7.1 - 7.3 (m, 6 $\text{H}_i$ ), 7.45 - 7.6 (m, 2 $\text{H}_j$ ), 8.2 (d, 2 $\text{H}_k$ ), 8.5 (d, 1 $\text{H}_l$ )

**FD-MS** (m/z): (100%) 693.5 ( $\text{M}^+$ ), calculated ( $\text{C}_{42}\text{H}_{65}\text{NO}_5\text{S}$ ) = 696.05, (60%) 1389.5 ( $\text{M} + \text{M}^+$ ), calculated ( $2 \times \text{C}_{42}\text{H}_{65}\text{NO}_5\text{S}$ ) = 1392.1, (30%) 2086.5 ( $2\text{M} + \text{M}^+$ ), calculated ( $3 \times \text{C}_{42}\text{H}_{65}\text{NO}_5\text{S}$ ) = 2088.2, (12%) 2783.9 ( $3\text{M} + \text{M}^+$ ), calculated ( $4 \times \text{C}_{42}\text{H}_{65}\text{NO}_5\text{S}$ ) = 2784.2

#### Reaction d:

#### Cleavage of the benzyl group



Product **49** (560 mg, 0.8 mmol, 696.05 g/mol) was dissolved in a mixture of EtOH/Cyclohexene (6/3 ml) in a round bottom flask, and the catalyst Pd/C was added. The flask was heated until the temperature reached 90°C. The reaction was followed by TLC. Additional amounts of catalyst were added for the completion of the reaction. After 2 days, the reaction was stopped, and the mixture was filtrated. The solvent was evaporated under vacuum. The product **50** was purified by column chromatography. Eluents: DCM to DCM/Ac (gradient to 25/1).

**Yield:** 300 mg, (61%)

**TLC:** PE/THF (5/1),  $R_f = 0.53$

**$^1\text{H NMR}$**  (250 MHz,  $\text{d}_8$  - THF, RT)  $\delta_{\text{H}}$ , ppm: 0.8 - 1.0 (m, 15 $\text{H}_a$ ), 1.0 - 1.7 (m, 24 $\text{H}_b$ ), 2.9 (s, 6 $\text{H}_c$ ), 3.3 - 3.7 (m, 5 $\text{H}_d$ ), 3.95 - 4.3 (m, 2 $\text{H}_e$ ), 7.3 (d, 1 $\text{H}_f$ ), 7.6 - 7.8 (m, 2 $\text{H}_g$ ), 8.3 (t, 2 $\text{H}_h$ ), 8.7 (d, 1 $\text{H}_i$ )

**FD-MS** (m/z): (100%) 605.5 ( $\text{M}^+$ ), calculated ( $\text{C}_{35}\text{H}_{59}\text{NO}_5\text{S}$ ) = 605.9, (47%) 1212.3 ( $\text{M} + \text{M}^+$ ), calculated ( $2 \times \text{C}_{35}\text{H}_{59}\text{NO}_5\text{S}$ ) = 1211.8, (38%) 1819.7 ( $2\text{M} + \text{M}^+$ ), calculated ( $3 \times$



was monitored by TLC. A few drops of water were added to quench excess of NaH. Precipitated salts were centrifuged (15 minutes at 9000 rpm). The solvent was evaporated in vacuum. The product **52** was purified by column chromatography. Eluents: HE/Et<sub>2</sub>O (1/1 gradient to 1/3.5).

**Yield:** 2.24 g, (95%)

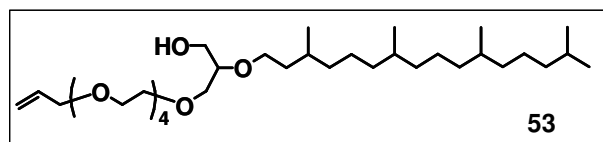
**TLC:** HE/Et<sub>2</sub>O (1/1), R<sub>f</sub> = 0.25

**<sup>1</sup>H NMR** (250 MHz, CDCl<sub>3</sub>, RT) δ<sub>H</sub>, ppm: 0.8 (m, 15H<sub>a</sub>), 1.0 - 1.7 (m, 24H<sub>b</sub>), 3.4 - 3.75 (m, 23H<sub>c</sub>), 4.0 (d, 2H<sub>d</sub>), 4.5 (s, 2H<sub>e</sub>), 5.1 - 5.3 (m, 2H<sub>f</sub>), 5.8 - 6.0 (m, 1H<sub>g</sub>), 7.2 - 7.35 (m, 5H<sub>h</sub>)

**FD-MS** (m/z): (100%) 678.9 (M<sup>+</sup>), calculated (C<sub>41</sub>H<sub>74</sub>O<sub>7</sub>) = 679.04, (50%) 1358.5 (M + M<sup>+</sup>), calculated (2 x C<sub>41</sub>H<sub>74</sub>O<sub>7</sub>) = 1358.08

### Reaction g:

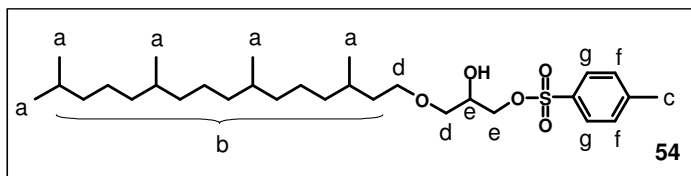
**Cleavage of benzyl group with chlorosulfonyl isocyanate (CSI) - NaOH**



Na<sub>2</sub>CO<sub>3</sub> (790 mg, 7.45 mmol, 105.99 g/mol) was suspended in anhydrous DCM (19 ml), followed by addition of CSI (0.43 ml, 4.95 mmol, 141.53 g/mol) and product **52** (2.24 g, 3.3 mmol, 679.04 g/mol) in inert atmosphere. The reaction mixture was refluxed for 2 days, and then was cooled to 0°C. MeOH (13 ml) and NaOH (0.66 g, 16.5 mmol, 40 g/mol) were added and stirred for 1 h at RT. DCM was evaporated, and the residue was dissolved in H<sub>2</sub>O. The solution was neutralized with 1N HCl and extracted with EtAc. The organic layer was washed with H<sub>2</sub>O and brine, dried over MgSO<sub>4</sub> and concentrated in vacuum. The FD-MS has shown only the presence of the intermediate.

**Yield:** failed

**FD-MS** (m/z): (100%) 701.6 (**52** + Na<sup>+</sup>), calculated (C<sub>41</sub>H<sub>74</sub>O<sub>7</sub>) = 702.04, (75%) 1381.6 (2 x **52** + Na<sup>+</sup>), calculated (2 x C<sub>41</sub>H<sub>74</sub>O<sub>7</sub> + Na<sup>+</sup>) = 1381.08, (70%) 745.2 (intermediate without sulfonylchloride group + Na<sup>+</sup>), calculated (C<sub>42</sub>H<sub>75</sub>NO<sub>8</sub> + Na<sup>+</sup>) = 745.07, (20%) 843.0 (intermediate + Na<sup>+</sup>), calculated (C<sub>42</sub>H<sub>74</sub>ClNO<sub>10</sub>S) = 843.58 (Figure 2.24)

**Figure 2.22****Reaction a:****Opening of the epoxy ring**

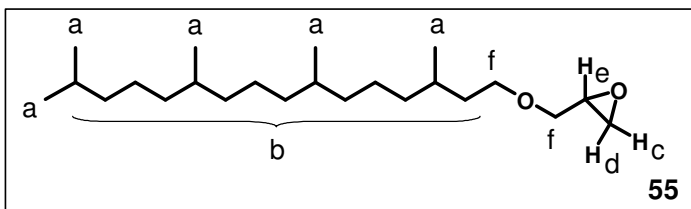
All glassware used in reactions **a**, **c**, **d** and **e** was dried and purged with Ar prior to use. Phytanol **2** (3.7 g, 12.4 mmol, 298.5 g/mol) and glycidyl tosylate **39** (2.5 g, 10.86 mmol, 230.28 g/mol) were placed in 2 neck round bottom flask and dissolved in dry DCM (38 ml). The solution was stirred until all of the glycidyl tosylate was dissolved, and then one drop of  $\text{BF}_3\text{Me}_2\text{O}$  was added at RT. The reaction continued to stir overnight at RT until all glycidyl tosylate had been consumed (monitored by TLC). After the completion of the reaction, water (38 ml) was added to quench the catalyst. The aqueous phase was washed with DCM 3 times. The organic layers were collected, dried over  $\text{MgSO}_4$ , filtered and the solvent was evaporated. The product **54** was isolated by column chromatography. Eluents: HE/EtAc (5/1).

**Yield:** 3.98 g, (69%)

**TLC:** HE/EtAc (5/1),  $R_f = 0.25$

**$^1\text{H NMR}$**  (250 MHz,  $\text{CDCl}_3$ , RT)  $\delta_{\text{H}}$ , ppm: 0.8 (m,  $15\text{H}_a$ ), 1.0 - 1.65 (m,  $24\text{H}_b$ ), 2.4 (s,  $3\text{H}_c$ ), 3.3 - 3.5 (m,  $4\text{H}_d$ ), 3.85 - 4.15 (m,  $3\text{H}_e$ ), 7.3 (d,  $2\text{H}_f$ ), 7.78 (d,  $2\text{H}_g$ )

**FD-MS** (m/z): (100%) 526.7 ( $\text{M}^+$ ), calculated ( $\text{C}_{30}\text{H}_{54}\text{O}_5\text{S}$ ) = 526.8, (30%) 1052.6 ( $\text{M} + \text{M}^+$ ), calculated ( $2 \times \text{C}_{30}\text{H}_{54}\text{O}_5\text{S}$ ) = 1053.7

**Reaction b:****Forming of the oxirane ring**

Product **54** (3.98 g, 7.55 mmol, 526.83 g/mol) was dissolved in MeOH (87 ml) in a 3 neck round bottom flask equipped with a thermometer. The solution was cooled down to  $0^\circ\text{C}$ , and the catalyst  $\text{K}_2\text{CO}_3$  (2.09 g, 15.1 mmol, 138.21 g/mol) was added. The reaction mixture was allowed to slowly warm up to RT and was stirred overnight. A TLC check revealed the formation of the product and consumption of the starting materials. The reaction mixture was poured in sat.  $\text{NH}_4\text{Cl}$  solution. The water layers as well as the precipitated tosylate salts were extracted with diethyl ether 3 times. The organic layers



were collected and washed with sat. NaCl until the pH reached 7.0. The combined organic phase was dried over MgSO<sub>4</sub>, filtered, and the solvent was evaporated. The product **55** was used without further purification.

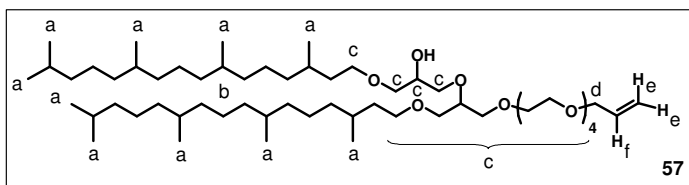
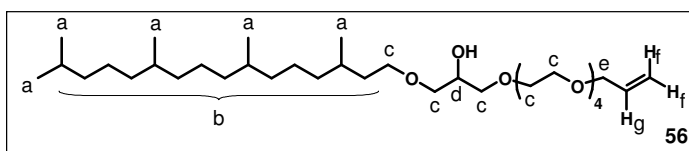
**Yield:** 2.54 g, (95%)

**TLC:** He/EtAc (7/3), R<sub>f</sub> = 0.75

**<sup>1</sup>H NMR** (250 MHz, CDCl<sub>3</sub>, RT) δ<sub>H</sub>, ppm: 0.8 (m, 15H<sub>a</sub>), 1.0 - 1.7 (m, 24H<sub>b</sub>), 2.55 - 2.63 (m, 1H<sub>c</sub>), 2.8 (t, 1H<sub>d</sub>), 3.1 - 3.2 (m, 1H<sub>e</sub>), 3.3 - 3.75 (m, 4H<sub>f</sub>)

**Reaction c:**

**Introduction of the hydrophilic part**



1-Allyl-tetraethylene glycol **9** (1.87 g, 7.98 mmol, 234.29 g/mol), **55** (2.54 g, 7.16 mmol, 354.62 g/mol) and BF<sub>3</sub>Me<sub>2</sub>O (0.03 ml, 0.36 mmol, 113.87 g/mol) dissolved in dry DCM (25 ml) were placed in 2 neck round bottom flask. The solution was allowed to stir overnight at RT. The FD-MS and the TLC check revealed the reaction of the product **56** with excess reactant **55** forming a competing side product **57**. About 5 ml water was added to stop the reaction. The resulting water layer was extracted with DCM three times. The organic layers were collected, dried over MgSO<sub>4</sub>, filtrated, and the solvent was evaporated. Products **56** and **57** were isolated by flash chromatography. Eluents: HE/EtAc (1/1 to 1/2).

**Yield:** **56:** 850 mg, (20%), **57:** 1.05 g, (16%), overall 1.9 g, (36%)

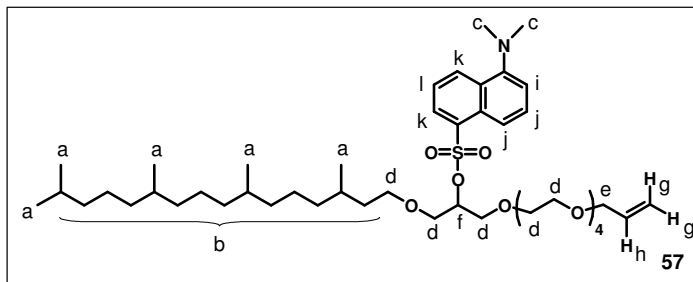
**TLC:** HE/EtAc (1/1), **56:** R<sub>f</sub> = 0.17; **57:** R<sub>f</sub> = 0.34

**<sup>1</sup>H NMR** (250 MHz, CDCl<sub>3</sub>, RT) δ<sub>H</sub>, ppm: **56:** 0.8 (t, 15H<sub>a</sub>), 0.9 - 1.7 (m, 24H<sub>b</sub>), 3.3 - 3.75 (m, 22H<sub>c</sub>), 3.85 - 4.0 (m, 1H<sub>d</sub>), 4.0 (d, 2H<sub>e</sub>), 5.1 - 5.3 (m, 2H<sub>f</sub>), 5.8- 6.0 (m, 1H<sub>g</sub>); **57:** 0.8 (t, 30H<sub>a</sub>), 0.9 - 1.7 (m, 48H<sub>b</sub>), 3.3 - 3.9 (m, 30H<sub>c</sub>), 4.0 (d, 2H<sub>d</sub>), 5.1 - 5.3 (m, 2H<sub>e</sub>), 5.8- 6.0 (m, 1H<sub>f</sub>)

**FD-MS** (m/z): **56:** (100%) 588.4 (M<sup>+</sup>), calculated (C<sub>34</sub>H<sub>68</sub>O<sub>7</sub>) = 588.9, (40%) 1177.2 (M +

M<sup>+</sup>), calculated (2 x C<sub>34</sub>H<sub>68</sub>O<sub>7</sub>) = 1177.8; **57**: (100%) 965.1 (M + Na<sup>+</sup>), calculated (C<sub>57</sub>H<sub>114</sub>O<sub>9</sub> + Na) = 966.5, (40%) 1887.3 (M + M<sup>+</sup>), calculated (2 x C<sub>57</sub>H<sub>114</sub>O<sub>9</sub>) = 1887.1

**Reaction d:**  
**Preparation of**  
**fluorescent precursor 51**



Product **56** (300 mg, 0.51 mmol, 588.92 g/mol), NaH (12 mg, 0.51 mmol, 24 g/mol) and dry DCM (10 ml) were placed in a Schlenk flask. The reaction mixture was stirred for 1 h at RT. The alkoxide of **56** and triethylamine (0.14 ml, 0.99 mmol, 101.2 g/mol) were added dropwise to dansyl chloride (550 mg, 2.04 mmol, 269.75 g/mol) dissolved in dry DCM (10 ml) at 40°C. Additional amounts of NaH and dansyl chloride were added during the reaction. After 5 days, the TLC analysis revealed consumption of the reactants. The reaction was stopped. A few drops of water were added to quench excess of NaH. Precipitated salts were centrifuged (15 minutes at 9000 rpm). The solvent was evaporated in vacuum. The product **51** was purified by column chromatography. Eluents: HE/EtAc (1/1).

**Yield:** 270 mg, (64%)

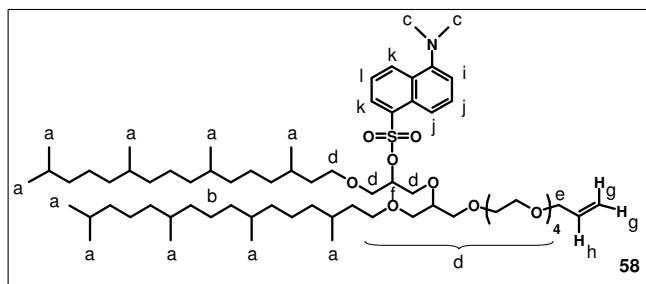
**TLC:** HE/EtAc (1/1), R<sub>f</sub> = 0.55

**<sup>1</sup>H NMR** (250 MHz, CDCl<sub>3</sub>, RT) δ<sub>H</sub>, ppm: 0.65 - 0.9 (t, 15H<sub>a</sub>), 1.0 - 1.6 (m, 24H<sub>b</sub>), 2.85 (s, 6H<sub>c</sub>), 3.1 - 3.7 (m, 22H<sub>d</sub>), 3.9 (d, 2H<sub>e</sub>), 4.6 (p, 1H<sub>f</sub>), 5.1 - 5.3 (m, 2H<sub>g</sub>), 5.8 - 6.0 (m, 1H<sub>h</sub>), 7.16 (d, 1H<sub>i</sub>), 7.45 - 7.6 (m, 2H<sub>j</sub>), 8.25 (t, 2H<sub>k</sub>), 8.56 (d, 1H<sub>l</sub>)

**FD-MS** (m/z): (100%) 820.2 (M<sup>+</sup>), calculated (C<sub>46</sub>H<sub>79</sub>NO<sub>9</sub>S) = 822.21, (95%) 1642.4 (M + M<sup>+</sup>), calculated (2 x C<sub>46</sub>H<sub>79</sub>NO<sub>9</sub>S) = 1644.42, (35%) 2465.3 (2M + M<sup>+</sup>), calculated (3 x C<sub>46</sub>H<sub>79</sub>NO<sub>9</sub>S) = 2466.6

**<sup>13</sup>C NMR** (CD<sub>2</sub>Cl<sub>2</sub>) δ<sub>C</sub>, ppm: 135, 133, 131, 130, 128, 123, 117, 115, 80, 72, 71, 70, 69, 46, 39, 37, 36, 33, 30, 28, 25, 24, 23, 20

**Reaction e:**  
**Preparation of**  
**fluorescent precursor 58**



Product **57** (300 mg, 0.32 mmol, 943.54 g/mol), NaH (20 mg, 0.83 mmol, 24 g/mol) and dry DCM (10 ml) were placed in a Schlenk flask. The reaction mixture was stirred for 1 h at RT. The alkoxide of **57** and triethylamine (0.08 ml, 0.59 mmol, 101.2 g/mol) were added dropwise to dansyl chloride (340 mg, 1.26 mmol, 269.75 g/mol) dissolved in dry DCM (10 ml) at 40 °C. Additional amounts of NaH and dansyl chloride were needed during the reaction. After 2 days, the TLC analysis revealed the complete consumption of reactants. A few drops of water were added to quench the excess of NaH. Precipitated salts were centrifuged (15 minutes at 9000 rpm). The solvent was evaporated in vacuum. Product **58** was isolated by column chromatography. Eluents: HE/EtAc (2/1 to 1/1).

**Yield:** 220 mg, (59%)

**TLC:** HE/EtAc (1.5/1),  $R_f = 0.43$

**$^1\text{H NMR}$**  (250 MHz,  $\text{CDCl}_3$ , RT)  $\delta_{\text{H}}$ , ppm: 0.65 - 0.9 (t, 30 $\text{H}_a$ ), 0.9 - 1.65 (m, 48 $\text{H}_b$ ), 2.85 (s, 6 $\text{H}_c$ ), 3.1 - 3.75 (m, 30 $\text{H}_d$ ), 4.0 (d, 2 $\text{H}_e$ ), 4.55 - 4.65 (m, 1 $\text{H}_f$ ), 5.1 - 5.3 (m, 2 $\text{H}_g$ ), 5.8 - 6.0 (m, 1 $\text{H}_h$ ), 7.16 (d, 1 $\text{H}_i$ ), 7.45 - 7.6 (m, 2 $\text{H}_j$ ), 8.25 (t, 2 $\text{H}_k$ ), 8.55 (d, 1 $\text{H}_l$ )

**FD-MS** (m/z): (100%) 1173.3 ( $\text{M}^+$ ), calculated ( $\text{C}_{69}\text{H}_{125}\text{NO}_{11}\text{S}$ ) = 1176.8, (65%) 2349.8 ( $\text{M} + \text{M}^+$ ), calculated ( $2 \times \text{C}_{69}\text{H}_{125}\text{NO}_{11}\text{S}$ ) = 2353.7

## Literature

1. Michalke, A.; Galla, H.J.; Steinem, C., *Eur. Biophys. J.*, **2001**, *30*, 421-429.
2. Kryszinski, R.; Zebrowska, A.; Michota, A.; Bukowska, J.; Becucci, L.; Moncelli, M. R., *Langmuir*, **2001**, *17*, 3852-3857.
3. Munro, J.C.; Frank, C. W., *Langmuir*, **2004**, *20*, 10567-10575.
4. Hong, Q.; Terrettaz, S.; Ulrich, W. P.; Vogel, H.; Lakey, J. H., *Biochem. Soc. Trans*, **2001**, *29(Part 4)*, 578-582.

5. Heyse, S.; Ernst, O. P.; Dienes, Z.; Hofmann K. P.; Vogel, H., *Biochemistry*, **1998**, *37*(2), 507-522.
6. Reimhult, E., *On the formation of supported phospholipids bilayers*, Goeteborg, Sweden, **2004**.
7. Pantusa, M.; Bartucci, R.; Marsh, D.; Sportelli, L., *Biochimica et Biophysica Acta*, **2003**, *1614*, 165-170.
8. Cornell, B. A.; Braach-Maksvytis, V. L. B.; King, L. G.; Osman, P. D. J.; Raguse, B., Wieczorek, L.; Pace, R. J., *Nature*, **1997**, *387*, 580-583.
9. De Rosa, M.; Gambacorta, A.; Gliozzi, A., *Microbiol. Rev.* **1986**, *50*, 70-80.
10. Terrettaz, S.; Mayer, M.; Vogel, H., *Langmuir*, **2003**, *19*, 5567-5569.
11. Schiller, S. M.; Naumann, R.; Lovejoy, K.; Kunz, H.; Knoll, W., *Angew. Chem. Int. Ed.*, **2003**, *42*(2), 208-211.
12. Bhattacharya, S.; Dileep, P. V., *Bioconjugate Chem.*, **2004**, *15*, 508-519.
13. Stewart, L. C.; Kates, M., *Chem. Phys. Lipids*, **1989**, *50*, 23-42.
14. Sita, L. R., *J. Org. Chem.*, **1993**, *58*, 5285-5287.
15. Cornell, B. A.; Krishna, G.; Osman, P. D.; Pace, R. D.; Wieczorek, L., *Biochem. Soc. Trans.*, **2001**, *29*, 613-617.
16. Joo, C. N.; Shier, T.; Kates, M., *J. Lipid Res.*, **1968**, *9*, 782-788.
17. Krishna, G.; Schulte, J.; Cornell, B. A.; Pace, R. J.; Osman, P. D., *Langmuir*, **2003**, *19*, 2294-2305.
18. Hato, M., *Curr. Opin. Colloid Interface Sci.*, **2001**, *6*, 268-276.
19. Theato, P.; Zentel, R.; Schwarz, S., *Macromol. Biosci.*, **2002**, *2*, 378-394.
20. Burns, C. J.; Field, L. D.; Morgan, J.; Petteys, B. J.; Prashar, J.; Ridley, D. D.; Sandanayake, K. R. A. S.; Vigneovich, V., *Aust. J. Chem.*, **2001**, *54*, 431-438.
21. Sharma, M. K.; Jattani, H.; Lane M. Gilchrist, J., *Bioconjugate Chem.*, **2004**, *15*, 942-947.
22. Moncelli, M. R.; Becucci, L.; Schiller, S. M., *Bioelectrochemistry*, **2004**, *63*, 161.
23. Breffa, C., *New synthetic strategies to tethered bilayer lipid membranes*, **2005**, Johannes Gutenberg Universität: Mainz.
24. Wagner, M. L.; Tamm, L. K., *Biophys. J.*, **2000**, *79*, 1400-1414.
25. Atanasov, V.; Knorr, N.; Duran, R. S.; Ingebrandt, S.; Offenhaeusser, A.; Knoll, W.; Köper, I., *Biophysical Journal*, **2005**, *89*, 1780-1788.
26. Wagner, F.; Walton, E.; Boxer, G. E.; Pruss, M. P.; Holly, F. W.; Folkers, K., *J. Am. Chem. Soc.*, **1956**, *78*, 5079-5081.

- 
27. Atanasov, V.; Atanasova, P. P.; Vockenroth, I. K.; Knorr, N.; Köper, I., *Bioconjugate Chemistry*, **2006**, *17*, 631-637.
  28. Braach-Maksvytis, V.; Raguse, B., *J. Am. Chem. Soc.*, **2000**, *122*, 9544-9545.
  29. Yamauchi, K.; Doi, K.; Kinoshita, M., *Biochimica et Biophysica Acta*, **1996**, 163-169.
  30. Yamauchi, K.; Doi, K.; Kinoshita, M.; Kii, F.; Fukuda, H., *Biochimica et Biophysica Acta*, **1992**, *1110*, 171-177.
  31. Romani, F.; Passaglia, E.; Aglietto, M.; Ruggeri, G., *Macromol. Chem. Phys.*, **1999**, *200*, 524-530.
  32. Padeken, H.-G.; Klamann, D., (1985) *In Methoden der Organischen Chemie, Organische Schwefel - Verbindungen.*, (Gundremann, K. D., and Huemke, K., Eds.) Vol. E11, pp 38-62, Georg Thieme Verlag, Stuttgart, New York.
  33. Burns, J. A.; Butler, J. M.; Whitesides, G. M., *J. Org. Chem.*, **1991**, *56*, 2648-2650.
  34. Getz, E. B.; Xiao, M.; Chakrabarty, T.; Cooke, R.; Selvin, P. R., *Analytical Biochemistry*, **1999**, *273*, 73-80.
  35. Vockenroth, I. K.; Atanasova, P. P.; Knoll, W.; Jenkins, A. T. A.; Köper, I., *IEEE Sensors 2005 - The 4-th IEEE Conference on Sensors. Irvine, CA: IEEE Sensors*, **2005**, 608-610.
  36. Knoll, W.; Frank, C.W.; Heibel, C.; Naumann, R.; Offenhausser, A.; Rühle, J.; Schmidt, E.K.; Shen, W.W.; Sinner, A., *Reviews in Molecular Biotechnology*, **2000**, *74*, 137-158.
  37. Sinner, A.; Knoll, W., *Current opinion in chemical biology*, **2001**, *5*, 705-711.
  38. Giess, F.; Friedrich, M. G.; Heberle, J.; Naumann, R. L.; Knoll, W., *Biophysical Journal*, **2004**, *87*, 3213-3220.
  39. McGillivray, D. J.; Lösche, M.; Vanderah, D. J.; Kasianowicz, J. J.; Valincius, G., *NIST Special Publication 1045*, **2005**, 22-23.
  40. Köper, I., *not published results*.
  41. Raguse, B.; Braach-Maksvytis, V. L. B.; Cornell, B. A.; King, L. G.; Osman, P. D. J.; Pace, R. J.; Wiczorek, L., *Langmuir*, **1998**, *14*, 648-659.
  42. Krishna, G.; Schulte, J.; Cornell, B. A.; Pace, R. J.; Wiczorek, L.; Osman, P. D., *Langmuir*, **2001**, *17*, 4858-4866.
  43. Munro, J. C.; Frank, C. W., *Langmuir*, **2004**, *20*, 3339-3349.
  44. Jeuken, L. J. C.; Connell, S. D.; Nurnabi, M.; O'Reilly, J.; Henderson, P. J. F.; Evans, S. D.; Bushby, R. J., *Langmuir*, **2005**, *21*, 1481-1488.
  45. Yin, P.; Burns, C. J.; Osman, P. D.; Cornell, B. A., *Biosensors and Bioelectronics*, **2003**, *18*, 389-397.

- 
46. Valincius, G.; McGillivray, D. J.; Febo-Ayala, W.; Vanderah, D. J.; Kasianowicz, J. J.; Lösche, M., *The Journal of Physical Chemistry, B*, **2006**, *110*, 10213-10216.
  47. Baumgart, T.; Kreiter, M.; Lauer, H.; Naumann, R.; Jung, G.; Jonczyk, A.; Offenhäuser, A.; Knoll, W., *Journal of Colloid and Interface Science*, **2003**, *258*, 298-309.
  48. He, L.; Robertson, J. W. F.; Kärcher, J. Li, I.; Schiller, S. M.; Knoll, W.; Naumann, R., *Langmuir*, **2005**, 11666-11672.
  49. Dollmann, B., *Modellmembranen auf Siliziumoxid-Oberflächen*, **2006**, Johannes Gutenberg Universität: Mainz.
  50. Shibata, A.; Ikawa, K.; Shimooka, T.; Terada, H., *Biochimica et Biophysica Acta*, **1994**, *1192*, 71-78.
  51. Corcelli, A.; Lobasso, S.; Palese, L. L.; Saponetti, M. S.; Papa, S., *Biochemical and Biophysical Research Communications*, **2007**, *354*, 795-801.
  52. Christie, W. W., *The lipid library*, <http://www.lipidlibrary.co.uk/index.html>.
  53. Schiller, S., *not published results*.
  54. Berkowitz, W. F.; Pan, D.; Bittman, R., *Tetrahedron Letters*, **1993**, *34*(27), 4297-4300.
  55. Rasmussen, H., *Science*, **1970**, *170*, 404-412.
  56. Ohki, S.; Arnold, K., *Journal of Membrane Biology*, **1990**, *114*, 195-203.
  57. Devaux, P. F.; Fellmann, P.; Herve, P., *Chemistry and Physics of Lipids*, **2002**, *116*, 115-134.
  58. Sarcinaa, M.; Muratab, N.; Tobinc, M. J.; Mullineauxa, C. W., *FEBS Letters*, **2003**, *553*, 295-298.
  59. Ayuyan A. G.; Cohen F. S., *Chemphyschem.*, **2006**, *7*(11), 2409-2418.
  60. Korlach, J.; Baumgart, T.; Webb, W. W.; Feigenson, G. W., *Biochimica et Biophysica Acta – Biomembranes*, **2005**, *1668*(2), 158-163.
  61. Van IJzendoorn, S. C. D.; Hoekstra, D., *Journal of Cell Biology*, **1998**, *142*, 683-696.
  62. Riggers, R. J.; Pomorski, T.; Holthuis, J. C.; Kalin, N.; Van Meer, G., *Traffic*, **2000**, *1*, 226-234.
  63. Kraayenhof, R.; Sterk, G. J.; Sang, H. W., *Biochemistry*, **1993**, *32*, 10057-10066.
  64. Roy, B. C.; Peterson, R.; Mallik, S.; Campiglia, A. D., *Journal of Organic Chemistry*, **2000**, *65*, 3644-3651.
  65. Kim, J. D.; Lee, M. H.; Lee, M. J.; Jung, Y. H., *Tetrahedron Letters*, **2000**, *41*, 5073-5076.

### 3. Investigation the properties of thiolated lipid monolayers (DPTT, DPHT, DPOT and DDPTT)

#### 3.1. General principles of Langmuir film balance and Langmuir – Blodgett technique

In 1774, Benjamin Franklin has reported the phenomena of floating fatty monolayers on the water surface. This has been studied systematically by Irving Langmuir over two hundred years later.<sup>1</sup> In his honour, these layers are named “Langmuir films”. As the first detailed description of the monolayer transfer onto solid supports was given by Katherine Blodgett<sup>2</sup>, the transferred monolayer assemblies are referred to as Langmuir-Blodgett films.

With a Langmuir film balance, one studies in general the assembly of amphiphilic molecules at the air-water interface. The design of the set-up is illustrated in Figure 3.1. A solution of an amphiphile in a volatile and water insoluble solvent is spread on the water surface of the Teflon trough and the amphiphilic molecules cover homogeneously the available area.

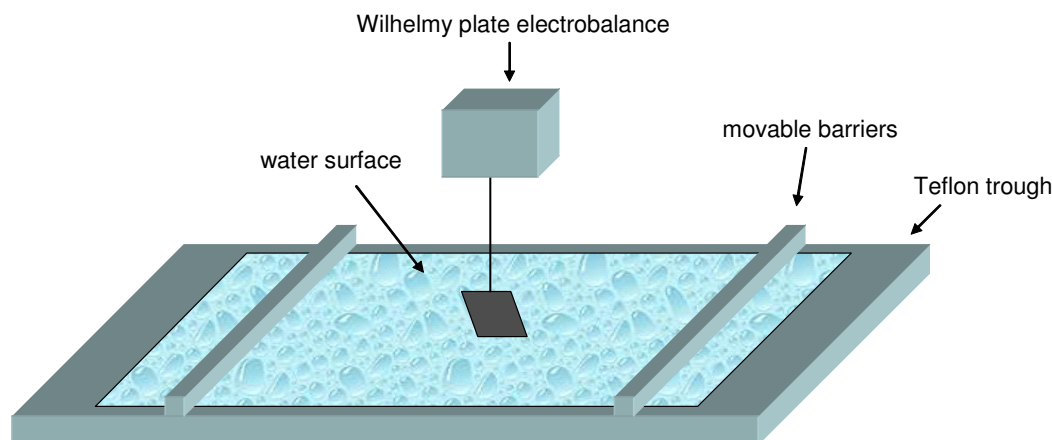


Figure 3.1. Schematic representation of a Langmuir film balance with a Wilhelmy plate electrobalance

The amphiphilic nature of the lipids defines their orientation at the interface. The polar head groups immerse in the water and the hydrocarbon chains point towards the air.

The surface area of the trough can be varied by movable barriers. The decrease of the average area per lipid molecule ( $A$ ) causes an increase of the surface pressure ( $\pi$ ). The two parameters,  $A$  and  $\pi$  are continuously monitored during the compression. The surface pressure is measured by a Wilhelmy plate, which is partially immersed in the water. The plate is connected to a precise balance, and since the water meniscus acts on the plate, the surface tension can be measured.  $\pi$  can be calculated as a reduction of the surface tension of the pure water by addition of the amphiphiles:

$$\pi = \gamma_0 - \gamma \quad (3.1)$$

where  $\gamma_0$  is the surface tension of the pure water ( $\sim 73$  mN/m) and  $\gamma$  is the surface tension after addition of the amphiphile.

Typically, an experiment is performed at a constant temperature. The barriers move at a constant velocity, and the surface pressure is given as a function of the mean area per molecule. The resulting curve is known as a  $\pi - A$  isotherm and provides useful information about the monolayer properties.<sup>3</sup>

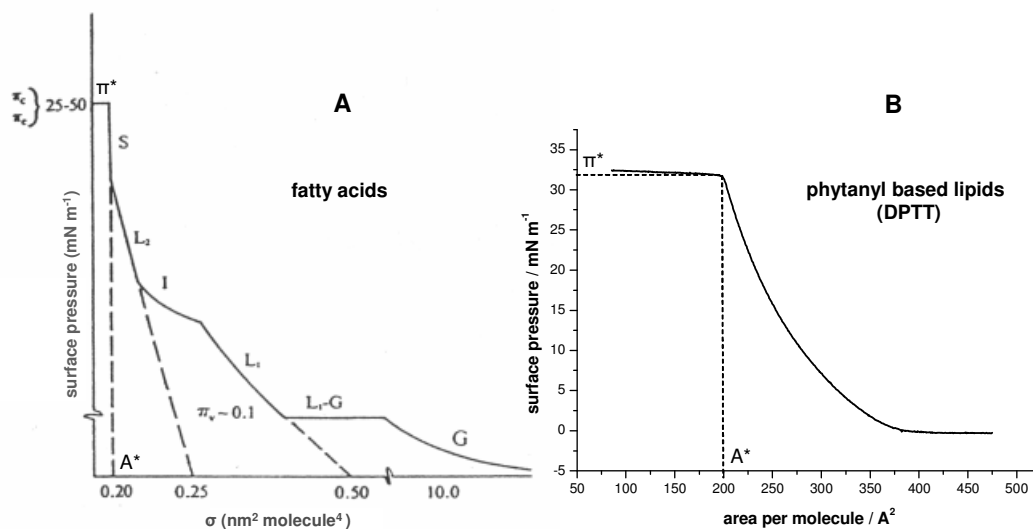


Figure 3.2. Schematic  $\pi - A$  isotherms of fatty acids (A) and phytanyl based lipids (DPTT) (B)



When the monolayer is compressed, one can distinguish different phases. At low  $\pi$ -values, the lipid interactions are weak and the monolayer acts as a two-dimensional gas (G in Figure 3.2, A). Compression of the layer leads to a reduction of the mean molecular area and the molecules start to exhibit repulsive forces on each other and undergo transitions: first to a liquid-expanded ( $L_1$ ) and later to a liquid-condensed ( $L_2$ ) state. At higher densities the monolayer reaches a solid state (S). Upon further compression, the monolayer will collapse into three-dimensional structures. The surface pressure at this point is known as collapse pressure ( $\pi^*$ ), and  $A^*$  is the corresponding mean molecular area.

The phytanyl chains of our molecules are branched and this characteristic feature dictates the shape of the isotherm. In comparison with the isotherm of lipids with straight chains in the hydrophobic part, the isotherm of the phytanyl based lipids is characteristic of a liquid expanded monolayer. A smooth curve, without any plateaus can be observed (Figure 3.2,B). The most important points are the molecular area at which a pronounced increase in the surface pressure is observed and the collapse pressure  $\pi^*$  with the corresponding  $A^*$ .

The Langmuir-Blodgett technique is a powerful tool for the preparation of transferred homogeneous monolayers with precise thickness. The monolayer is transferred, as schematically shown in Figure 3.3, by raising of a hydrophilic solid substrate from the water subphase through the monolayer while simultaneously keeping the  $\pi$  constant by a computer controlled feedback.

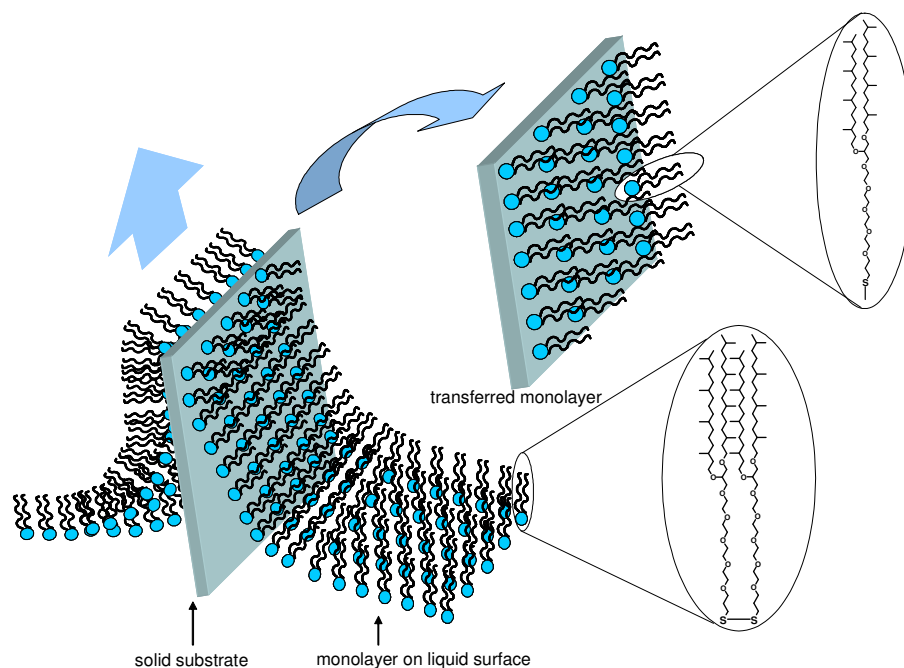


Figure 3.3. Deposition of a floating monolayer on a solid substrate

*Langmuir film balance setup:*

A KSV 5000 (KSV, Helsinki) instrument equipped with a Wilhelmy balance was used. The subphase consisted of ion-exchanged Millipore filtered water (Millipore Milli-Q system,  $R > 18 \text{ M}\Omega \text{ cm}$ ). If not otherwise stated, experiments were carried out at  $20 \pm 1^\circ\text{C}$ . The operational area of the trough was  $81000 \text{ mm}^2$ . The speed of the barriers during the compression was constantly held at  $10 \text{ mm/min}$ . Monolayers were obtained by spreading  $25 \mu\text{l}$  of a solution of the corresponding lipid in chloroform on the water surface. The organic solvent was allowed to evaporate for 20 min before compression of the film.

*Lipids:*

The structures of all lipids used in the current study are shown in Figure 3.4. The anchor lipids (DPTT, DPHT, DPOT and DDPTT) and diphytanyl glycerol (DPG) were synthesized according to the synthetic procedure described in section 2.2.5 and 2.6.4. 1,2-Diphytanoyl-*sn*-glycero-3-phosphatidylethanolamine (DPhyPE) was purchased from Avanti Polar Lipids, and was used without further purification. Lipid mixtures were

prepared by dissolving the compounds in chloroform (2 mg/ml) followed by 10 min sonication prior to use in order to receive a more homogeneous mixture.

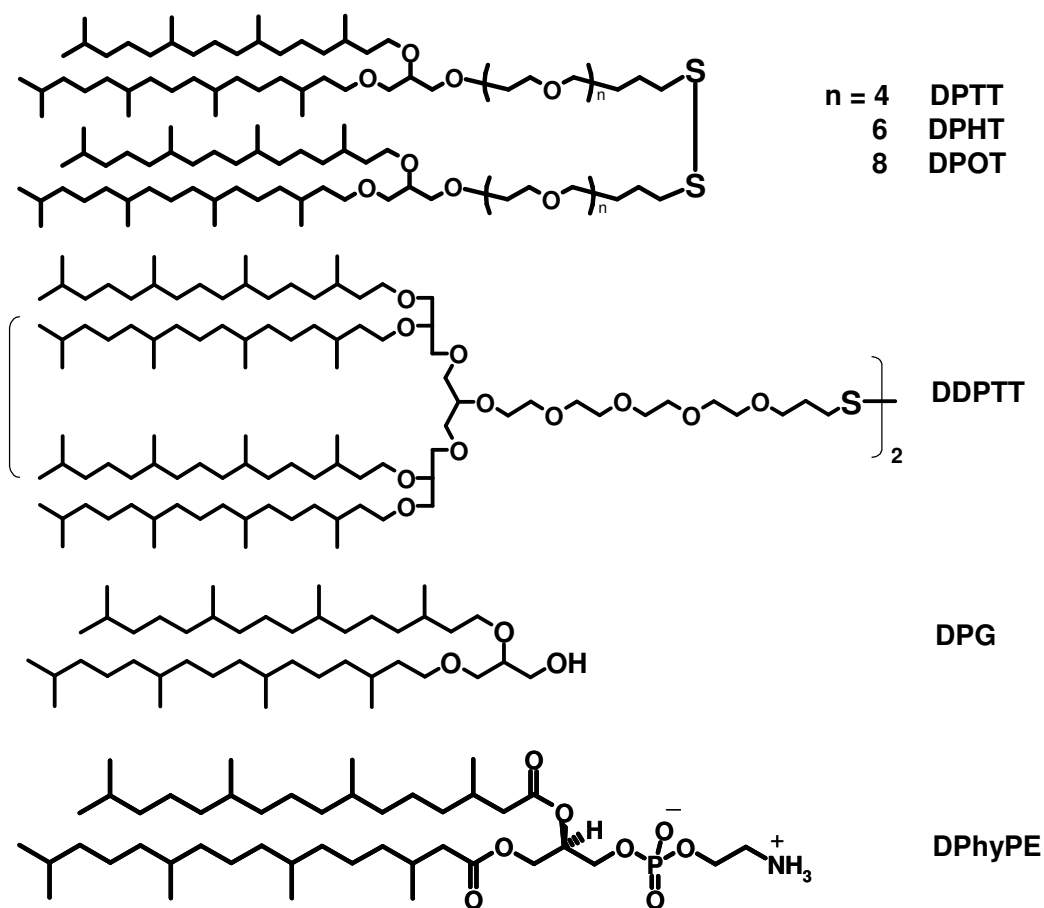


Figure 3.4. Structure of the lipids utilized in the current study.

### 3.2. Introduction and motivation

For tBLMs, homogeneous and not too dense monolayers are required to allow for the incorporation of complex membrane proteins in a functional form. However, dense tethered lipid monolayers are commonly prepared by self-assembly.<sup>4,5</sup> Dilution of the tethered layer was proposed<sup>6,5</sup> by mixing with small surface active molecules, which can intercalate between the anchor lipids. This approach might yet lead to a phase-separation of the anchor lipid from the lateral spacer, which would lower the reproducibility and the quality of the membrane, especially in terms of its electrical

sealing properties. Furthermore, the molecular assembly of the mixed lipid system in a self-assembly process is rather difficult to control.

Pre-organization of the lipid monolayer at the air-water interface of a Langmuir film-balance was chosen as an alternative way to achieve a better control of the lipid distribution. The dilution of the anchor lipids is controlled via the surface pressure and the mean area per molecule. This allows controlling the distribution and the concentration of anchor lipids on the water surface. Subsequent transfer of the lipid film onto a solid substrate and further vesicle fusion can then lead to the formation of a tBLM.

The characteristics of the lipid films as well as films consisted of lipids with long hydrophilic spacers have been studied extensively.<sup>7-9</sup> However, in most of the cases the studies have been restricted to the description of the film properties in terms of compressibility and phase behavior. The current approach is motivated by the fact that the lipid films will later on be used as monolayers in tBLMs, which have already shown practical application in the biosensing field.<sup>10,11</sup>

The anchor lipids used in this study consist of a lipophilic (hydrophobic) and a lipophobic (hydrophilic) part and thus they act as surfactants on the water surface. Films have been prepared using pure lipids or mixtures of anchor lipids and free lipids. Therefore, the concentration of the individual components in the film, and then, later on in the inner-membrane architecture of a tBLM can be controlled.

In this chapter, the properties of the surface monolayer will be described in terms of surface pressure, structure of the lipid molecule, content of lipid mixtures, temperature and relaxation features.

### **3.3. Results and discussion**

#### **3.3.1. Influence of the lipid structure**

In order to investigate the influence of the spacer length of the anchor lipid,  $\pi$  – A isotherms of lipids with tetra-, hexa- and octathylene glycol spacers (DPTT, DPHT and DPOT) were recorded at 20°C. The experimental data is depicted in Figure 3.5. All isotherms show a smooth transition from gaseous phase over an expanded phase to a condensed phase, and no explicit plateau region can be seen.

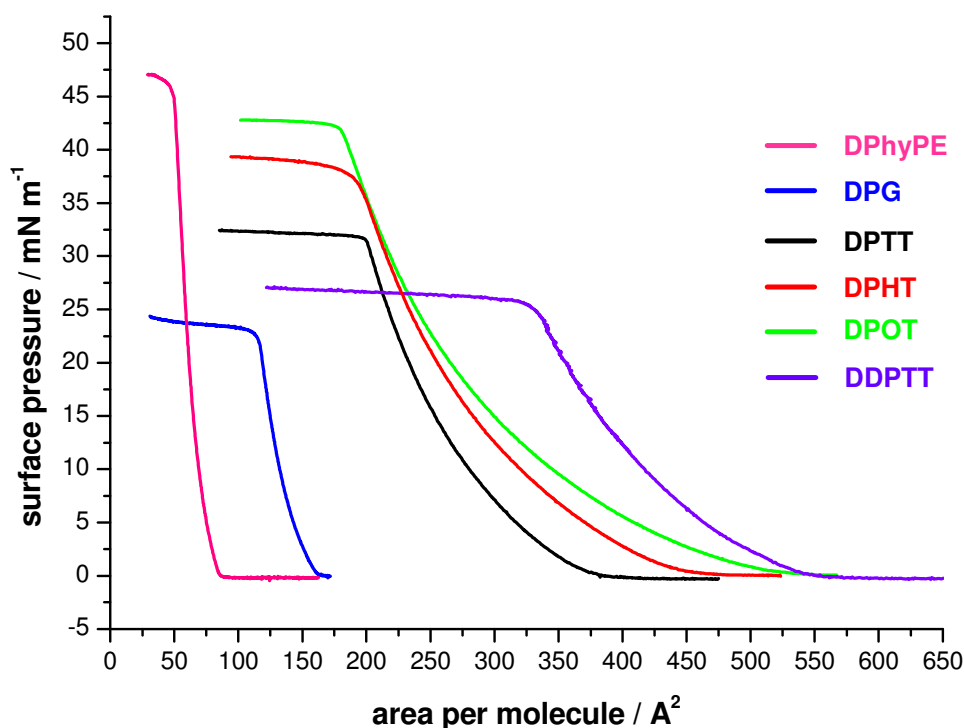


Figure 3.5.  $\pi - A$  isotherms of DPhyPE, DPG, DPTT, DPHT, DPOT and DDPTT at 20°C.

After continuous compression, DPTT, DPHT and DPOT undergo a phase transition and kinks in the isotherms at 31, 37 and 42 mN/m respectively are observed. These kinks correspond to the collapse of the monolayer and the formation of three-dimensional structures in the water sub phase. Comparably, relatively low collapse surface pressures have already been reported for similar phytanyl-based (archaeal-type) lipid monolayers.<sup>12</sup> Kitano *et al.* have compared the collapse pressure of 32-37 mN/m for archaea lipids with values of 54-56 mN/m for conventional lipids possessing straight, saturated hydrophobic chains. It has been proposed that the decrease in the collapse pressure of archaeal phytanyl-based lipids is due to the exceptionally high conformational disorder of the branched chains.<sup>13</sup> Nevertheless, membranes formed of archaeal lipids have been shown to provide a high bilayer stability and low ion leakage.<sup>14,15</sup>

In Figure 3.5, the isotherm of the free lipid DPG is compared with the isotherms of DPTT, DPHT and DPOT. One can see that the isotherms of the anchor lipids are

broader and shifted to higher areas per molecules. Compared to DPG, the larger hydrophilic parts (tetra-, hexa- and octaethylene glycol) cause interactions between the anchor lipids at much higher area per molecule. This is due to the fact that ethylene glycol is only poorly soluble in water at low surface pressure.<sup>16</sup> Therefore, at low surface pressure, the lipid molecules might lie planar on the water surface and thus cover a large area. With increasing  $\pi$ , the ethylene glycol chains become more soluble and orient the lipid molecules more perpendicular to the water surface.

However, DPhyPE shows an opposite effect. Even if DPhyPE is a larger molecule than DPG, the isotherm is narrower and is shifted to smaller areas per molecule in comparison with that of DPG. This effect is due to the higher hydrophilicity of phosphoethanolamine in DPhyPE<sup>13</sup> compared to hydroxyl group of DPG. Thus, DPhyPE is immersed more deeply into the water sub phase than DPG, and orientated more perpendicular to the water surface. This reduces the average area per molecule and allows for compression to much higher surface pressure. The DPhyPE films collapse at an area per molecule of  $72 \text{ \AA}^2$ , which is in a good agreement with the value shown in the literature ( $76 \text{ \AA}^2$ ).<sup>17</sup>

Similarly, the increase of the collapse surface pressure of the anchor lipids can be explained by the increase in length of the ethylene oxide (EO) chains. Hence, increasing the number of EO units in the spacer allows for the formation of a denser monolayer. Thus, the collapse area per molecule decreases from  $\sim 200 \text{ \AA}^2$  for DPTT to  $\sim 180 \text{ \AA}^2$  for DPOT. However, it should be taken into account that the reported values for area per molecule in Figure 3.5 were obtained for the lipid-dimers. Once those dimers are transferred to a gold surface, they become monomers that bind to the gold. Therefore, the actual area per monomeric molecule has to be taken as  $\sim 100 \text{ \AA}^2$  for DPTT and  $\sim 90 \text{ \AA}^2$  for DPOT. In comparison, the area per lipid molecule of the similar DPTL self-assembled on gold surface was determined with different methods. Reductive desorption gave an area per molecule at  $51^{18} - 55^{19} \text{ \AA}^2$ . A van der Waals modeling results in values of  $\sim 65 \text{ \AA}^2$ . Kunze *et al.*<sup>19</sup> have proposed values of  $\sim 78 \text{ \AA}^2$  using a new method based on chronocoulometry. Since the average area per molecule obtained for the lipids investigated in the current study are larger than the referred data from self-assembly, one can conclude that the lipid monolayers obtained by LB transfer will be less densely packed than those from self-assembly technique. The reason is yet unclear.

Finally, the influence of the number phytanyl chains connected to the hydrophilic spacer part on the collapse pressure value can be evaluated comparing the isotherms of DPTT (two phytanyl chains) and DDPTT (four phytanyl chains) (Figure 3.4). Since both lipids have the same spacer part (TEG), all differences in the isotherms should be due to the different number phytanyl chains. In Figure 3.5, one can see that the collapse pressure of DDPTT is lower (25 mN/m) in comparison with DPTT (31 mN/m). Moreover, the first pronounced increase of the surface pressure in the isotherm of DDPTT is shifted to much higher area per molecule causing a shift of the whole isotherm and  $\sim 330 \text{ \AA}^2$  ( $\sim 165 \text{ \AA}^2$  for a monomer) area per lipid molecule at the collapse pressure. This experiment clearly shows that an increase of the phytanyl chains number increases drastically the disorder in the hydrophobic part. The latter hinders the achievement of higher collapse pressure and lower area per molecule.

### 3.3.2. Influence of the temperature

In Figure 3.6, the temperature dependence of the DPTT and DPOT isotherms is shown. Measurements were conducted at 4°C, 20°C and 40°C for a given lipid concentration (25  $\mu\text{l}$ , 2 mg/ml). As reported in the literature,<sup>12</sup> higher temperatures lead to a decrease of the collapse pressure and an increase of the corresponding area per molecule. For instance, in the case of the DPTT isotherms (Figure 3.6, A), the collapse pressure at 4°C is recorded at 35 mN/m and at an area per molecule of  $\sim 196 \text{ \AA}^2$  in comparison with 31 mN/m and  $\sim 200 \text{ \AA}^2$ , respectively, obtained at 20°C. On the other hand, increasing the temperature to 40°C is combined with a drop of the collapse pressure to 25 mN/m and  $\sim 207 \text{ \AA}^2$  area per molecule. With increasing the temperature, the hydration of the EO chain decreases,<sup>8,16</sup> leading to a decrease of the solubility of the hydrophilic heads and thus to a collapse of the monolayer at lower surface pressure. Therefore, at lower temperatures, more densely packed monolayers could be prepared. The DPOT isotherms in Figure 3.6,B are broader and have kinks at higher surface pressure in comparison with those of DPTT. The temperature effect is similar to that observed by DPTT. Thus, among DPTT, DPHT and DPOT, the most densely packed monolayers can be prepared by using DPOT at 4°C which layer can be compressed to 45 mN/m reaching the smallest area per molecule.

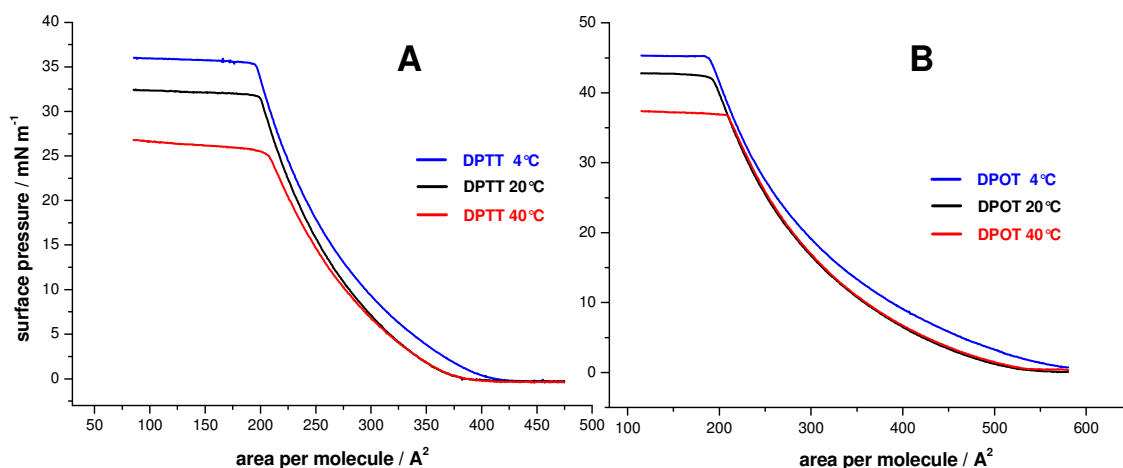


Figure 3.6.  $\pi - A$  isotherms at 4, 20 and 40°C of DPTT and DPOT.

### 3.3.3. Investigation of anchor and free lipids mixed monolayers

One approach towards formation of anchor lipid monolayers with lower area per molecule at the collapse pressure might be the dilution of the anchor lipids with free, non-bound lipids. This approach would be a further step for preparation of more complex membrane architectures that resemble more the natural analogues, which are composed of various lipids and other compounds. Isotherms of mixed anchor and a free lipid (DPTT/DPhyPE) for various mixing ratios are shown in Figure 3.7.

In contrast to isotherms of pure lipids, those of mixed lipids show two kinks instead of one. With increasing the amount of the anchor lipid in the mixture, the kink at lower surface pressure becomes more pronounced and the  $\pi - A$  isotherms shift to higher mean molecular areas by nearly constant collapse surface pressure (30-35  $\text{mN/m}$ ). The curve in Figure 3.8 depicts a typical isotherm of mixed lipids. When a solution of mixed lipids is spread on the water surface, the lipids molecules are in gaseous phase and do not or minimally interact with each other (a). Further barrier compression causes decrease of the area per molecule and hence, intermolecular interactions (b). The ethylene glycol chains start to dissolve gradually with increasing the surface pressure in the water sub phase resulting in steeper isotherm (b).<sup>16</sup> The kink at low surface pressure (30-35  $\text{mN/m}$ ) correlates very well to the collapse pressure of pure



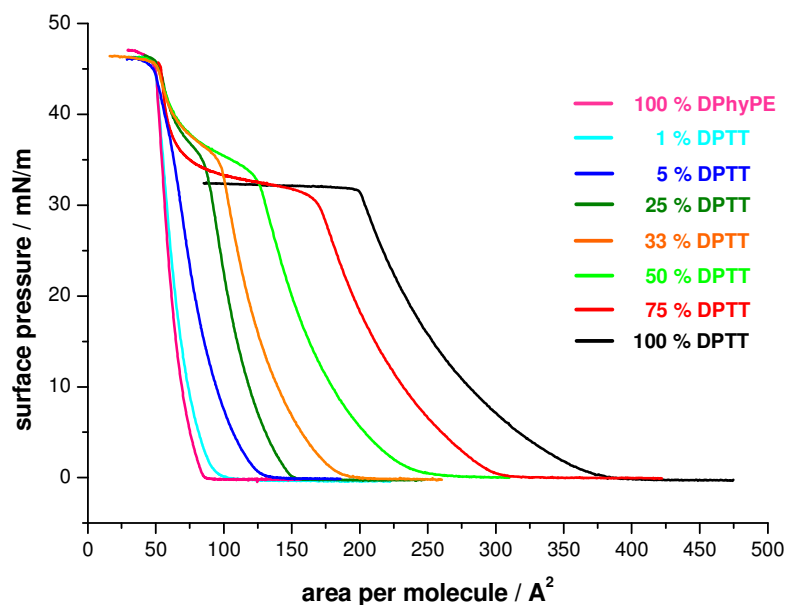


Figure 3.7.  $\pi - A$  isotherms of different DPTT / DPhyPE mixtures at 20 °C

DPTT (32 mN/m). We propose that once the mixed lipid monolayer reaches the collapse pressure of DPTT, the anchor lipids collapse gradually (c + d) until a pure DPhyPE film is formed (e). After that, the monolayer behaves as a pure DPhyPE monolayer and therefore, the isotherm matches the isotherm of pure DPhyPE (f). The kink at higher surface pressure (45-47 mN/m) matches the collapse pressure of DPhyPE. Similar isotherms were recorded for mixtures of DPHT/DPhyPE and DPOT/DPhyPE (data not shown). In these cases, both the kinks were hard to be distinguished due to the proximity of the collapse-pressure of DPHT, DPOT to that of DPhyPE.

Isotherms with double kink shape have already been reported for mixtures of pegylated and free lipids<sup>20</sup>. However, the kinks have been observed at significantly lower surface pressure ( $\sim 10$  mN/m) and have been attributed to conformational changes of the much longer PEG chains underneath the water surface. Such a low surface pressure kink was observed neither for pure anchor lipids (Figure 3.5) nor for mixed lipids (Figure 3.7). Similarly, there was no kink visible in the isotherms of DPHT and DPOT that would correspond to conformational change of the PEG unit. It was proposed that this absence is due to the much shorter PEG chains (4, 6 and 8

ethylene glycol units for DPTT, DPHT and DPOT, respectively). Therefore, it was proposed that the conformational changes do not dominate the interactions of hydrophobic (phytanyl) chains and are additively added to the surface properties of the whole molecule.

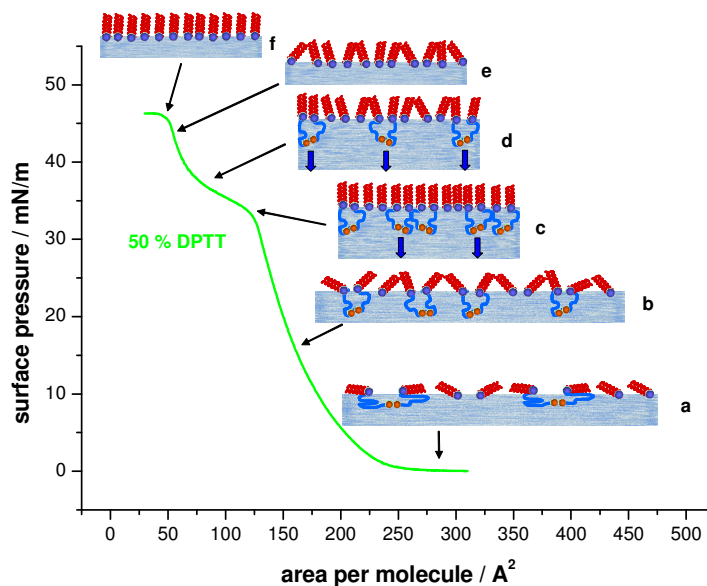


Figure 3.8. Schematic representation of the proposed lipid behavior in mixtures by surface compression

In order directly to verify the proposed lipid monolayer behavior between the first and the second kink, a series of LB-deposition on gold substrates was conducted. Initially, a pure anchor lipid (DPTT) monolayer was transferred (speed up 5 mm/min) at surface pressure before (75% from the corresponding  $\pi^*$ ) and after the collapse. The microscope images in Figure 3.9 (before (A) and after (B) the collapse pressure) are taken by an optical microscope. Obviously, in the region before the collapse pressure, the monolayer is smooth and no structural deformations on the substrate are observed. However, a monolayer compression after the collapse pressure results in destruction of the monolayer and creation of tri-dimensional (globular) structures as shown in Figure 3.9, B.

Similarly, a second series of experiments with mixed monolayers (DPTT/DPhyPE) was done. They were transferred on gold substrates before the first (24.8 mN/m) and before the second kink (43 mN/m). The optical images of the monolayers transferred before the first kink are similar to Figure 3.9, A (data is not shown).

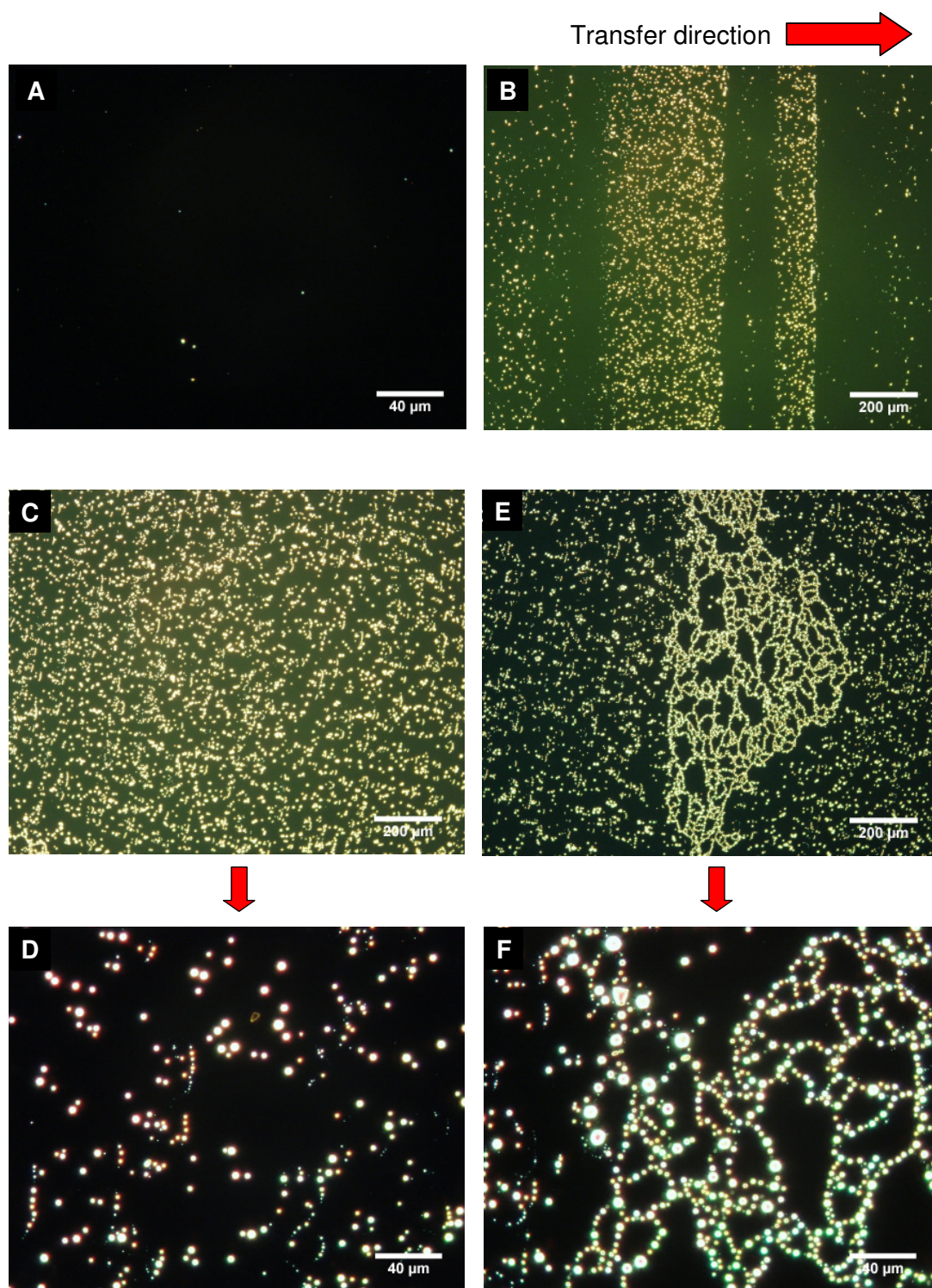


Figure 3.9. Optical microscope images of pure lipid monolayers (A) before (75% from  $\pi^*$ ) and (B) after the collapse kink, and of mixed lipid monolayers (DPTT/DPhyPE) (C, D, E, F) before the second collapse kink (75% from  $\pi^*$ ). D is a magnification of C, F is magnification of E

However, structures on the gold surface obtained by deposition before the second kink were observed with the naked eyes. These structures (Figure 3.9, C, D) were similar to those observed by collapsed pure anchor lipid (Figure 3.9, B). Additionally, from the microscope images in Figure 3.9, (E, F) is seen, that the surface is covered with bigger conglomerates surrounded by smaller structures with average diameter of 1 – 10  $\mu\text{m}$ . In conclusion, the formation of agglomerates between the first and second kink might be due to further rearrangement of the lipid globular aggregates.

### 3.3.4. Investigation the miscibility of lipid monolayers

One important criterion when investigating lipid mixtures is the miscibility of the individual compounds. With respect to the use of the mixed layers as a platform for the preparation of tBLMs which can host proteins, we are interested to study the lateral distribution of the anchor and free lipids. Thus, it will be possible by control of the experimental conditions to prepare lipid layers without any phase segregation that might affect both the incorporation and functionality of embedded proteins. Therefore, the behavior of their mixed monolayers was analyzed according to an additive rule.<sup>21</sup> Basically, ideal mixtures of two components should fulfill the additive rule, where the molecular area ( $A_{id}$ ) for a given pressure should be the sum of the area of both components multiplied by their corresponding molar fractions:

$$A_{id} = x_{\text{DPTT}}A_{\text{DPTT}} + x_{\text{DPhyPE}}A_{\text{DPhyPE}} \quad (3.2)$$

where  $x_{\text{DPTT}}$  and  $x_{\text{DPhyPE}}$  are the molar fractions of DPTT and DPhyPE in the mixed monolayer, and  $A_{\text{DPTT}}$  and  $A_{\text{DPhyPE}}$  are the corresponding areas per molecule of the pure compounds at the same surface pressure.

The interaction between DPTT and DPhyPE molecules in the mixed monolayers can be examined by analysis of the excess area ( $A_{ex}$ ).<sup>22,23</sup> The latter can be calculated by comparing  $A_{id}$  (calculated by equation 3.2) and the average area per molecule ( $A_{exp}$ ) obtained experimentally by recording the  $\pi$ -A isotherm of a certain lipid mixture at a given surface pressure:

$$A_{ex} = A_{exp} - A_{id} = A_{exp} - (x_1A_1 + x_2A_2) \quad (3.3)$$

When the  $A_{ex}$  is equal to zero, the two compounds are immiscible or form an ideal mixture, where no chemical or physical interactions between the compounds occur. Any deviation from  $A_{ex} = 0$  provides evidence for partial miscibility in the film. Moreover, the  $A_{ex}$  gives information about the type of interactions (attractive or repulsive). For instance, negative  $A_{ex}$  ( $A_{exp} < A_{id}$ ) indicate that attractive interactions occurred between the hetero-molecules resulting in decrease of the  $A_{exp}$ . Conversely, positive  $A_{ex}$  ( $A_{exp} > A_{id}$ ) is caused by repulsive intermolecular interactions, and thus, expanded  $A_{exp}$  in comparison with  $A_{id}$  is observed.

Practically, in order to distinguish between the different possibilities, the mean area per molecule recorded at different surface pressures is plotted as a function of the composition (Figure 3.10). The points present the  $A_{exp}$  at the particular surface pressure and the lines express the  $A_{id}$  calculated with equation 3.2. A linear behavior of the  $A_{exp}$  ( $A_{ex} \sim 0$  in the surface interval between 2.5 – 30 mN/m) can be attributed to either ideal mixing or complete segregation of DPTT and DPhyPE.

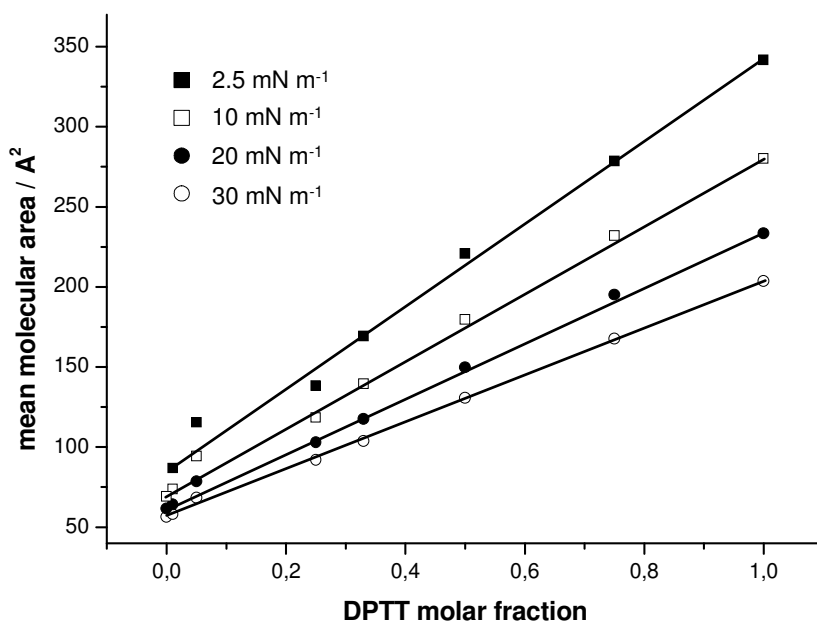


Figure 3.10. Mean molecular area as a function of DPTT molar fraction in mixed DPTT / DPhyPE monolayers taken at 2.5, 10, 20 and 30 mN/m.

Further information to distinguish these two situations can be extracted by thermodynamic analysis of DPTT/DPhyPE  $\pi - A$  isotherms and evaluation of the

excess free energy change of mixing ( $\Delta G_{ex}$ ).  $\Delta G_{ex}$  represents the deviation of free energy change of mixed system from that of an ideal mixed one. The  $\Delta G_{ex}$  values can be determined by integration of  $A_{ex}(\pi)$  from  $\pi = 0$  mN/m to the desired surface pressure.<sup>21</sup>

$$\Delta G_{ex} = \int_0^{\pi} (A_{exp} - A_{id}) d\pi = \int_0^{\pi} (A_{exp} - (x_1 A_1 + x_2 A_2)) d\pi \quad (3.4)$$

If  $\Delta G_{ex} = 0$ , the mixing is ideal. Positive  $\Delta G_{ex}$  values indicate that the intermolecular interactions between the hetero-molecules are weaker in comparison with that between the lipids of the same type.<sup>24</sup> Negative  $\Delta G_{ex}$  values point to the presence of a mutual attractive interactions of the mixed compounds.

The calculation of  $\Delta G_{ex}$  was conducted according the following steps. Firstly, the function describing the isotherms  $\pi(A)$  was presented as  $A(\pi)$ . The obtained curves were fitted with polynomal function of 9 order including 1000 points. Then, a function  $A_{exp} - (x_{DPTT} A_{DPTT} + x_{DPhyPE} A_{DPhyPE})$  was built and integrated from 0 consecutive to 2.5, 10, 20 and 30 mN/m fulfilling the equation 3.4. Thus,  $\Delta G_{ex}$  for each particular molecular fraction (0.1, 0.25, 0.33, 0.50, 0.75) at different surface pressures was found and presented as  $\Delta G_{ex}(x_{DPTT})$  in Figure 3.11.

As it seen, at low surface pressures the lowest values of  $\Delta G_{ex}$  are obtained (except  $x_{DPTT} = 0.1$  and 0.33) indicating a better miscibility at lower surface pressure. The tendency for positive deviations from ideal mixing with increasing the surface pressure might induce the lateral phase separation at high surface pressures. Solely, the monolayer composed of 33% DPTT has negative  $\Delta G_{ex}$  values indicating attractive interactions between the different type molecules at all surface pressures. Thus, relatively low positive  $\Delta G_{ex}$  values and fluctuation feature of the function  $\Delta G_{ex}(x_{DPTT})$  around zero proposed a good miscibility of the mixed lipids.

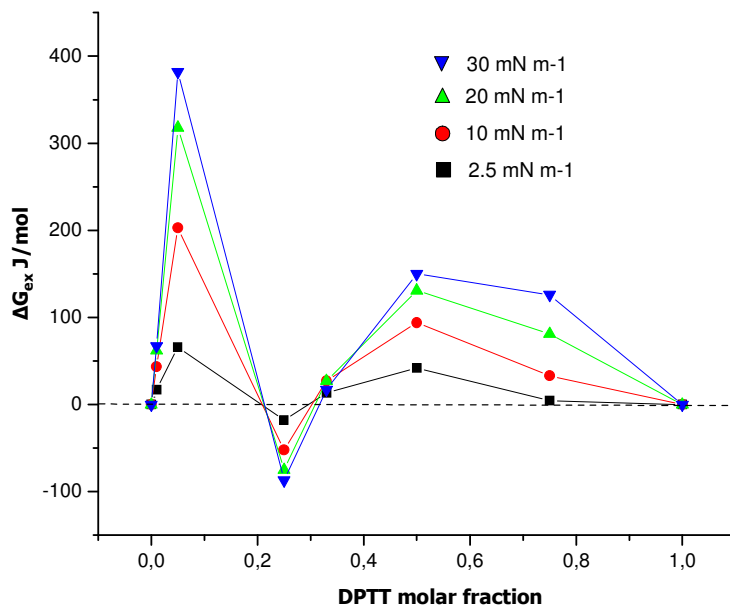


Figure 3.11. Excess free energy of mixing ( $\Delta G_{\text{ex}}$ ) as a function of DPTT molar fraction for 30, 20, 10 and 2.5 mN/m

### 3.3.5. Hysteresis of the pure anchor lipids

As it was already mentioned, after the collapse, the investigated phytanyl based lipids exhibit a very smooth isothermal line. This is a characteristic feature observed and reported for similar phytanyl based lipids.<sup>12</sup> It has been attributed to the formation of amorphous monolayers, which are softer than straight-chain lipid monolayers. The latter tend to form stiff crystalline phases that usually show rough isothermal shapes after the collapse. The reversibility of the collapse process has been proven for DPTL recording a hysteresis with an upper limit above the collapse pressure.<sup>19</sup> At such conditions the hysteresis should register significant material loss. However, such a loss has not been observed. Thus, it has been proposed that during the decompression of the already collapsed film, the lipid molecules in the water phase efficiently recovered the released surface area. The homogeneous mixing of the lipids is also a result of the lack of nonspecific intermolecular interaction. This statement is supported by the results obtained by recording the hysteresis of DPTT as described in Figure 3.12. The shape of the hysteresis does not show any irregularity of compression-expansion cycles. A decrease of  $\sim 2 \text{ \AA}$  in molecular area upon the

hysteresis cycle can be observed. This might be due to partial destruction of the monolayer (dissolution and collapse of the monolayer) and relaxation of the film.

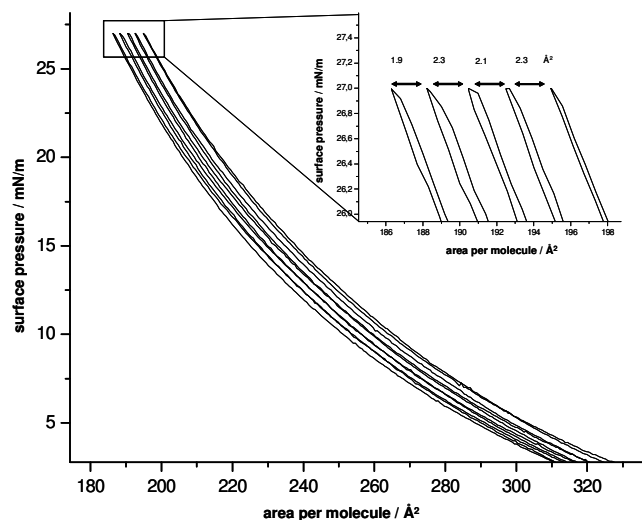


Figure 3.12. Hysteresis of DPTT at 20°C, compression rate 10 mm/min

### 3.3.6. Relaxation time investigation of the monolayers

Additionally, isobaric creep experiments were performed at a pressure of 31 mN/m as shown in Figure 3.13. The isobaric curve is relatively steep during the first 1.5 – 2 hours (1.5% area loss at 2 hours). Later on it follows a slow and constant decrease of  $A/A_0$  with the time. Similar behavior has been observed for lipids as well as surfactant molecules.<sup>25,26</sup> The effect was called “initial area loss” and was attributed to a structural rearrangement in terms of relieving surface inhomogeneities. They appear as a result of pushing together of condensed film islands as described by the nucleation theory for growth in supersaturated monolayers).<sup>27</sup> It has been found that the magnitude of the “initial area loss” depends directly on the compression rate. Thus, the effect is considerable at high rate of compression and is insignificant at lower one.



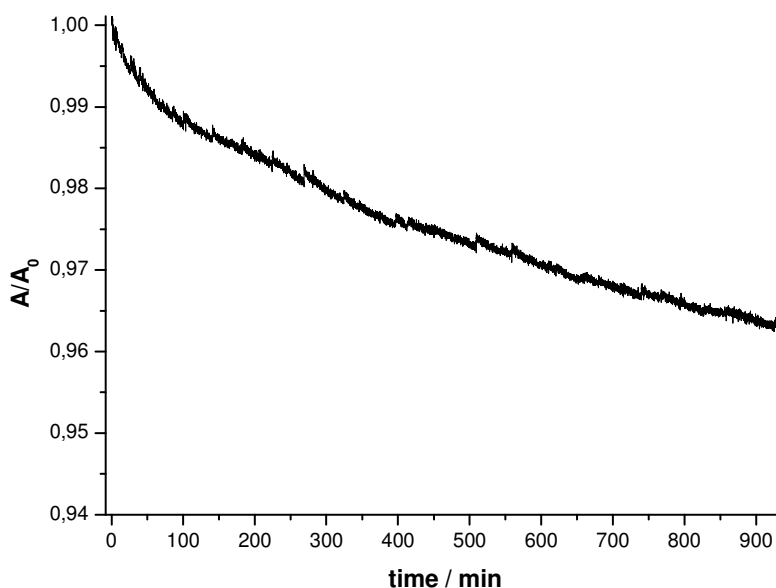


Figure 3.13. Relaxation curve of DPOT

### 3.4. Conclusion

The behavior and monolayer properties of four new thiolated anchor lipids on the air-water interface have been reported. Monomolecular films on Langmuir film balance can be used as a model system for membrane architectures. The results give useful information for the preparation of tBLMs, when the monolayer is transferred to a solid substrate. In this study, the packing density and mixing behavior at the air-water interface were investigated. Mixing of anchor lipids with free lipids might result in a decreased packing density, which might allow for the incorporation of complex membrane proteins.

The results indicated that an increase in the hydrophobicity (PEG chain length) of the anchor lipids leads to a higher packing density. A decrease in the temperature results in a similar trend. Furthermore, mixing the anchor lipids with free lipids can homogeneously dilute the anchor lipid monolayers. Thus, a full control over lateral arrangement of the lipid monolayers is possible and should now allow for a controlled transfer to solid substrates, leading to an adjustable platform for solid supported membranes.

## Literature

1. Langmuir, I.; Schäfer, V. J., *Journal of the American Chemical Society*, **1938**, *60*(6), 1351-1360.
2. Blodgett, K., *Journal of the American Chemical Society*, **1935**, *57*(6), 1007-1022.
3. Möhwald, H., *Annu. Rev. Phys. Chem.*, **1990**, *41*, 441-476.
4. Terrettaz, S.; Vogel, H., *MRS Bulletin*, **2005**, *30*, 207-210.
5. Valincius, G.; McGillivray, D. J.; Febo-Ayala, W.; Vanderah, D. J.; Kasianowicz, J. J.; Losche, M., *Journal of Physical Chemistry B*, **2006**, *110*(21), 10213-10216.
6. He, L. H.; Robertson, J. W. F.; Li, J.; Karcher, I.; Schiller, S. M.; Knoll, W.; Naumann, R., *Langmuir*, **2005**, *21*(25), 11666-11672.
7. Minamikawa, H.; Hato, M., *Langmuir*, **1997**, *13*(9), 2564-2571.
8. Mitchell, D. J.; Tiddy, G. J. T.; Waring, L.; Bostock, T.; McDonald, M. P., *Journal of the Chemical Society-Faraday Transactions I*, **1983**, *79*, 975-1000.
9. Smith, R. D.; Berg, J. C., *Journal of Colloid and Interface Science*, **1980**, *74*, 273-286.
10. Sackmann, E., *Science*, **1996**, *271*, 43-48.
11. Cornell, B. A.; Braach-Maksvytis, V. L. B.; King, L. G.; Osman, P. D. J.; Raguse, B., Wieczorek, L.; Pace, R. J., *Nature*, **1997**, *387*, 580-583.
12. Kitano, T.; Onoue, T.; Yamauchi, K., *Chemistry and Physics of Lipids*, **2003**, *126*, 225-232.
13. Gauger, D. R.; Binder, H.; Vogel, A.; Selle, C.; Pohle, W., *Journal of Molecular Structure*, **2002**, *614*, 211-220.
14. Lindsey, H.; Petersen, N. O.; Chan, S. I., *Biochimica Et Biophysica Acta*, **1979**, *555*, 147-167.
15. Braach-Maksvytis, V.; Raguse, B., *J. Am. Chem. Soc.*, **2000**, *122*, 9544-9545.
16. Baekmark, T. R.; Elender, G.; Lasic, D. D.; Sackmann, E., *Langmuir*, **1995**, *11*, 3975-3987.
17. Shinoda, K.; Shinoda, W.; Baba, T.; Mikami, M., *Journal of Chemical Physics*, **2004**, *121*, 9648-9654.
18. Naumann, R.; Schiller, S. M.; Giess, F.; Grohe, B.; Hartman, K. B.; Kaercher, I.; Köper, I.; Lübben, J.; Vasilev, K.; Knoll, W., *Langmuir*, **2003**, *19*, 5435-5443.
19. Kunze, J.; Leitch, J.; Schwan, A. L.; Faragher, R. J.; Naumann, R.; Schiller, S.; Knoll, W.; Dutcher, J. R.; Lipkowski, J., *Langmuir*, **2006**, *22*, 5509-5519.
20. Kim, K.; Shin, K.; Kim, H.; Kim, C.; Byun, Y., *Langmuir*, **2004**, *20*(13), 5396-5402.

- 
21. Petty, M. C., *Langmuir-Blodgett Films: An Introduction Cambridge University Press*, **1996**
  22. Lee, Y. L.; Lin, J. Y.; Chang, C. H., *Journal of Colloid and Interface Science*, **2006**, 296, 647-654.
  23. Sanchez, J.; Badia, A., *Thin Solid Films*, **2003**, 440, 223-239.
  24. Maget-Dana, R., *Biochimica et Biophysica Acta - Biomembranes*, **1999**, 1462 (1-2), 109-140.
  25. Smith, R. D.; Berg, J. C., *Journal of Colloid and Interface Science*, **1980**, 74, 273-286.
  26. Feria, J. d. I. F.; Patino, J. M. R., *Langmuir*, **1994**, 10, 2317-2324
  27. Vollhardt, D., *Advances in Colloid and Interface Science*, **1993**, 47, 1-23.

## 4. Electrical properties of diluted tBLMs

### 4.1. Introduction

All the efforts to synthesize the anchored lipids described in Chapter 2 are united in one goal: preparation of stable and flexible tBLMs. The quality of the membranes is judged from their electrical sealing properties. Since the artificial tBLMs aim to mimic the natural membranes in terms of ability to host functional membrane proteins, they should be simultaneously highly resistive against ion flow through the bilayer and fluid enough in order to ensure effective function of the embedded ion channels.

In general, tBLMs are prepared in a two-step procedure. The first step is the preparation of the monolayer, where different methods could be used. The most commonly used are LB-transfer and self-assembly, where the proximal leaflet, consisting of tether lipids, is covalently attached to the substrate. The next step to complete the formation of the lipid bilayer can be done by either vesicle fusion or solvent exchange. Finally, the incorporation of a protein (added during or after the membrane formation) examines the properties and quality of the membrane.

The electrical parameters of tBLMs as well as the evaluation of the functional protein incorporation can be measured by Electrochemical Impedance Spectroscopy (EIS). It is proven to be a powerful and accurate method for investigating the function of ion-channels and the influence of the membrane characteristics on their ability to transport ions across the membrane.

In this chapter, some preliminary EIS measurements of bilayer formation and protein incorporation are discussed.

## 4.2. Characterisation techniques

### 4.2.1. Electrochemical Impedance Spectroscopy

#### 4.2.1.1. Theory

Electrochemical Impedance Spectroscopy (EIS) is a useful technique to describe electrical parameters of a complex system. For solid supported membranes, where the support can act as an electrode, EIS can be used to study for example the resistive and capacitive components of a membrane. Several applications have been summarized by Terretaz et al.<sup>1</sup>

In principle, EIS describes the response of a system to an electrical stimulus. In an ideal case, a system simply follows Ohms law. The system can then be described in terms of simple elements, i.e. resistors and capacitors. However, in a complex system, these simple assumptions are no longer valid and the elements have to be replaced by complex elements.

In a typical EIS experiment, one applies a low frequency alternating current between a working and a counter electrode, controlled by a defined reference electrode. In our membrane experiments, the substrate is used as working electrode. If the amplitude  $E_0$  of the excitation signal is small (5-10 mV), one can obtain a linear response of the system. For an sinusoidal excitation signal of the frequency  $\omega$ ,

$$E = E_0 \sin (\omega t) \quad (4.1)$$

the current signal will have the same form with a reduced amplitude and a shifted phase:

$$I = I_0(\omega) \sin (\omega t + \varphi) \quad (4.2)$$

Figure 4.1 systematically visualizes this relationship.

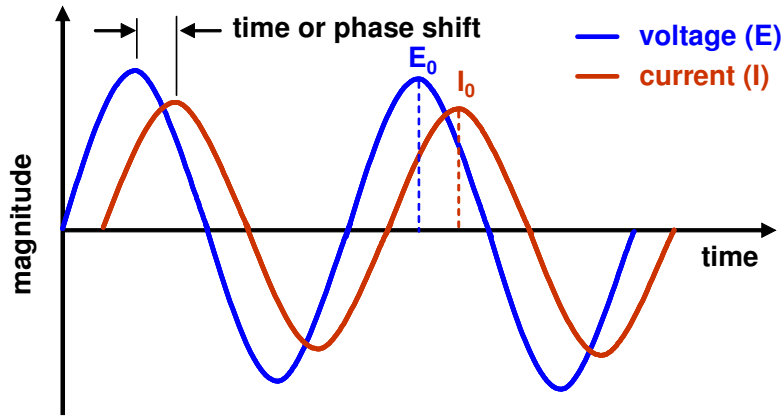


Figure 4.1. Current and voltage as a function of time

The impedance of the system can be expressed as

$$|Z(\omega)| = \frac{|E(\omega)|}{|I(\omega)|} \quad (4.3)$$

Bode plots are often used to visualize the response of the system. As shown in Figure 4.2,A, the absolute impedance is plotted as a function of the applied frequency, which typically is varied over various orders of magnitude. In this presentation, resistive elements can be seen as a horizontal line, while capacitive elements show a slope of -1. On the second axis of the Bode plot, the phase angle is plotted. Here, resistive parts show a low phase angle, while ideal capacitive elements have a phase angle of  $90^\circ$ .

The experimental data can be simulated using simple resistive and capacitive elements. For example, the curves in Figure 4.2 are a result of a simulation of a simple circuit model (Fig. 4.2,B). In our experiments, we will use a model, where two RC elements are in series with a resistor and a capacitance (Fig 4.2,C).

In this case, R1 represents the resistance of the electrolyte. The first RC element describes the lipid bilayer, while the second RC element described the spacer region. The last capacitor has to be added in order to take account of the electrochemical double layer at the electrode interface. This model circuit is more complicated than models used in former studies of similar systems. For example, in the DPTL system,

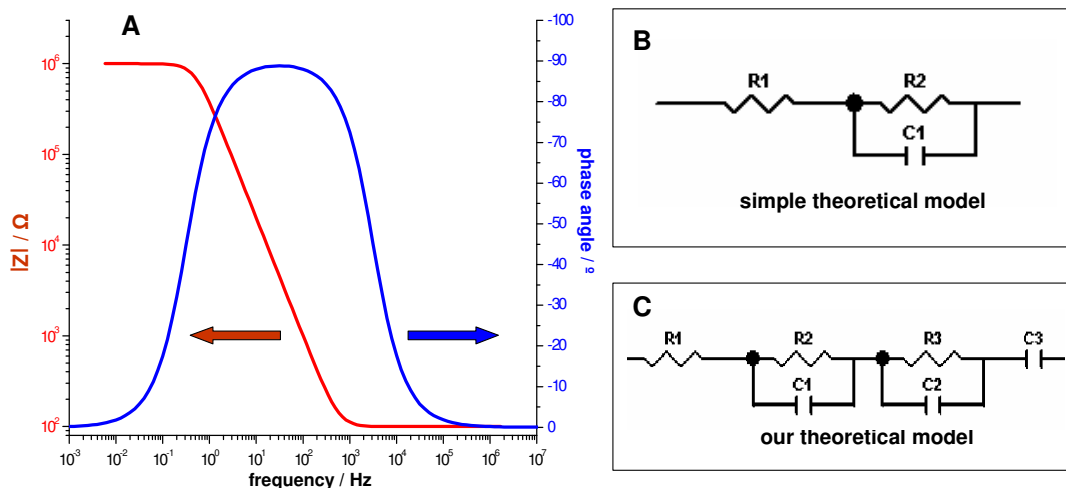


Figure 4.2. Representation of (A) the impedance  $Z$  and the phase shift  $\theta$  as a function of the frequency on a Bode plot, (B) simple theoretical model, and (C) double RC circuit fitting our experimental data

the second RC element and the electrochemical double layer often superimpose to a single capacitance. However, as shown later on, the experimental data clearly show two significantly different RC elements.

#### 4.2.1.2. Measurements

The impedance spectra were recorded using an Autolab Pgstat 12 impedance spectrometer with FRA (Frequency Response Analysis) software. The amplitude of the excitation signal was 10 mV. The frequency was changed in range from 100 kHz to 2 mHz and recorded at 30 different frequencies.

The experiments were conducted using in-house Teflon cells with the substrates as a working electrode, a coiled platinum wire (0.8 mm diameter, 99.9% purity, Mateck, Jülich, Germany) as a counter electrode and Dri Ref-2 reference electrode (World Precision Instruments, Berlin, Germany) immersed in 1 ml buffer solution above the substrate. The opened electrode area was  $0.2 \text{ cm}^2$ .

The raw data were analysed using ZVIEW software package (Version 2.9, Scribner Associates, NC, USA). The obtained values were normalized to the electrode surface area.

### 4.2.2. Atom Force Microscopy

Atomic force microscopy (AFM) is a type scanning probe microscopy measuring the local properties of the sample such as height, optical adsorption or magnetism with a tip placed very close to the sample. The forces between the sample and the tip can be repulsive or attractive. In repulsive “contact” mode, the tip at the end of the cantilever slightly touches the sample. The instrument drags the tip over the sample, and a detection apparatus measures the vertical deviation of the cantilever, which indicates the local sample height. In noncontact mode, AFM operates with measurement of the attractive forces. In this case, the tip does not touch the sample.

By using AFM, one can achieve a resolution in sub nanometer scale, and it can image the non-conducting surfaces. These advantages make AFM a suitable technique to solve processing and material problems in bioscience.

AFM scans were obtained by computer controlled device Dimension 3100 CL (Veeco Instruments, USA) by tapping mode. Single beam silicon cantilevers (Olympus OMCL-AC160TS-W2 Tapping Mode) with spring constants of  $\sim 45$  N/m and resonant frequencies of  $\sim 300$  kHz have been used. Tapping mode allowed us to study the roughness of the LB monolayers. Measurements were performed in ambient conditions. Dimensions of scans varied between  $5\mu\text{m} \times 5\mu\text{m}$  and  $3\mu\text{m} \times 3\mu\text{m}$ . Obtained images were processed using software Nanoscope Version 5.12r5.

### 4.2.3. Contact angle

Contact angle measurements provide information about the hydrophilicity (wetting properties) of the investigated surface. Direct information can be extracted by measuring the contact angle ( $\theta$ ) (Figure 4.4) between the baseline of a water droplet standing on the solid surface and the tangent at the drop boundary. For hydrophilic surfaces, the contact angle approaches  $0^\circ$ . On highly hydrophobic surfaces, the water droplet exhibit a large contact angle ( $>90^\circ$ ).



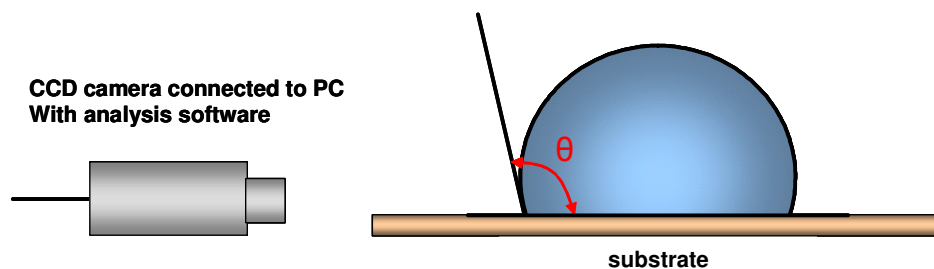


Figure 4.4. Contact angle measurement

The measurements of static, advancing and receding contact angles of pure DPTT, DPHT and DPOT LB monolayers were conducted on experimental setup DSA 10 from Krüss CA, Germany. The shape of a 5  $\mu\text{l}$  drop was recorded with a CCD camera. The contact angles were simulated with software Drop Shape analysis vl.5. The static contact angles of all other monolayers were derived on experimental setup OCA 15 plus SCA 20 software. The mean value was obtained by averaging 7 measurements per substrate.

## 4.3. Materials and methods

### 4.3.1. Anchor and free lipids, solutions

**Anchor lipids:** All anchor lipids used for tBLMs formation are synthesized as described in Chapter 2 and the purity is verified by  $^1\text{H}$  NMR and FD-MS.

**Free lipids:** DPhyPE used by preparation of LB-mixed monolayers as well as DPhyPC needed for the bilayer formation are commercial lipids from Avanti Polar Lipids (Alabaster, AL, USA)

**Buffer solutions:** KCl and NaCl were purchased from Acros organics, Geel, Belgium and are of ACS purity. Water from a Millipore purification system (Millipore GmbH, Eschborn, Germany) with specific resistance of  $> 18 \text{ M}\Omega \text{ cm}^{-1}$  was used for the 0.1M buffer solutions.

### 4.3.2. Substrates

All LB and SA monolayers needed for the electrochemical measurements in this study were prepared on Template Stripped Gold (TSG). TSG surfaces are useful for surface studies because a very consistent flat gold surface with few defects can be easily prepared. These characteristics are in great demand for fabrication of the extremely thin tBLMs.

For our study, TSG surfaces were produced according to Naumann et al.<sup>2</sup> The procedure includes the following steps. 50 nm gold films were deposited by electrothermal evaporation on clean silicon wafers (CrysTec, Berlin, Germany) with an Edwards evaporation machine. The gold surface was glued with an optical glue EPO-TEK (Epoxy Technology, USA) to glass slides (BK7, Menzel GmbH, Germany) and cured at 150°C for 1h. After cooling down, the slides are ready for use. In this state, they can be stored for weeks. Immediately before the experiment, the silicon wafer is stripped away, the gold surface is cleaned from mechanical impurities under an air stream, and it is immersed either into a self-assembly solution (by self-assembly) or into water sub phase (by LB-deposition).

### 4.3.3. Monolayer formation

The formation of tBLMs involves two consecutive steps. The first one consists in the formation of a monolayer. The monolayers should be densely packed in order to achieve sufficient hydrophobicity. Such highly ordered monolayers ensure the preparation of robust tBLMs with high insulating electrical properties. There are different methods to obtain monolayers, such as self-assembly, Langmuir-Blodgett transfer and lipid-detergent vesicles.

#### *Self-assembly*

Self-assembly is commonly used to create dense monolayers. It is preferred because of the small amount material needed and the ease of preparation.

The principle of this method is not fully understood, but in general is concentrated on spontaneous molecular assembly on the substrate caused by different types of interactions. In our case, the self-assembly of the anchor lipids is based on the strong sulfur-gold binding between the disulfide anchor group and the gold substrate, while

the hydrophobic forces between the hydrocarbon chains define the organization at the surface.

For self-assembled monolayers, a freshly stripped gold slide was placed for 24 hours either in an ethanolic solution (DPOT) or in a THF solution (DDPTT) containing 0.2 mg/ml of the corresponding thiolipid. Then, the slide was taken out, rinsed with EtOH, and dried in a nitrogen stream. The coated slides were immediately used for EIS measurements, but they can be used up to one month after the preparation.

It should be taken into account that even negligible impurities could cause significant influence on the electrical properties of the resulting membranes. Therefore, the self-assembly solution and the substrate surface purity should be controlled.

#### *Langmuir-Blodgett transfer*

Since one of the main goals in this study is to obtain less densely packed monolayers, Langmuir-Blodgett (LB) transfer could help to deposit diluted layers, which have been pre-arranged on the air-water interface. Controlled dilution in the proximal layer could increase the membrane fluidity, and thus, the incorporation of larger proteins.

The principle of the monolayer formation by Langmuir film balance as well as the experimental conditions was described in details in Chapter 3, section 3.1. The LB-transfer was conducted as a freshly stripped gold slide cleaned thoroughly in a nitrogen stream was immersed vertically into water sub phase. Then, the chloroform solution of the corresponding thiolipid was spread on the water surface. After relaxation for 20 min, the lipid molecules were compressed to the desired surface pressure. The substrate was pulled out of the sub phase with a speed 0.6 mm/min. The LB-monolayers were immediately investigated by EIS.

#### **4.3.4. Bilayer formation**

The second final step in the tBLM formation is the completion of the bilayer. The outer leaflet of the bilayer consists of free lipids. In our study, 1,2-Di-*O*-phytanoyl-*sn*-glycero-3-phosphoholine (DPhyPC), shown in Figure 4.5, was chosen because of the similarity to the hydrophobic part of the tethered lipids in the inner leaflet. This step has two important aspects: formation of the outer leaflet and filling the defects in the inner one in order to improve the sealing properties. As a result, an increase of the resistance and decrease of the capacitance is observed by EIS measurement.

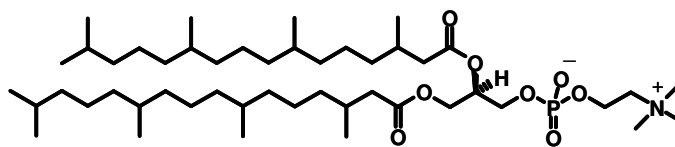


Figure 4.5. Structure of 1,2-Diphytanoyl-*sn*-Glycero-3-Phosphocholine (DPhyPC)

Two different strategies were used for the formation of the bilayer: vesicle fusion and solvent exchange.

#### *Vesicle fusion*

The bilayer in this case is formed by fusion of small unilamellar vesicles. The fusion is believed to occur in three steps: adhesion of the vesicles, bursting of the vesicles and spreading of the membrane patches towards formation of the second layer. Vesicles are prepared as follows: DPhyPC lipids are dissolved in MilliQ water at a concentration of 2 mg/ml. A turbid solution resulted by heating to 65°C and vortexing was extruded up to 21 times through a polycarbonate membrane with 50 nm pores to give a clear solution of vesicles. This solution was used during the next three days. 20  $\mu$ l of the vesicle solution were injected into the measuring cell having a volume of 1 ml, yielding a final lipid concentration of 0.04 mg/ml. Vesicle fusion was left 12 hours, while the impedance spectra were recorded every 60 min to follow the vesicle fusion process in situ.

#### *Solvent exchange*

This alternative approach turned out to be more appropriate for our systems. Solvent exchange was introduced by Miller et al<sup>3</sup> and consists of self-assembly of lipids on a hydrophobic surface during the exchange of solvent from ethanol to aqueous solution. After recording the impedance spectra of the monolayer, the buffer solution in the measuring cell was removed. 30  $\mu$ l ethanolic solution of DPhyPC (5 mg/ml) were spread above the monolayer. In 10 min, the bilayer formation was initiated spontaneously by rinsing the ethanolic solution in the cell with buffer at a very low speed. After about 60 min, the impedance spectra showed a steady state.

#### 4.3.5. Incorporation of valinomycin

The main application of the artificial tBLMs is to serve as a stable platform for protein incorporation where the function of the proteins could be investigated. Therefore, the quality of the obtained membranes, hence, the ability to host proteins in active form should be verified. A simple but useful test could be performed consisted in incorporation of small proteins and monitoring of their function. Since the time was limited, only preliminary experiments with valinomycin were conducted.

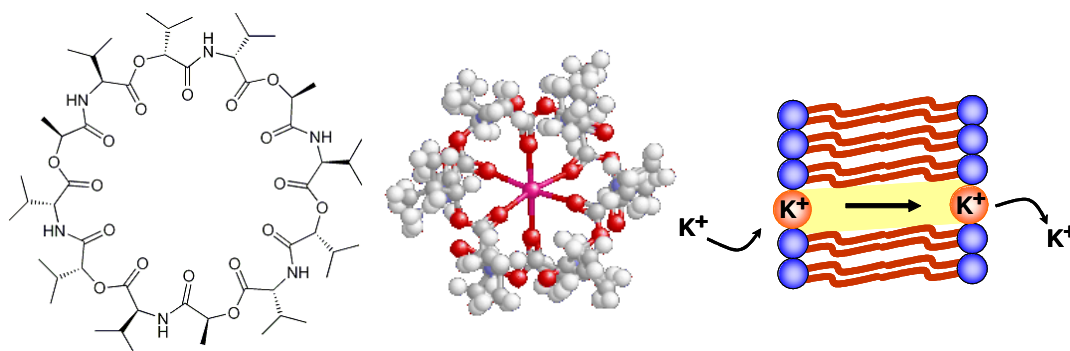


Figure 4.6. Structure of valinomycin and principle ion transfer through the membrane

Valinomycin is a dodecadepsipeptide (Figure 4.6) that consists of twelve alternating amino acids connected in a macrocyclic molecule. It is obtained from the cells of several *Streptomyces* strains and is a member of the group of natural neutral ionophores due to the lack a residual charge. It consists of enantiomers D-Valine and L-Valine, D-Hydroxyvaleric acid and L-Lactic acid. Structures are alternated bound via amide and ester bridges. Valinomycin is an ion carrier, highly selective for potassium ions. It functions as a potassium-specific transporter and facilitates the movement of potassium ions through lipid membranes in access of an electrochemical potential gradient.

## 4.4. Results and discussion

### 4.4.1. Application of DPTT, DPHT and DPHDL

Systematic investigation of the electrical properties of the self-assembled monolayers and the quality of the resulting tBLMs obtained from DPTT, DPHT and DPHDL is performed by my colleague Inga Vockenroth (MPIP, Mainz, Prof. Knoll's group).

The resistance and capacitance determined by EIS measurements has confirmed the expected lower density of the DPHDL-based monolayers, while the DPTT and DPHT-based monolayers have shown resistance in megaohm range. The bilayers built by fusion of vesicles have exhibited highly insulating properties, needed to ensure electrical measurement of ion flow only through the embedded proteins. The membranes are stable over weeks and robust towards rinsing.<sup>4</sup>

Several membrane proteins in terms of carrier, channels and pores have been incorporated in their functional form. For instance, valinomycin has been incorporated in DPTT.<sup>4</sup> It is an ion carrier selective to potassium cations. Decrease of the resistance with increasing potassium concentration in the buffer solution has been observed. Controlled and reproducible incorporation of synthesized M2 peptides into tBLMs based on DPHT has been reported.<sup>5</sup> DPHT (containing longer spacer part and one anchor group) compared with DPTL has shown incorporation of higher amount of functional ion channels. Finally,  $\alpha$ -Haemolysin, a pore forming toxin has been functionally embedded in DPTT and DPHDL-based tBLMs. The less densely packed DPHDL-based membrane has shown significant decrease of the resistance in comparison with DPTT. Moreover, the concentration of  $\alpha$ -Haemolysin needed to produce a detectable effect in a DPTT-based tBLM has found to be relatively higher than the detection limit of the DPHDL-based membrane. The latter could be explained with the higher fluidity of the DPHDL-tBLMs, hence, ability to incorporate higher amount of protein (paper in preparation).

### 4.4.2. Membrane formation based on LB-diluted monolayers

The use of Langmuir film balance technique allowed for the investigation of the influence of parameters such as temperature, surface pressure, structure of the lipids,

content of the lipid mixture and relaxation time on the packing density of the monomolecular lipid films at the air-water interface. Control of these parameters is decisive for the proper lipid monolayers transfer to solid substrates. The observed behaviour of the lipids on the air-water interface, described in Chapter 3, allowed us to conclude that the lowest mean molecular area of the lipids and the highest collapse pressure can be achieved with DPOT. The density of the lipids on the LB through can be increased if the pure tether lipids are mixed with free lipids (DPhyPE). Therefore, the DPOT/DPhyPE mixed lipid system was mainly used for preparation of denser lipid monolayers for further tBLM formation. Thus, mixed monolayers with different DPOT/DPhyPE ratio were transferred on gold substrates at different surface pressure (50% and 75% from  $\pi^*$ ). The static contact angles showed values above 90°. The obtained very high hydrophobicity of the monolayers is prerequisite for successful bilayer formation.

Unfortunately, the electrical properties of the monolayers in terms of resistance and capacitance determined by EIS were not satisfactory and further vesicle fusion did not result in a stable membrane. According to the results from EIS and CA measurements, we concluded that, in spite of the high hydrophobicity caused by the phytanyl chains, the mixed monolayers prepared by LB-transfer are rather diluted. Since the concentration of the tether lipids in the mixture is lower than that of the pure tether lipid monolayers, the gold surface can not be completely covered and the LB monolayers are not stable enough to prepare robust tBLMs. In spite of the fact that the mixed monolayers are denser, it was found that the presence of non anchor lipids does not facilitate and might even hinder the vesicle fusion process.

To improve the surface coverage, further experiments with pure DPTT, DPHT and DPOT anchor lipids were performed. The monolayers were deposited close to the collapse pressure at 80% from  $\pi^*$ . Then, the covered substrates were washed with ethanol and sonicated for 5 min in ethanol in order to remove the rest of not covalently attached lipids. The roughness of the lipid monolayers was measured by AFM. The AFM images, depicted in Figure 4.7, show a large smooth area and low roughness from 0.418 nm for DPTT to 0.533 nm for DPOT (25 $\mu\text{m}^2$ ). This slightly increase of the roughness from DPTT through DPHT to DPOT is probably due to increase of the molecular weight (length) of the molecules containing tetra, hexa and octaethylene glycol, respectively as a spacer part. The increase of the spacer part will cost increase

the number of the possible conformations, and thus will increase the roughness. However, the obtained roughness values are comparable to the roughness of bare TSG (0.358 nm).<sup>6</sup>

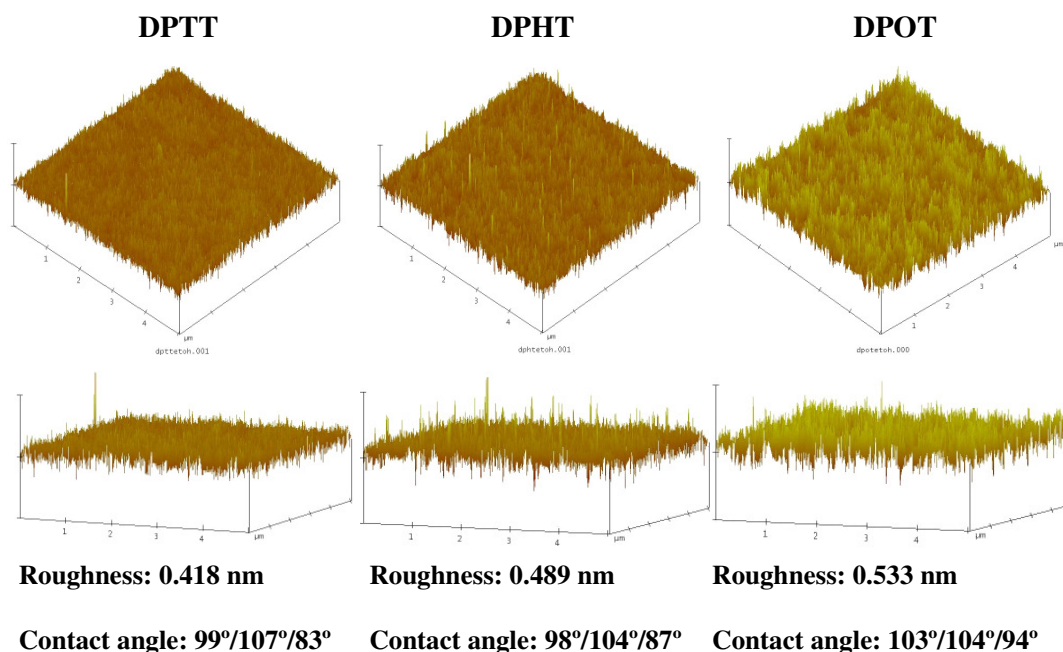


Figure 4.7. AFM images and contact angle (static / advancing / receding) of DPTT, DPHT and DPOT lipid monolayers obtained by LB-transfer on TSG

Additionally, the contact angles (Figure 4.7) are around 100°, which is characteristic for highly hydrophobic surfaces. The impedance spectra of these monolayers still did not show better results and subsequent vesicle fusion only slightly improved the electrical parameters.

Different parameters were varied in order to tune the transfer conditions. For instance, the transfer pressure was decreased. Furthermore, to get denser and homogeneous monolayers, the temperature was lowered. A different attempt to reach such properties was relaxation of the monolayers on the surface for a certain period of time before transfer. Unfortunately, all the attempts in this direction failed.

The reason is supposed to be in the more diluted monolayers obtained by LB than by SA technique. In principle, the lowest area per molecule reached with our tether lipids by Langmuir film balance (DPOT, 4°C) is  $\sim 95 \text{ \AA}^2$ , while the reported mean molecular area for the similar self-assembled DPTL is between 51 - 75  $\text{\AA}^2$ .<sup>7</sup>



It was reported<sup>6,8,9</sup> that tBLMs formation on diluted SAMs can be successfully performed when solvent exchange is applied. Therefore, in the following experiment, the ability to form membrane on LB-monolayer was examined comparing vesicle fusion and solvent exchange. LB-transfer of DPOT at lower surface pressure ( $\pi = 31.5$  mN/m, 75% from  $\pi^*$  and speed up 0.6 mm/min) was conducted.

The contact angle slightly decreased to 94°. After 12 hrs vesicle fusion, the resistance changed slightly, and the decrease of the capacitance was negligible. However, the solvent exchange method was successfully applied and proved the formation of bilayer. 30  $\mu$ l DPPC in an ethanolic solution were injected in the EIS cell above the lipid monolayer. In 10 min, the surface was rinsed with 0.1M KCl (~ 5 ml) at very low speed. The formation of the bilayer was initiated simultaneously by changing the ethanolic with buffer solution. The impedance spectra depicted in the Bode plot (Figure 4.8) was derived recording the system at steady state. The bilayer formation is observed by appearance of a characteristic shoulder in the impedance curve and phase shift plateau at high frequencies.

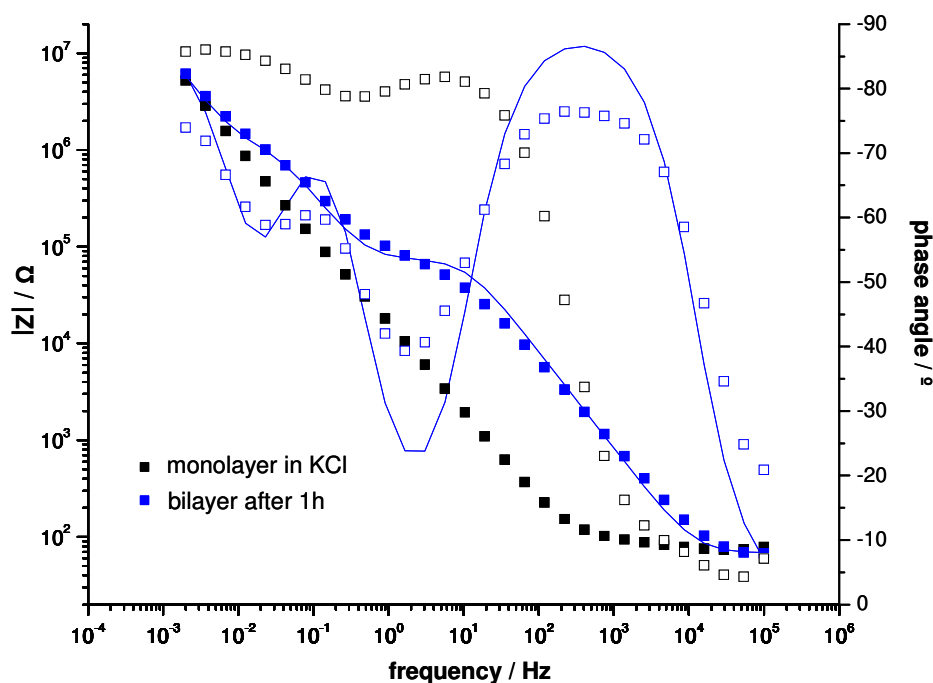


Figure 4.8. Bilayer formation *via* solvent exchange on DPOT-based LB-monolayer

The data are fitted with addition of a second RC element in the equivalent circuit. The calculated electrical parameters fitted with the model shown in Figure 4.2 are presented in Table 1. The resistance increases by factor of 5, while the capacitance drops steady down after the bilayer formation.

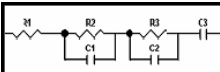
	$R_2$ [ $k\Omega \text{ cm}^2$ ]	$C_1$ [ $\mu\text{F}/\text{cm}^2$ ]	$R_3$ [ $M\Omega \text{ cm}^2$ ]	$C_2$ [ $\mu\text{F}/\text{cm}^2$ ]	$C_3$ [ $\mu\text{F}/\text{cm}^2$ ]
<b>monolayer</b>	<b>4.56</b>	<b>60.71</b>	<b>14.10</b>	<b>53.57</b>	-
<b>bilayer</b>	<b>20</b>	<b>0.71</b>	<b>0.20</b>	<b>25</b>	<b>50</b>

Table 1. Calculated equivalent circuit values for bilayer formation based on DPOT LB-monolayer

The calculated value of  $C_2$  ( $25 \mu\text{F}/\text{cm}^2$ ) is comparable with the Helmholtz capacitance ( $10\text{-}30 \mu\text{F}/\text{cm}^2$ ). The appearance of double-layer capacitance implies that the gold surface is not completely covered with lipid molecules. The appearance of  $C_3$  remains unclear. However, the second RC element ( $R_2C_1$ ) clearly shows the formation of a bilayer with a capacitance very close to the natural membranes and a resistance in kilohm range.

#### 4.4.3. Membrane formation of DPOT-based self-assembled monolayers

We compared also the electrical parameters of membranes prepared from pure DPOT using LB and SA technique.

The self-assembly monolayer was obtained on a gold substrate (stripped immediately before the experiment) immersed in an ethanolic solution of DPOT ( $0.2 \text{ mg/ml}$ ) for 24h. The coated gold slide was thoroughly rinsed with ethanol prior to use. A contact angle of  $107^\circ$  was obtained. Similarly to DPOT-based LB-monolayer, solvent exchange was chosen to form a bilayer. One hour after solvent exchange, a steady state was achieved and no further change in the impedance spectra depicted in Figure 4.9 was observed. In the impedance spectra, it is seen that two RC elements appear due to the bilayer formation. Double RC model (Figure 4.2) was used to fit the data. The capacitance in

both RC elements is in range of a natural membrane (Table 2). The resistance related to the RC element at higher frequencies is very low, but the RC element at lower frequency has value in megaohm range.

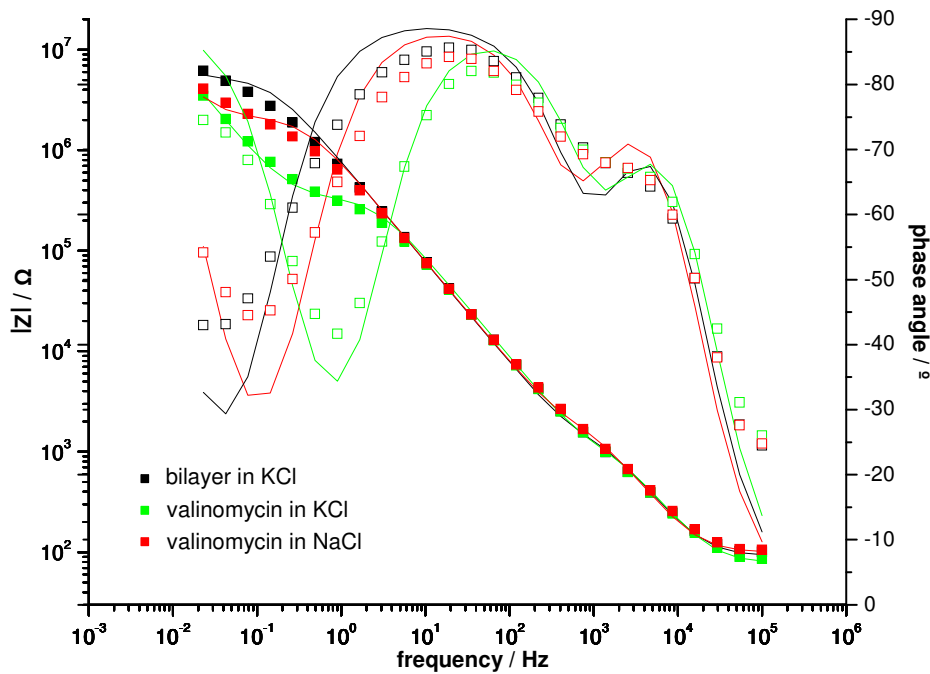
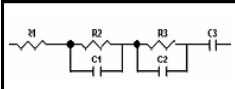


Figure 4.9. DPOT-based bilayer formation *via* solvent exchange and valinomycin incorporation

The relatively longer spacer part of DPOT may start to affect the electrical properties of the resulting membrane. Since both RC elements have very low capacitance similar to the native membrane, we supposed that these two RC elements are due to the bilayer formation. Moreover,  $R_2C_1$  element at higher frequencies is due to the spacer part, while the other ( $R_3C_2$ ) is caused from the bilayer. Finally, the appearance of another capacitance ( $C_3$ ) could be related to the Helmholtz capacitance that implies a presence of lateral space between the tethered lipids on the gold substrate. One can conclude that the appearance of second RC element and Helmholtz capacitance might explain the presence of ionic reservoir beneath the membrane.



	$R_2$ [ $k\Omega \text{ cm}^2$ ]	$C_1$ [ $\mu\text{F}/\text{cm}^2$ ]	$R_3$ [ $M\Omega \text{ cm}^2$ ]	$C_2$ [ $\mu\text{F}/\text{cm}^2$ ]	$C_3$ [ $\mu\text{F}/\text{cm}^2$ ]
<b>bilayer</b>	<b>0.209</b>	<b>0.54</b>	<b>1.36</b>	<b>0.79</b>	<b>10.71</b>
<b>valinomycin 0.1 M KCl</b>	<b>0.252</b>	<b>0.54</b>	<b>0.08</b>	<b>0.71</b>	<b>6.79</b>
<b>valinomycin 0.1 M NaCl</b>	<b>0.336</b>	<b>0.61</b>	<b>0.48</b>	<b>0.79</b>	<b>9.29</b>

Table 2. Calculated equivalent circuit values for DPOT SA-based bilayer built by solvent exchange and valinomycin incorporation

The membrane formation and its ability to serve as a platform for protein incorporation in their functional form are commonly verified by incorporation of small proteins or ion carriers.<sup>6-11</sup> In our case, the incorporation of valinomycin was examined. The presence of potassium ions causes drop of the resistance of a membrane containing valinomycin. Figure 4.9 shows the EIS data of a DPOT-based membrane with incorporated valinomycin (green curve). Further exchange of the 0.1M KCl with 0.1M NaCl blocks the ion carrier and leads to reversible increase of the resistance (red curve). The obtained values for the resistance and capacitance are listed in Table 2. In presence of valinomycin, the resistance in  $R_3C_2$  drops by 2 orders of magnitude, while the capacitance stays almost constant. However, in the other  $R_2C_1$  element not only the capacitance but also the resistance do not change significantly. Hence,  $R_2C_1$  is not influenced by the peptide incorporation. This confirms the statement that  $R_2C_1$  is due to the spacer part, while the  $R_3C_2$  element related to the bilayer is strongly influenced by the valinomycin incorporation.

#### 4.4.4. Membrane formation of DDPTT-based self-assembled monolayers

The need of less densely packed in the spacer part monolayers suited to study the incorporation of proteins with large subunits led to the synthesis of DDPTT. This molecule has two main advantages. It contains extended hydrophobic part to reduce the leakage through the membrane and defines lower two-dimensional packing density beneath the membrane.

The LB-isotherm of DDPTT (section 3.3.1) has shown lower collapse pressure at higher area per lipid molecule in comparison with the other synthesized lipids. Therefore, self-assembly was chosen to form a monolayer followed by solvent exchange proved to be successful by membrane formation. Some preliminary EIS experiments were conducted to determine the electrical properties of the DDPTT-based tBLM.

Since DDPTT contains four phytanyl chains, the high hydrophobicity did not allow to dissolve it in ethanol. Thus, the gold substrate was immersed in a THF solution (0.2 mg/ml) of DDPTT for 24 hours. The measured static contact angle is about  $100^\circ$ .

Two RC elements in the impedance spectra presented in Figure 4.10 can be observed. The dataset was fitted with the same theoretical model used by DPOT. The calculated values listed in Table 3 point capacitance characteristic for the nature membranes and a resistance in megaohm range.

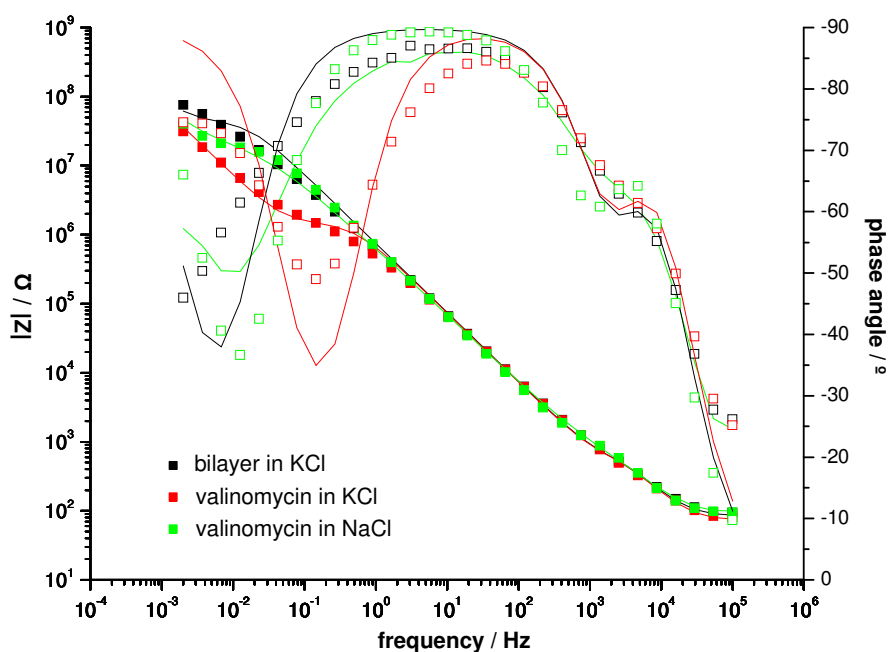



Figure 4.10. DDPTT-based bilayer formation via solvent exchange and valinomycin incorporation

Similarly to DPOT, valinomycin was successfully incorporated in DDPTT-based membrane as can be seen in Figure 4.11. The fitted data (Table 3) indicate decrease of the resistance after complete peptide incorporation followed by reversible increase when potassium buffer is exchanged with sodium buffer.



	$R_2$ [ $k\Omega \text{ cm}^2$ ]	$C_1$ [ $\mu\text{F}/\text{cm}^2$ ]	$R_3$ [ $M\Omega \text{ cm}^2$ ]	$C_2$ [ $\mu\text{F}/\text{cm}^2$ ]	$C_3$ [ $\mu\text{F}/\text{cm}^2$ ]
<b>bilayer</b>	<b>0.01</b>	<b>0.61</b>	<b>10.95</b>	<b>0.86</b>	<b>6.55</b>
<b>valinomycin 0.1 M KCl</b>	<b>0.14</b>	<b>0.61</b>	<b>0.36</b>	<b>0.86</b>	<b>7.86</b>
<b>valinomycin 0.1 M NaCl</b>	<b>0.14</b>	<b>0.61</b>	<b>4.20</b>	<b>0.96</b>	<b>7.86</b>

Table 3. Calculated equivalent circuit values for DPOT bilayer built by solvent exchange and valinomycin incorporation

In spite of the fact that the presented data are derived only from some preliminary results, it was shown that the bilayer formation based on self-assembled DPOT and DDPTT monolayers has potential. Further detailed investigations are needed to prove the promising application of these diluted but resistive membranes in incorporation of larger proteins.

#### 4.5. Conclusion

All anchor lipids synthesized in this work showed ability to form bilayers and incorporate functional proteins.

Briefly, the electrical properties and the successful incorporation of several proteins such as an ion carrier (valinomycin), an ion channel (M2) and a pore ( $\alpha$ -Haemolysin) in membranes based on DPTT, DPHT and DPHDL, respectively, accomplished by Inga Vockenroth were presented.

The expected lower density of the DPHDL-based membranes due to the “self-diluted” character of the molecule was confirmed, while the DPTT-based membranes has shown, similarly to DPTL high resistance due to the dense assembly of the tethered lipids on the gold surface. DPHT containing longer than DPTT spacer part formed bilayer with lower, but still in megaohm range resistance. Nevertheless, these membranes demonstrated ability to incorporate higher amount of functional protein. Finally, the membranes itself are stable over few weeks and robust against rinsing.

Several attempts towards preparation of diluted LB-monolayers based on pure DPTT, DPHT, DPOT and mixed lipids (DPOT/DPhyPE) in different ratio and transfer pressure were performed. Unfortunately, in spite of the high contact angle (hydrophobicity) of the monolayers, the electrical parameters measured by EIS were not sufficient. This may be due to the fact that for our lipids the use of Langmuir film balance did not allow to approach low enough areas per molecule needed to build stable membranes. However, it was shown that a LB-monolayer based on pure DPOT transferred at 75% of  $\pi^*$  could form a bilayer by solvent exchange. tBLMs obtained in this way showed low stability and therefore are disabled to incorporate proteins.

Some preliminary investigations of the electrical sealing properties of self-assembled DPOT and DDPTT-based mono- and bilayers were conducted. Solvent exchange was applied to complete the bilayers. It was found that the longer spacer in DPOT and the bigger space between the DDPTT molecules ensured by their extended hydrophobic parts essentially influence the electrical parameters of the membrane. The space beneath the membrane is clearly visible in impedance spectra by the appearance of a second RC element. The latter exhibits low resistance, but the capacitance is similar to the natural membranes. DPOT and DDPTT-based membranes showed high resistance in megaohm range and low capacitance comparable with that of the natural one.

Finally, the ability to host proteins in their functional form was tested with incorporation of the small ion carrier valinomycin. In both types of membranes, a drop of the resistance in the valinomycin containing membranes was observed followed by reversible increase of the resistance caused by exchange of the potassium ions with sodium buffer.

Systematic investigation towards optimisation the electrical properties of the DPOT and DDPTT-based membranes as well as better understanding the contribution of the space beneath the membrane will be object of further research. Additionally, the influence of the latter to the membrane fluidity could be tested by incorporation of larger proteins.

## Literature

1. Terrettaz, S.; Vogel, H., *MRS Bulletin*, **2005**, 30(3), 207-210.
2. Naumann, R.; Schiller, S. M.; Giess, F.; Grohe, B.; Hartman, K. B.; Karcher, I.; Köper, I.; Lübben, J.; Vasilev K.; Knoll, W., *Langmuir*, **2003**, 19, 5435-5443.
3. Miller, C.; Cuendet, P.; Gratzel, M., *Journal of Electrochemical Chemistry*, **1990**, 278, 175-192.
4. Vockenroth, I.; Atanasova, P.P.; Knoll, W.; Köper, I., *IEEE sensors*, **2005**.
5. Vockenroth, I.; Atanasova, P.P.; Long, J. R.; Jenkins, A. T. A.; Knoll, W.; Köper, I., *Biochimica et Biophysica Acta (BBA) – Biomembranes*, **2007**, 1768(5), 1114-1120.
6. Breffa, C., *New synthetic strategies to tethered bilayer lipid membranes*, **2005**, Johannes Gutenberg Universität: Mainz.
7. Kunze, J.; Leitch, J.; Schwan, A. L.; Faragher, R. J.; Naumann, R.; Schiller, S.; Knoll, W.; Dutcher, J. R.; Lipkowski, J., *Langmuir*, **2006**, 22, 5509-5519.
8. Valincius, G.; McGillivray, D. J.; Febo-Ayala, W.; Vanderah, D. J.; Kasianowicz, J. J.; Lösche, M., *The Journal of Physical Chemistry, B*, **2006**, 110, 10213-10216.
9. Store, T.; Lakey, J. H.; Vogel, H., *Angew. Chem., Int. Ed. Engl.*, **1999**, 38, 389.
10. Atanasov, V.; Knorr, N. Duran, R. S.; Ingebrandt, S.; Offenheusser, A.; Knoll, W.; Köper, I., *Biophysical Journal*, **2005**, 89(3), 1780-1788.
11. Knoll, W.; Yu, F.; Neumann, T.; Schiller, S.; Naumann, R., *Physical Chemistry Chemical Physics*, **2003**, 5(23), 5169-5175.



## 5. Conclusion and outlook

Tethered lipid bilayers, as model membranes, became recently a subject of many research activities. They mimic the cytoplasmic membrane of the biological cell and are similarly composed of two amphiphilic layers. The proximal layer is based on so-called anchor lipids. They have a hydrophobic tails connected to a hydrophilic spacer. The latter is covalently attached *via* anchor to the substrate. The bilayer is formed by spreading a second monolayer of free phospholipids onto the tethered lipid monolayer. tBLMs are robust and fluid systems stable over months. They are densely packed and have high sealing properties. Therefore, tBLMs are an excellent platform for investigation the incorporation and function of transmembrane proteins and further for biosensing applications. However, tBLMs on gold surface often suffer from the very dense tethered lipid layer. Thus, proteins containing large submembrane units can not be embedded into the bilayer. Therefore, the increase of the ionic reservoir beneath the membrane is of great importance.

The main goal in this study was to develop a suitable approach to increase the submembrane space in tBLMs. The challenge in this task is to create a tBLM with lower lipid density in order to increase the membrane fluidity, but to avoid defects that might appear due to increase in the lateral space within the tethered monolayers. Therefore, various synthetic strategies and different monolayer preparation techniques were examined to obtain a system fulfilling these requirements.

Synthetic attempts to achieve a large ionic reservoir were made in two directions: increasing the spacer length of the tether lipids and increasing the lateral space of the lipids in the monolayer. The latter resulted in the synthesis of a small library of tether lipids that were characterized by  $^1\text{H}$ - $^{13}\text{C}$  NMR, FD-MS, ATR, DSC and TGA.

In the frame of this work, a new synthetic strategy for preparation of tether lipids suitable for different substrates was established. This approach includes the synthesis of a “universal” lipid precursor with double bond anchor that can be easily modified for different substrate (*e.g.* metal and metaloxide). Since this study is focused on the preparation of tBLMs on gold surface, a very simple and fast procedure was applied to modify the double bond into a thiol group. It was shown that the spacer length of the tether lipids can be tuned by varying the length of the ethylene glycol chains in the

spacer. Thus, a series of three new tether lipids DPTT, DPHT and DPOT was obtained. Differential scanning calorimetry derived  $T_g$  values lower than  $-20^\circ\text{C}$  that is a prerequisite for preparation of fluid membranes in ambient conditions. FD-MS has shown that the obtained lipids exist as dimers. However, all lipids have good solubility and are surface active.

The synthesis of the tether lipid precursor with octadecaethylene glycol (ODEG) in the spacer part was demonstrated. However, following a multiple step procedure, the product was obtained in a very low yield mainly due to significant material lost by isolation and purification. In order to improve the efficiency, a further optimization of the synthetic strategy should include coupling with the hydrophobic part in the beginning of the synthesis. The phytanyl chains will lower the polarity of the precursors and thus facilitate their detection and isolation.

Two new tetraethylene glycol thiolated spacer molecules were obtained in good yields. The molecules have been used by Jing Li (thesis in preparation) within a project concerning preparation of mixed monolayers and thus to lower the packing density of the tethered lipids on the surface.

Another approach towards preparation of monolayers with decreased two-dimensional packing density of the lipids was the synthesis of a novel tether lipid DPHDL containing two lipoic anchor moieties. This "self-diluted" lipid provides additional lateral space excluding the need of a spacer molecule that might lead to phase separation. Additionally, the molecule was designed in a way to provide higher number of thiol functionality and thus to prevent eventual lipid desorption in solution.

The extended lipophilic part of DDPTT should lead to the preparation of more homogeneously diluted, leakage free proximal layers that will facilitate the completion of the bilayer. The synthetic route includes the preparation of an intermediate with a double bond functionality that could be modified according to the required surface. Modification with silane anchor for silicon oxide surfaces could be very useful for solving the problem with rather diluted SAMs obtained on silicon wafers. Within current study the double bond of the "universal precursor" was converted to thiol for binding to gold surface.

Our tool-box of tether lipids was completed with two fluorescent labelled lipid precursors. Two different synthetic approaches were examined. Although the first one was not successful, the second led to preparation of two precursors with one and two phytanyl chains in the hydrophobic region and a dansyl group as a fluorophore. The fluorescent activity of the lipids was verified by measuring the absorption and emission spectra compared to those of the dansyl chloride. The use of such fluorescently marked lipids is supposed to give additional information for the lipid distribution on the air-water interface. Thus, further modification of the double bond to chloro- or alkoxy-silane anchors will enable direct monitoring of distribution of the deposited monolayers on the silicon oxide (*e.g.* glass) substrate.

The Langmuir film balance was used to investigate the monolayer properties of four of the synthesized thiolated anchor lipids DPTT, DPHT, DPOT and DDPTT. The packing density and mixing behaviour were examined. The derived results have shown that mixing anchored with free lipids can homogeneously dilute the anchored lipid monolayers. Moreover, an increase in the hydrophilicity (PEG chain length) of the anchored lipids leads to a higher packing density. A decrease in the temperature results in a similar trend. Opposed to these results, increasing the number of phytanyl chains per lipid molecule is shown to decrease in the packing density.

DPTT, DPHT and DPHDL were assembled for preparation of tBLMs. The incorporation of functional proteins in these membranes was investigated by Inga Vockenroth using EIS. Self-assembled DPTT-based membranes have shown high resistance in megaohm range supported with dense monolayers that could incorporate mostly small proteins such as valinomycin and gramicidin. However, DPHT having longer spacer demonstrated the ability to incorporate larger amount of functional M25 protein in comparison with DPTL possessing shorter spacer.

The expected lower density of the DPHDL-based tBLMs caused by the special design of the molecule was confirmed with the observed lower resistance of the membrane. Nevertheless, the enhanced fluidity of these membranes allowed for incorporation of higher amount of bigger proteins such as  $\alpha$ -Haemolysin.

LB-monolayers based on pure DPTT, DPHT, DPOT and mixed lipids (DPOT/DPhyPE) in different ratio and transfer pressure were tested to form tBLMs with diluted inner

layer. In spite of the high contact angle, the electrical parameters did not show formation of bilayers with good electrical sealing properties. It was found that the use of Langmuir film balance technique did not allow approaching low enough areas per molecule needed to build-up stable membranes. However, a combination of the LB-monolayer transfer with the solvent exchange method accomplished successfully the formation of tBLMs based on pure DPOT.

Some preliminary investigations of the electrical sealing properties and protein incorporation of self-assembled DPOT and DDPTT-based tBLMs were conducted. The bilayer formation successfully performed by the solvent exchange technique resulted in membranes with high resistance in megaohm range and comparable with the natural membrane capacitance. The appearance of space beneath the membrane is clearly visible in the impedance spectra expressed by a second RC element. The latter brings the conclusion that the longer spacer in DPOT and the bigger lateral space between the DDPTT molecules in the investigated systems essentially influence the electrical parameters of the membrane. Finally, we could show the functional incorporation of the small ion carrier valinomycin in both types of membranes.

The DPOT and DDPTT-based membranes should be systematically investigated in order to improve their electrical properties. Additional information concerning the influence of space beneath the membrane to the sealing properties of these systems is needed. Additionally, an object of further research will be evaluation of the membrane fluidity tested by incorporation of transmembrane proteins with submembrane parts. Furthermore, the fluidity and the sealing properties of the membrane can be optimized by mixing different anchor lipids.

Different surface-sensitive techniques commonly used to investigate supported membranes such as SPR, QCM and FRAP could be applied to our membranes to extract further information about their characteristics.

## Abbreviations

Ac	acetone
AFM	Atom Force Microscopy
AIBN	azobisisobutyronitrile
ATR	Attenuated Total Reflection
CDCl <sub>3</sub>	deuterated chloroform
CH	cyclohexane
CSI	chlorosulfonyl isocyanate
DCM	dichloromethane
DMAP	dimethylaminopyridine
DPhyPC	diphytanyl phosphatidylcholine
DPhyPE	diphytanyl phosphatidylethanolamine
DPG	diphytanyl glycerol
DSC	Differential Scanning Calorimetry
EDC	1-Ethyl-3-(3-dimethylaminopropyl)-carbodiimide
EO	ethylene oxide
EtAc	ethylacetate
Et <sub>2</sub> O	diethyl ether
EIS	electrochemical impedance spectroscopy
EtOH	ethanol
FC	flash chromatography
FD-MS	Field Desorption Mass Spectroscopy
FRAP	Fluorescence Recovery After Photobleaching
HE	hexane
LB	Langmuir – Blodgett
MeOH	methanol
NMR	Nuclear Magnetic Resonance
PE	petrol ether
PEG	polyethylene glycol
QCM	Quartz Crystal Microbalance
RT	room temperature
SA	self-assembly
SAM	self assembly monolayer
SE	solvent exchange
sBLM	supported Bilayer Lipid Membrane
SPR	Surface Plasmon Resonance
TEA	triethylamine
T <sub>g</sub>	glass transition temperatures
TGA	thermogravimetric analysis
tBLM	tethered Bilayer Lipid Membrane
THF	tetrahydrofuran
TLC	thin layer chromatography
TSG	template stripped gold
VF	vesicle fusion

**Synthetic lipids**

DPTL	2,3-di-O-phytanyl-sn-glycerol-1-tetraethylene glycol-D,L-lipoic acid ester lipid
DPTT	2,3-di-O-phytanyl-glycerol-1-tetraethylene glycol-3'-mercaptopropyl ether lipid
DPHT	2,3-di-O-phytanyl-glycerol-1-hexaethylene glycol-3'-mercaptopropyl ether lipid
DPOT	2,3-di-O-phytanyl-glycerol-1-octaethylene glycol-3'-mercaptopropyl ether lipid
DPHDL	2-(2',3'-di-O-phytanyl-glycerol-1'-hexaethylene glycol)-glycerol-1,3-di-O-D,L-lipoic acid ester lipid
DDPTT	1,3-di-(2',3'-di-O-phytanyl-glycerol)-glycerol-2-tetraethylene glycol-3''-mercaptopropyl ether lipid

**Number Names of the compounds used in the synthetic part**

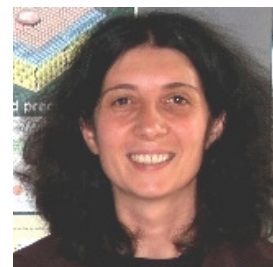
<b>1</b>	3,7,11,15-Tetramethyl-hexadec-2-en-1-ol (phytol)
<b>2</b>	3,7,11,15-Tetramethyl-hexadecan-1-ol (phytanol)
<b>3</b>	1-Bromo-3,7,11,15-tetramethyl-hexadecane (phytanyl bromide)
<b>4</b>	[2,3-Bis-(3,7,11,15-tetramethyl-hexadecyloxy)-propoxymethyl]-benzene
<b>5</b>	2,3-Bis-(3,7,11,15-tetramethyl-hexadecyloxy)-propan-1-ol (DPG)
<b>6</b>	Tetraethylene glycol (TEG)
<b>7</b>	Hexaethylene glycol (HEG)
<b>8</b>	Octaethylene glycol (OEG)
<b>9</b>	Allyl-tetraethylene glycol
<b>10</b>	Allyl-hexaethylene glycol
<b>11</b>	Allyl-octaethylene glycol
<b>12</b>	Toluene-4-sulfonic acid (allyl-tetraethylene glycol) ester
<b>13</b>	Toluene-4-sulfonic acid (allyl-hexaethylene glycol) ester
<b>14</b>	Toluene-4-sulfonic acid (allyl-octaethylene glycol) ester
<b>15</b>	3-[2,3-Bis-(3,7,11,15-tetramethyl-hexadecyl)-glycerol-1-tetraethylene glycol]-propene
<b>16</b>	3-[2,3-Bis-(3,7,11,15-tetramethyl-hexadecyl)-glycerol-1-hexaethylene glycol]-propene

- 
- 17 3-[2,3-Bis-(3,7,11,15-tetramethyl-hexadecyl)-glycerol-1-octaethylene glycol]-propene
- 18 Thioacetic acid S-{3-[2,3-bis-(3,7,11,15-tetramethyl-hexadecyl)- glycerol-1-tetraethylene glycol]-propyl} ester
- 19 Thioacetic acid S-{3-[2,3-bis-(3,7,11,15-tetramethyl-hexadecyl)- glycerol-1-hexaethylene glycol]-propyl} ester
- 20 Thioacetic acid S-{3-[2,3-bis-(3,7,11,15-tetramethyl-hexadecyl)- glycerol-1-octaethylene glycol]-propyl} ester
- 21  $\alpha,\omega$ -Bis-tosyl-hexaethylene glycol
- 22 Trityl-hexaethylene glycol
- 23  $\alpha,\omega$ -di-Trityloxy-octadecaethylene glycol
- 24 Octadecaethylene glycol (ODEG)
- 25 Allyl-octadecaethylene glycol
- 26 Toluene-4-sulfonic acid (allyl-octadecaethylene glycol) ester
- 27 3-[2,3-Bis-(3,7,11,15-tetramethyl-hexadecyl)-glycerol-1-octadecaethylene glycol]-propene
- 28 Tetraethylene glycol monomethylether
- 29 3-(Methoxy-tetraethylene glycol)-propene
- 30 Thioacetic acid S-[3-(methoxy-tetraethylene glycol)-propyl] ester
- 31 3-(Methoxy-tetraethylene glycol)-propane-1-thiol
- 32 Toluene-4-sulfonic acid (trityl-tetraethylene glycol) ester
- 33 2,3-Bis-(3,7,11,15-tetramethyl-hexadecyl)- glycerol-1-(trityl-hexaethylene glycol)
- 34 2,3-Bis-(3,7,11,15-tetramethyl-hexadecyl)-glycerol-1-hexaethylene glycol
- 35 1,3-Bis-benzyloxy-propan-2-ol
- 36 Toluene-4-sulfonic acid 2-benzyloxy-1-benzyloxymethyl-ethyl ester
- 37 1,3-Bis-benzyl-2-[(2,3-Bis-(3,7,11,15-tetramethyl-hexadecyl)-glycerol-1-hexaethylene glycol] glycerol
- 38 2-[2,3-Bis-(3,7,11,15-tetramethyl-hexadecyloxy)-glycerol-1-hexaethylene glycol] glycerol
- 39 Glycidyl tosylate
- 40 Toluene-4-sulfonic acid-3-[2,3-bis-(3,7,11,15-tetramethyl-hexadecyloxy)-propoxy]-2-hydroxy-propyl ester
- 41 2-[2,3-Bis-(3,7,11,15-tetramethyl-hexadecyloxy)-propoxymethyl]-oxirane

- 42 1,3-Bis-[2,3-bis-(3,7,11,15-tetramethyl-hexadecyloxy)-propoxy]-propan-2-ol
- 43 3-[1,3-Bis-{(2,3-bis-(3,7,11,15-tetramethyl-hexadecyloxy)-propoxy)-glycerol-2-tetraethylene glycol] propene
- 44 Thioacetic acid S-[3-[1,3-bis-{2,3-bis-(3,7,11,15-tetramethyl-hexadecyloxy) - propoxy)-glycerol-2-tetraethylene glycol]-propyl] ester
- 45 1,3-di-(2',3'-di-O-phytanyl-glycerol)-glycerol-2-tetraethylene glycol-3''-mercaptopropyl ether lipid (DDPTT)
- 46 2-Phenyl-[1,3]dioxan-5-ol
- 47 2-Phenyl-5-(3,7,11,15-tetramethyl-hexadecyloxy)-[1,3]dioxane
- 48 3-Benzyloxy-2-(3,7,11,15-tetramethyl-hexadecyloxy)-propan-1-ol
- 49 5-Dimethylamino-naphthalene-1-sulfonic acid 3-benzyloxy-2-(3,7,11,15-tetramethyl-hexadecyloxy)-propyl ester
- 50 5-Dimethylamino-naphthalene-1-sulfonic acid 3-hydroxy-2-(3,7,11,15-tetramethyl-hexadecyloxy)-propyl ester
- 51 5-Dimethylamino-naphthalene-1-sulfonic acid 3-[(allyl-tetraethylene glycol)-2-(3,7,11,15-tetramethyl-hexadecyloxy)-propyl ester
- 52 [3-(Allyl-tetraethylene glycol)-2-(3,7,11,15-tetramethyl-hexadecyloxy)-propoxymethyl]-benzene
- 53 3-(Allyl-tetraethylene glycol)-2-(3,7,11,15-tetramethyl-hexadecyloxy)-propan-1-ol
- 54 Toluene-4-sulfonic acid 2-hydroxy-3-(3,7,11,15-tetramethyl-hexadecyloxy)-propyl ester
- 55 2-(3,7,11,15-Tetramethyl-hexadecyloxymethyl)-oxirane
- 56 1-(Allyl-tetraethylene glycol)-3-(3,7,11,15-tetramethyl-hexadecyloxy)-propan-2-ol
- 57 1-[1-(2-{2-[2-(2-Allyloxy-ethoxy)-ethoxy]-ethoxy}-ethoxymethyl)-2-(3,7,11,15-tetramethyl-hexadecyloxy)-ethoxy]-3-(3,7,11,15-tetramethyl-hexadecyloxy)-propan-2-ol
- 58 5-Dimethylamino-naphthalene-1-sulfonic acid 2-[1-(2-{2-[2-(2-allyloxy-ethoxy)-ethoxy]-ethoxy}-ethoxymethyl)-2-(3,7,11,15-tetramethyl-hexadecyloxy)-ethoxy]-1-(3,7,11,15-tetramethyl-hexadecyloxymethyl)-ethyl ester



## Curriculum Vitae

**Petia Pavlinaova Atanasova****Personal**

*Family:* Atanasova  
*Name:* Petia  
*Surname:* Pavlinaova  
*Sex:* Female  
*Marital status:* Married with a daughter (born 2001)  
*Nationality:* Bulgarian  
*Date of birth :* 19 January 1973  
*Place of birth:* Pleven, Bulgaria  
*Address:* Dimitar Blagoev Str. 7  
*City:* 5869 Gorna Mitropolia  
*Country:* Bulgaria

**Education and career**

**07/2004** - PhD, **Max-Planck-Institute for Polymer Research**,  
Mainz/Germany, Material science group

**Topic:**

*A molecular approach towards tethered bilayer lipid membranes:  
Synthesis and characterization of novel anchor lipids*

**01/2001-05/2004** - Motherhood

**02/1998 - 01/2001** Chemistry scientist, **Institute of Polymers by  
Bulgarian Academy of Science**, Sofia / Bulgaria

**03/1997 - 11/1997** Master-student „**St. Kliment Ohridsky**“  
**University of Sofia**, Sofia / Bulgaria

**Diploma Thesis:**

*1,4-Addition of N,N-disubstituted phenylacetamides to 2-arylmethylene-4-butanolids.*

Grade – excellent 6.00 (out of 6.00)

**10/1992 – 02/1997** Student „**St. Kliment Ohridsky**“ **University of Sofia**, Sofia / Bulgaria

Master of Science degree in Organic and Analytic Chemistry

Grade – very good 5.69 (out of 6.00)

**09/1981 – 06/1992** Technical school for milk-production, Pleven / Bulgaria

High School Diploma

Grade – excellent 6.00 (out of 6.00)

Option: Biotechnological synthesis

**Publications**

1. Atanasova, P. P.; Atanasov, V.; Köper, I., *Langmuir*, **2007**, accepted.
2. Vockenroth, I.; Atanasova, P.P.; Long, J. R.; Jenkins, A. T. A.; Knoll, W.; Köper, I., *Biochimica et Biophysica Acta (BBA) – Biomembranes*, **2007**, 1768(5), 1114-1120.
3. Atanasov, V.; Atanasova, P. P.; Vockenroth, I. K.; Knorr, N.; Köper, I., *Bioconjugate Chemistry*, **2006**, 17, 631-637.
4. Vockenroth, I.; Atanasova, P.P.; Knoll, W.; Köper, I., *IEEE sensors*, **2005**.
5. Christova, D.; Ivanova, S. D.; Velichkova, R. S.; Tzvetkova, P.; Mihailova, P.; Lakov, L.; Peshev, O., *Designed Monomers and Polymers*, **2001**, 4(4), 329-341.
6. Cholakova, T. P.; Dobrev, A. A.; Kanchev, A. B.; Mihailova, P. P., *Journal of Chemical Research (S)*, **1999**, 546-547.